THE CHARACTERISTICS OF VAPOUR-LIQUID DISPERSIONS FORMED ON SIEVE TRAYS AND THEIR INFLUENCE ON DISTILLATION TRAY PERFORMANCE.

A Thesis submitted to the University of London in partial satisfaction of the requirements for the award of the degree of Doctor of Philosophy in the Faculty of Engineering (Chemical Engineering)

by

William Pattie Macmillan
B.Sc. (New South Wales)

Department of Chemical Engineering
and Chemical Technology,
Imperial College of Science and Technology,
London, S.W.7.

August 1962

ABSTRACT

A gamma ray absorption technique has been used to determine the dispersion density profiles and the liquid hold ups on sieve plates in a 4" diameter distillation column.

Plate efficiency studies have been performed for the n pentane-iso pentane system and related to the hydrodynamic parameter. A significant proportion of the total mass transfer process occurring on sieve plates was found to occur in the vapour-liquid dispersed region.

Experimental relationships have been established for the various factors contributing to the total pressure drop across the plate and it is shown that these combine to yield a reasonable prediction of plate pressure drop.

A pilot plant incorporating a 16 inch diameter distillation column has been designed and performance runs carried out.

Acknowledgments

The author wishes to express his most sincere thanks to Professor R.W.H. Sargent for his invaluable advice and encouragement during the course of this work and to Professor K.G. Denbigh for his interest in the project.

The assistance of Mr J. Oakley and his workshop staff, both in the design and construction of experimental apparatus is gratefully acknowledged, the skill and craftmanship of Mr John Harman making possible much of the specialised equipment used in the radio isotope work. Thanks are also due to Mr Len Tyley for his advice on counting techniques and to Ajoy Dey for his assistance in the photographic work connected with this thesis. The Departmental glassblowers were also most co-operative and fellow students gave much helpful advice.

The project has been sponsored in most generous fashion by the Joint ABCM/BCPMA Distillation Panel and most helpful discussion has arisen from contact with Panel members. The loan of a refrigeration compressor by the Directors of Messrs J.& E.Halls Ltd., is acknowledged with thanks. The award of Scholarships by the ABCM/BCPMA Panel and by the Commonwealth Scholarship Commissioners is gratefully acknowledged.

TABLE OF CONTENTS

1. Introduction 7

Part I. HYDRODYNAMIC STUDIES ON SIEVE PLATES.

2. Nature of the Vapour-Liquid Dispersed Region on Sieve Plates. 14

2.1. Determination of Liquid and Vapour Hold-ups in the Dispersion. 18

2.2. Methods Based on Tracer Additions.

2.2.1. Addition of Tracers to the Column Reboiler. 18

2.2.2. Measurement of Residence Time Distribution on the Plate. 15

2.3. Methods Based on Dispersion Density Determination.

2.3.1. Density Determination Based on Static Pressure Measurements. 21

2.3.2. Density Determination Based on Light Transmission Studies. 26

2.4. Radio Isotope Technique for Determining Dispersion Density Profiles. 27

3. Details of Experimental Rigs.

3.1. 4" Diameter Air-Water Column Simulator. 33

3.2. 4" Diameter Glass Distillation Column. 34

3.3. Gamma Ray Traverse System and Ancillary Counting Equipment. 37

4. Experimental Programme. 40

5. Discussion of the Experimental Data.

5.1. Validity of the Radio Isotope Density Measuring Technique. 44

5.2. Evaluation of Previous Methods of Liquid Hold-up Measurements.

5.2.1. Dynamic Head Manometers. 46

5.2	Evaluation of Pressure Probe Measurements for Liquid Hold up Determination	
5.2.1	Plate Manometer Measurements	46
5.2.2	Pressure Probe Traverse Measurements	49
6	Liquid Hold up Studies on Sieve Plates	54
7	Plate Pressure Drop Studies	
7.1	Evaluation of Previous Methods of Calculation	59
7.2	Analysis of Pressure Drop Experimental Data	69
Part II	Plate Efficiency Studies	
8	Concept of Plate Efficiency and its relation to Column Design Variables	79
8.1	Experimental Determination of Plate Efficiency Data	85
8.2	Discussion of Experimental Plate Efficiency Results	87
9	General Conclusion and Recommendations	93
Part III	Pilot Plant Distillation Column	
10	Flow Sheet Descriptions and Column Layout Details	96
10.1	Performance Proving Trial on Pilot Plant Column	107

Nomenclature 109

Bibliography 111

Appendix A 116

Appendix B 146

Appendix C 149

INTRODUCTION

1. Introduction.

In the highly competitive chemical industry of to-day, the elimination of over design in distillation columns would be a major breakthrough towards more efficient use of capital. The number of theoretical plates required to effect a given separation can be determined rather accurately, but there exists no reliable method for the estimation of the efficiency of a vapour-liquid contacting device for a given system.

The result of recent distillation research has been the development of general correlations to fit experimental data obtained on a large number of columns and for a wide variety of systems. Work sponsored by the American Institute of Chemical Engineers Research Committee and performed mainly by Gerster et al[28] at the University of Delaware is an excellent example of such a programme.

This work has led to improved methods of tower design and means of estimating plate efficiencies, but after at least five years concentrated effort no significant advance has been made in the understanding of the complex heat and mass transfer phenomena occurring on vapour-liquid contacting plates.

In 1958, the Distillation Panel of the Association of British Chemical Manufacturers (A.B.C.M.) and the British Chemical Plant Manufacturers Association (B.C.P.M.A.) was set up to evaluate the results of the A.I.Ch.E. Research Programme and to recommend specific topics that warranted further investigation. The

influence of the physical mechanism of contact of vapour and liquid on the mass transfer process was not known although the A.B.C.M./B.C.P.M.A. Panel favoured the view that,since mass transfer rates were higher during bubble formation, the bulk of the mass transfer occurred during bubble formation and subsequent rise of the bubble through the 'clear liquid' near the plate. Professor J.A. Gerster in his comments on the Panel's report was insistent that the results of the Delaware programme did not support this view and that a significant part of the mass transfer did occur in the foam[27].

This conflict of expert opinion coupled with the scarcity of information relating to the mechanism of formation of the vapour-liquid interfaces across which mass transfer occurs, led to the sponsorship of the present project, designed to elucidate some of these fundamental problems.

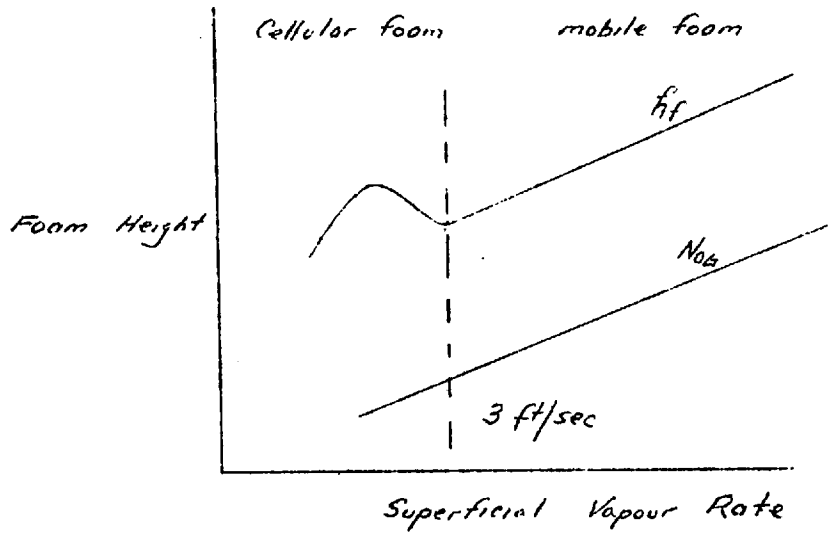
From the outset it was considered essential that all the data should be obtained in an actual distillation process even though this would make the experimental rigs more costly and techniques more complicated. There was a strong feeling that data obtained from the commonly used air-water systems were not directly applicable to distilling systems, due to differences in the physical mechanism of contacting liquid and vapour and differences in interfacial phenomena.

Sieve plates were chosen as the basic contacting plate to be studied. They are cheaply and easily fabricated and the

bubbling mechanism on any one plate is representative of sieve plates as a whole. The use of a bubble cap tray would yield data applicable to that type and size of cap only.

Two papers,[2][79] had already appeared in the literature showing the influence of liquid physical properties on the bubbling and foaming characteristics of binary mixtures. It was thus essential to choose a system in which the liquid physical properties were independent of composition to ensure that the effect of a change in an experimental parameter could be measured directly and not be obscured by attendant composition changes. A binary system comprising two hydrocarbon isomers would meet this requirement and a system boiling near room temperature was sought. This latter requirement was to facilitate visual and photographic studies on the column by eliminating undue condensation on the viewing sections. A mixture of normal and iso pentane was chosen as meeting these requirements. The liquid densities, viscosities and surface tensions are sufficiently close to each other that there is little composition effect and the boiling point of the mixture is of the order of 100°F.

There was also considerable evidence from the Russian literature that high mass transfer rates could be obtained by operation at superficial column velocities above 3 feet per second[63].



At low vapour rates, in the air-water system, a structural or cellular foam region was formed above the 'clear liquid' and was characterised by a typical honeycomb structure of vapour bubbles separated by thin liquid films. As the vapour rate was increased, the cell size decreased leading to a reduction in fcam height. At about 3 feet per second, the cellular structure disappeared and a highly turbulent, liquid-vapour dispersion, with no readily discernable structure, was formed. As one would expect, the number of gas phase transfer units was shown to be much higher in the mobile foam region than in the cellular region[55] and it appeared desirable to see if this rather particular result applied to distillation systems, many of which are considered to be examples of processes that are gas phase controlling.

The trend in commercial practice to towers of large diameters has accentuated the problems of maldistribution of liquid and vapour and its effect on the tray efficiency. It was considered

essential to work on as large a scale as possible, within the limits set by the College services and the financial resources available, so that plate mixing studies could be made. Feasibility studies showed that a three plate, 16" diameter column, capable of operation up to seven feet per second superficial velocity, was the largest size that could be provided for in the College. Design and erection of this pilot plate was reckoned to involve a long delay so it was decided to pilot the experimental techniques on a 4" diameter test rig.

It was considered that by determining the effect of design and operating variables on

(1) liquid hold-up on the tray

(2) dispersion density distribution above the tray

(3) distribution of the liquid hold-up between 'clear liquid' near the tray and the vapour-liquid dispersion above it, and

(4) the structure of this vapour-liquid dispersion

together with simultaneous plate efficiency measurements, that the effect of the physical mechanism of vapour-liquid contact on the mass transfer process could be elucidated.

The technique of measurement of plate efficiencies had been well developed whilst the use of high speed cinematography would allow the study of bubbling processes and dispersion structures. A previously developed technique, based on the absorption of gamma radiation by the dispersion[11], could be used for the determination of liquid hold-ups and the dispersion density profiles above the plate.

The first stage in this research was, then, the determination of the relative distribution of the liquid hold-up between 'clear liquid' and the dispersion and the effect on this distribution of changes in design and operating variables.

PART I. HYDRODYNAMIC STUDIES ON SIEVE PLATES.

2. Characteristics of Vapour-Liquid Dispersions formed on Sieve Plates.

Visual observation of an operating plate is the best method of demonstrating the futility of attempts to evaluate plate performance on the assumption that a single hydraulic regime exists on the plate. On the tray floor there is a pool of 'clear liquid' penetrated by the bubble streams rising from the plate orifices and above this a vapour-liquid dispersion, the nature and extent of each regime depending on the fluid physical properties and the column design and operating variables.

Much confusion has arisen in the past over the multiplicity of names given to these regimes and the tendency to call any dispersion a "foam". For convenience in describing the nomenclature used throughout this thesis, an over simplified account is given of the manner in which these various regimes are formed. When vapour passes at a low rate through a pool of clear liquid in a system with suitable fluid properties, a "cellular foam" is first formed. This has a characteristic "honeycomb" structure in which vapour, the dispersed phase, exists as polyhedral bubbles separated by thin liquid films. As the vapour velocity is increased, the vapour bubbles start to decrease in size and at slightly higher rates the liquid films rupture yielding a highly turbulent vapour-liquid dispersion. This ultimately degenerates at higher vapour rates into a coarse "spray" of liquid droplets suspended in the vapour stream.

There appears to be general agreement in the literature regarding the use of the terms cellular foam and spray, however there are many terms in current use to describe the vapour-liquid dispersed region. The Russian school refer to it as the mobile foam region[65] whilst Calderbank and Rennie[10] use the term froth, Helsby[37] preferring to call it a channelling region. The term, mobile foam, seems to be more expressive of the general nature of this regime than any of the alternatives and the terms, cellular foam, mobile foam and spray have been adopted in this thesis.

If a complete understanding of the mass transfer processes occurring on sieve trays is desired, then the contribution to the total mass transfer of each of the separate regimes must be evaluated. This would be achieved if the following data could be obtained:

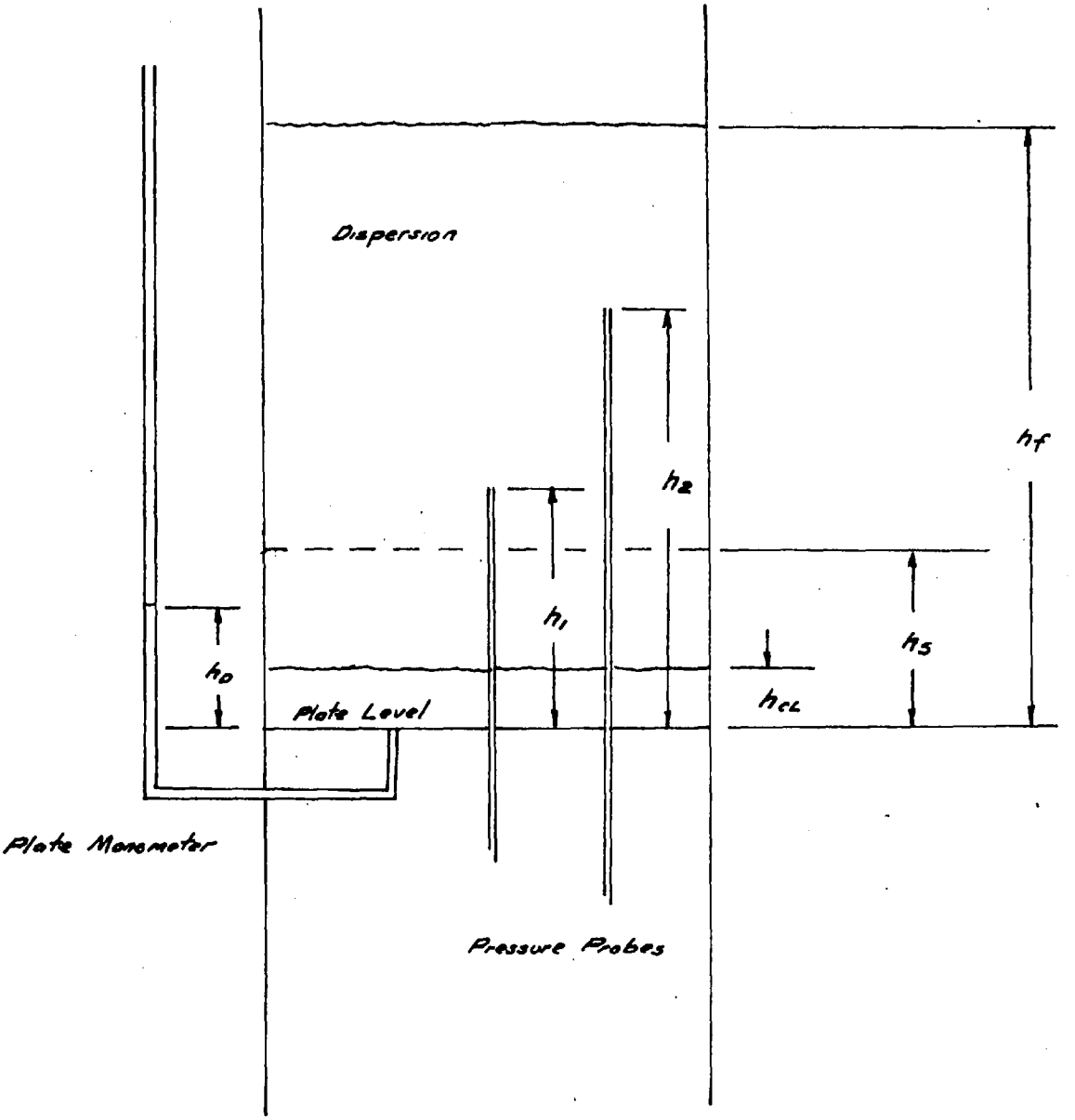
(1) Liquid and vapour hold-up in each regime

(2) Interfacial area of contact between the phases in each regime

(3) Physical mechanism of contact in each regime

(4) Liquid and vapour residence times in each regime.

The use of a high speed cine camera would yield information regarding the physical mechanism of contact of vapour and liquid in each regime whilst several methods exist for evaluation of liquid and vapour hold-ups. Techniques exist for the determination of liquid and vapour residence times but these apply to the total plate hold-up and it does not appear feasible to develop techniques specific to a given regime.



DENSITY DETERMINATION NOMENCLATURE

FIGURE 1

Various claims in the literature have been made that a linear relationship exists between the light transmitted through a dispersion and the interfacial area per unit volume and that with suitable calibration of the light probe, accurate data on interfacial areas can be obtained[8][13][14]. There is evidence that such a technique can be successfully employed to measure interfacial areas in liquid-liquid systems and in systems in which gas bubbles are dispersed in a liquid medium[11]. However the intense multiple scattering found in optically dense systems (such as are produced on sieve trays) would seem to invalidate the technique. One should also note that the light transmission technique has been used by Crozier and others to measure dispersion density and Crozier strongly insists that the light transmission through an optically dense dispersion is not a measure of interfacial area[15]. Calderbank et al[9] developed a reflectivity probe to measure interfacial area in optically dense dispersions but later admit that the technique is an error for cellular foams and describe a so called "pin dropping" technique to obtain the mean bubble diameter from dispersion photographs[10]. The results obtained from these techniques are encouraging,however no satisfactory method is available for determining the true interfacial area for the type of dispersion formed on sieve plates. The use of high speed cinematography to provide information on the mechanism of vapour-liquid contacting might also provide a means of measuring the interfacial area.

Thus the only way in which the contribution of each of the regimes to the total mass transfer can be elucidated is by measurement of the liquid and vapour hold-up in each regime. Knowledge of how the plate efficiency varies with changes in the distribution of hold-up between the regimes should allow general conclusions to be drawn regarding the mass transfer effectiveness of each regime.

2.1. Determination of Liquid and Vapour Hold-ups in the Dispersion.

For rigs in which there is no liquid cross flow the total liquid hold-up on the plate can be readily obtained by draining the plate at the end of a run. However, the technical problems involved in draining a plate in an operating column are so great that alternative techniques have to be used. Two general methods for the determination of liquid hold-ups are available, those based on the introduction of tracer materials either in the reboiler or more commonly on the test plate and those based on the measurement of the dispersion density on the test tray.

2.2. Methods Based on Tracer Additions.

2.2.1. Addition of Tracers to the Column Reboiler.

Rustin[69] developed a technique for estimating the liquid hold-up on bubble cap plates in a multi tray column used for the distillation of methyl cyclo hexane-toluene mixtures. A non-volatile, soluble tracer, benzoic acid, was added to the reboiler before start up and the total column hold-up determined by measurement of the increase in reboiler tracer concentration for the several

operating conditions studied. The actual column hold-up was then calculated by subtraction of the hold-up in the condenser and reflux lines, determining these hold-ups from the physical dimensions of their component parts. This method is only approximate in that it yields an average value for the individual plate hold-ups and cannot take into account variations in plate hold-up due to variation of plate composition in the column.

2.2.2. Measurement of Residence Time Distribution on the Plate.

Plate mixing phenomena cause some of the liquid to stay on the plate for periods longer or shorter than other portions of the liquid producing an entire spectrum of residence times ranging from zero to infinity. The implications of this have been discussed by Danckwerts[16] and general mathematical laws set up.

The experimental determination of liquid residence time distributions involves the injection of a non-volatile tracer into the inlet stream and the measurement of its concentration in the exit stream as a function of the time elapsed since injection. Two distinct types of residence time functions are obtained depending on whether a unit step impulse or an instantaneous pulse of tracer is introduced. The cumulative residence time curve obtained from the step input technique is readily obtained by integrating the instantaneous pulse curve.

For the case of a step input, Danckwerts has shown from a material balance that

$$1 - F(\theta) = \frac{V}{v} I(\theta)$$

where $F(\theta)$ = fraction of material in the outflow that has been in the system for a time less than θ

$I(\theta)$ = fraction of the material in the system having ages between θ and $(\theta + d\theta)$

v = volumetric liquid flow rate

V = volume of liquid hold-up.

Now $$\frac{v}{V} \int_0^{\infty} \{1 - F(\theta)\} \, d\theta = \int_0^{\infty} I(\theta) \, d\theta = 1$$

since the right hand integral represents the total fraction of the liquid on the plate having ages between zero and infinity, i.e. all the liquid present.

Thus $$\int_0^{\infty} \{1 - F(\theta)\} \, d\theta = \frac{V}{v}$$

leading to a method for finding V, the liquid hold-up on a plate.

Using a step input of a suitable tracer, $F(\theta)$ is obtained at the exit weir and plotted as $(1 - F(\theta))$ as a function of θ. This curve does not have to be integrated over the range zero to infinity as after a finite time has elapsed, the outlet tracer concentration is the same as the inlet concentration due to the ~~mobility~~ *mability* of the analytical technique to measure very small concentration differences. Examination of the experimental residence time curves presented by Foss et al[21] from data obtained on the air-water system using sieve plate sections, shows that small concentration differences between the outlet and inlet streams become

undetectable after a reasonable time has elapsed.

This technique for evaluation of liquid hold-up has the advantage that it is obtained at the same time as liquid mixing data, however since the project was not concerned with liquid mixing studies a simpler measuring technique was desired. These two tracer techniques have the disadvantage that non-surface active tracers specific to the system under study must be available. The addition of even small amounts of surface active dyes or salt solutions can alter the actual liquid hold-up on a plate due to changes in the nature of the dispersion. These techniques can only yield information regarding the total liquid hold-up on the plate and not as to its relative distribution between the several regimes.

2.3. Methods Based on Dispersion Density Determination.

For a homogeneous dispersion the liquid and vapour hold-ups may be readily calculated if the dispersion density and volume are known. Most workers in the past have assumed that the dispersions formed on operating plates are homogeneous and that the hold-ups are readily calculated by measuring the dispersion density and the dispersion height. Not only can the assumption of homogeneity be challenged but the methods used for measurement of dispersion density are also open to question.

2.3.1. Density Determinations Based on Static Pressure Measurements.

The greater bulk of past distillation research, including

the recent A.I.Chem.E. Research Programme, has been correlated using liquid hold-ups determined from 'static' pressure measurements at the base of the dispersion. The head at the bottom of the dispersion is considered to be due solely to the weight of the liquid in the dispersion and several methods have been proposed for its measurement. The most commonly used technique is to fit a U-tube manometer to the plate, one leg being flush with the plate with the other projecting into the vapour space above the dispersion. This manometer reading is considered to be the 'equivalent clear liquid height', i.e. the height to which the dispersion would collapse if there were no vapour present. Gilbert[33], amongst others, has pointed out the unreliability of these manometers but failed to appreciate that they measured the 'dynamic' rather than the static head on the plate.

Other workers have attempted to measure the head at the plate due to the dispersion as the difference between the wet and dry plate pressure drops. From results obtained on long rectangular test sections, up to 14 feet in length, with long calming lengths at each end, with no liquid cross flow, Kemp and Pyle[47] and Hutchinson et al[42] found that by increasing the liquid depth in the calming section, at constant vapour rate, the total plate pressure drop increased but by a lesser amount than the increase in clear liquid depths. They defined an aeration factor, β,

$$\beta = \frac{hT_1 - hT_2}{hS_1 - hS_2}$$

where hT_1 and hT_2 are the wet plate pressure drops corresponding to clear liquid depths, hS_1 and hS_2, both expressed as cms. of liquid. From a consideration of the hydraulic model involved, it can be shown that S_1 and S_2 are, in fact, the dynamic heads associated with the liquid and vapour flow on the plate and since $(\mathcal{L}_{T_1} - \mathcal{L}_{T_2})$ is proportional to $(hS_1 - hS_2)$, the difference in true static head of the liquid hold-up, then

$$\beta \propto \frac{hS_1 - hS_2}{hd_1 - hd_2}$$

β is thus dependent on the variation of both static and dynamic heads with F factor in the column and does not show directly changes in liquid hold-up on the tray.

Arnold et al[3] later modified this equation for the case of an actual column by substituting the liquid head at the weir, weir height plus weir crest, for the clear liquid heads of Kemp and Pyle. These relationships give the average aeration factor for the dispersion over two weir heights and the concept of aeration factor at a particular value of vapour rate, liquid rate and weir height was developed by Prince[66], Mayfield et al[54] and Yokota[78] as

$$\beta' \equiv \frac{hT - hDP}{hW}$$

where $\mathcal{L}_{DP}$ is the dry plate pressure drop and hW is the liquid head at the inlet weir. This method of defining the aeration factor tacitly assumes that the dispersion was formed from a pool

of liquid of depth equal to the liquid height at the weir and any difference between this depth and the static head at the base of the dispersion is due to the presence of vapour hold-up. Even a superficial examination of the validity of this assumption reveals that the head at the inlet weir is determined, in the main, by the head necessary to overcome the resistance of the rising bubble streams to liquid flow across the plate and need bear no direct relationship to the liquid hold-up. The relationship

$$\rho_f = \frac{hT - hDP}{hf}$$

(the symbols used in these expressions have the meanings assigned to them in Figure 1 (p.17) proposed by Hay and Johnson[35] determines an average value for the dispersion density rather than the aeration factor of previous workers and allows them to predict with some success the manner in which the hold-up varies with changes in design and operating variables.

There are two main objections to using relationships of this type to determine the liquid hold-up on the plate. The relationships are all based on the assumption that the pressure head in a dispersion formed by the flow of vapour through a pool of liquid on a perforated plate is due solely to the weight of liquid in the dispersion. No allowance whatever is made for kinetic effects associated with the vapour flow through the dispersion. More importantly from the viewpoint of this research, they can only yield an average value for dispersion density over the several regimes

present allowing no estimate to be made of the extent of each of the regimes.

For a non homogeneous dispersion, a vertical density traverse is necessary to determine both the relative extents of each regime and the total liquid hold-up on the plate. With the axes plotted in suitable units, the area under a dispersion density profile represents the static head of liquid per unit bubbling area of plate.

Two methods based on 'static' pressure measurements are available for determining the vertical dispersion density profile. One involves a measurement of the pressure necessary to force a bubble of inert gas through an orifice in the probe against the static pressure of the dispersion, whilst the other is a simple arrangement that uses the probe as one leg of a U-tube manometer. Both methods rely on the assumption that

$$\rho_f = \frac{d}{dh} (P \text{ static})$$

again considering the 'static' pressure to be due solely to the weight of liquid in the dispersion. Taking into consideration kinetic effects associated with the vapour flow, one would expect the measured pressure to be less than the head due to the liquid hold-up and that the divergence of these results would increase with increasing vapour rate. This has been confirmed experimentally by Kafarov and Vigdorov[45], at high vapour rates, the kinetic effects associated with liquid and vapour flow rates were so

pronounced that negative densities were determined in the region close to the plate.

As demonstrated in the experimental section of this thesis, the use of any relationship based on determination of the head due to the dispersion is not a reliable measure of the liquid hold-up on the plate. It is not considered feasible to correct such measurements for the kinetic effects associated with the fluid flow as they either yield an average value of dispersion density or require vertical probe traverses to obtain a density profile. The experimental difficulties in attempting any form of vertical traverse in a multi plate column are great and it appears that the technique ultimately chosen for determining the profile must allow traverses to be made external to the column.

2.3.2. Density Determination Based on Light Transmission Studies.

Crozier[15] has determined the density profile above a plate by measurement of the variation in light transmission through the dispersion, a method that does not employ probes of any description or the use of surface active tracers. It does, however, necessitate the use of a glass column or the provision of viewing windows in a metal column. The method depends on the assumption that the light absorbed by a given thickness of dispersion is an inverse function of the volume of liquid in the dispersion such that the fractional extinction of a light beam passing through the dispersion is a measure of the local dispersion density. The

mechanism of light extinction is assumed to be due to scattering at vapour liquid interfaces hence a change in the physical structure of the dispersion without altering the liquid hold-up could alter the amount of light transmitted and be interpreted as a change in dispersion density.

For this reason and from the fact that Calderbank puts forward equally cogent reasons to show that light absorption measurements yield data on interfacial areas, this method of density determination should be viewed with some caution. A better technique would be to use a much harder radiation, such as gamma radiation, that is more penetrating and less susceptible to reflection and to multiple scatter. The use of gamma radiation would obviate the need for glass viewing windows and would allow both horizontal and vertical traverses to be made using equipment completely external to the column.

2.4. Radio Isotope Technique for Determining Dispersion Density Profiles.

The use of gamma radiation to detect changes in level and the position of an interface within closed vessels is a well known technique[59]. It has been used by Grohse[34] to study density changes in gas-solid fluidised systems and by Hiwa and Beckmann[43] in the determination of liquid hold-up in packed beds whilst there are several instances of its application to density determination in gas-liquid dispersed systems.[9][32][74] The first recorded attempt to determine dispersion density within an

operating column was made by the Texas Co.Inc. in 1947 but the results of the investigation were never published.(17)

The absorption of a parallel, monoenergetic beam of gamma radiation by a homogeneous medium of density ρ and thickness x is described by an exponential law similar to Lambert's Law for parallel manochromatic light

$$I = I_0 \, e^{-\mu\rho x}$$

where I_0 and I are the intensities of the incident and transmitted radiation and μ is the mass absorption coefficient of the medium.

Now $I \propto \frac{1}{t}$ where t is the time taken to record a given number of counts, so that

$$\frac{1}{t} = \frac{1}{t_0} \, e^{-\mu\rho x}$$

$$\text{and } t_0 = t \, e^{-\mu\rho x}$$

$$\text{or } \ln t = \ln t_0 + u\rho x$$

The analysis above leads to a simple experimental procedure for measurement of dispersion density. The intensity of the transmitted beam is measured by the time taken to record a fixed number of counts. This count time is measured for the conditions of the column empty (t_0) and filled with liquid (t) and a straight line calibration curve drawn on semi log paper through the points ($\ln t_0, \rho = 0$) and $\ln t, \rho = 1$). The volume fraction liquid on the dispersion is then determined by measuring the time taken to record the fixed number of counts and reading the dispersion density directly from the calibration chart.

This analysis is only valid for the case of a parallel beam of monochromatic radiation passing through a homogeneous dispersion. The first requirements can be met by adequate collimation at both source and counter and by the selection of a suitable isotope. Calderbank[9] has shown that in a suitably collimated system using Caesium 137 as a mono energetic source, yielding 92% of gamma radiation with an energy of 0.66 MeV, that a linear relation does exist between log I and the dispersion density in accord with the theory outlined above.

Apart from brief mention by Cameron[11], the significance of errors due to non-homogeneity in the dispersion has not been fully evaluated. This is essential since the dispersions formed on sieve trays are inherently unstable and not homogeneous. Non homogeneity in the direction of the beam simply results in the measurement of the average of the point densities; however fluctuations with time during the counting period lead to the measurement of an apparent time average density of less magnitude than the true density.

The transmission law

$$\frac{dI}{dx} = -\mu\rho I$$

For constant ρ : $\quad I = I_0 e^{-\mu\rho x}$

For $\rho = \rho(x)$ $\quad \ln \frac{I}{I_0} = -\int_0^x \mu\rho\, dx$

$$= -u\int_0^x \rho\, dx$$

$$= -\mu \bar{\rho} x$$

i.e. $$I = I_0 e^{-\mu \bar{\rho} x}$$

For $\rho = \rho(t)$: Write $\rho = \bar{\rho} + r(t)$

thus $$\frac{1}{r}\int_0^r I dt = I_0 \frac{1}{r}\int_0^r e^{-\mu(\bar{\rho} + r)x} dt$$

$$= I_0 e^{-\mu \bar{\rho} x} \cdot \frac{1}{r}\int_0^r e^{-\mu r x} dt$$

For sufficiently long r $$\frac{1}{r}\int_0^r I dt = \langle I \rangle$$

and $$\frac{1}{r}\int_0^r e^{-\mu r x} dt = \langle e^{-\mu r x} \rangle$$

If r is a Gaussian noise of variance σ^2 (zero mean):

$$\langle e^{-\mu r x} \rangle = \int_{-\infty}^{+\infty} e^{-\mu r x} \frac{1}{\sqrt{2\pi\sigma^2}} e^{-\frac{r^2}{2\sigma^2}} dr$$

For the exponent $$\frac{-r^2}{2\sigma^2} - \mu r x = -\frac{1}{2\sigma^2}(r + \sigma^2 \mu x)^2 + \frac{\sigma^2 \mu^2 x^2}{2}$$

$$\therefore \langle e^{-urx} \rangle = e^{\frac{\sigma^2 \mu^2 x^2}{2}} \int_{-\infty}^{+\infty} \frac{1}{\sqrt{2\pi\sigma^2}} e^{\frac{1}{2\sigma^2}(r + \sigma^2 \mu x)^2} dr$$

$$= e^{\frac{\sigma^2 u^2 x^2}{2}}$$

If ρ' = apparent density defined by $\langle I \rangle = I_0 e^{-\mu \rho' x}$

then $$\langle I \rangle = I_0 e^{-\mu \rho' x} = I_0 e^{-\mu \bar{\rho} x} \cdot e^{\frac{\sigma^2 \mu^2 x^2}{2}}$$

$$\therefore \rho' = \bar{\rho} - \frac{\sigma^2 \mu x}{2}$$

Similarly for a pure sinusoidal fluctuation distribution

$$\rho' = \bar{\rho} - \frac{\mu x r_0^2}{4}$$

and for a Poisson distribution

$$\rho' = \bar{\rho}\ \frac{\sigma}{\mu x} \ln\ (1 + \frac{\mu x}{\sigma})$$

For measurements on a dispersion in which there is a fluctuation with time during the counting period, the magnitude of the error is directly related to the variance of the fluctuations, the path length and the value of the absorption coefficient of the medium. From this analysis the variance of the fluctuation in the non homogeneous dispersion formed on any sieve tray could be determined by measuring the time average density as a function of path length within the dispersion. For a Gaussian ~~raise~~ noise, a linear plot of ρ' against x should yield a straight line whose intercept is $\bar{\rho}$ at x = 0 and slope $-\frac{\sigma^2_u}{2}$. Fortunately, the experimental justification of this technique when applied to a dispersion of known hold-up shows, that for the range of variables studied, the time average density checks to within 5% of the true density, measured by independent means, so that detailed analysis of the fluctuation is not necessary.

Further sources of error in this method of density determination have been discussed by Hours[39]. Compton scattering of the radiation passing from the source to the counter could lead to the reception of secondary radiation at the counter. In this way an apparent density less than the true density would be measured. By using a fairly slender 'pencil' beam and by adequate collimation at the counter, this effect can be made negligible.

The intensity of the transmitted radiation is determined by the time necessary to obtain a fixed number of counts. The number of counts measured is chosen mainly on statistical grounds although a sufficiently long count time is necessary to eliminate errors in the timing device. Assuming that the random decay of a radio isotope follows a Poisson distribution, the timing of 50,000 counts should result in a 97% probability that a single measurement is within 1% of the true value.(75)

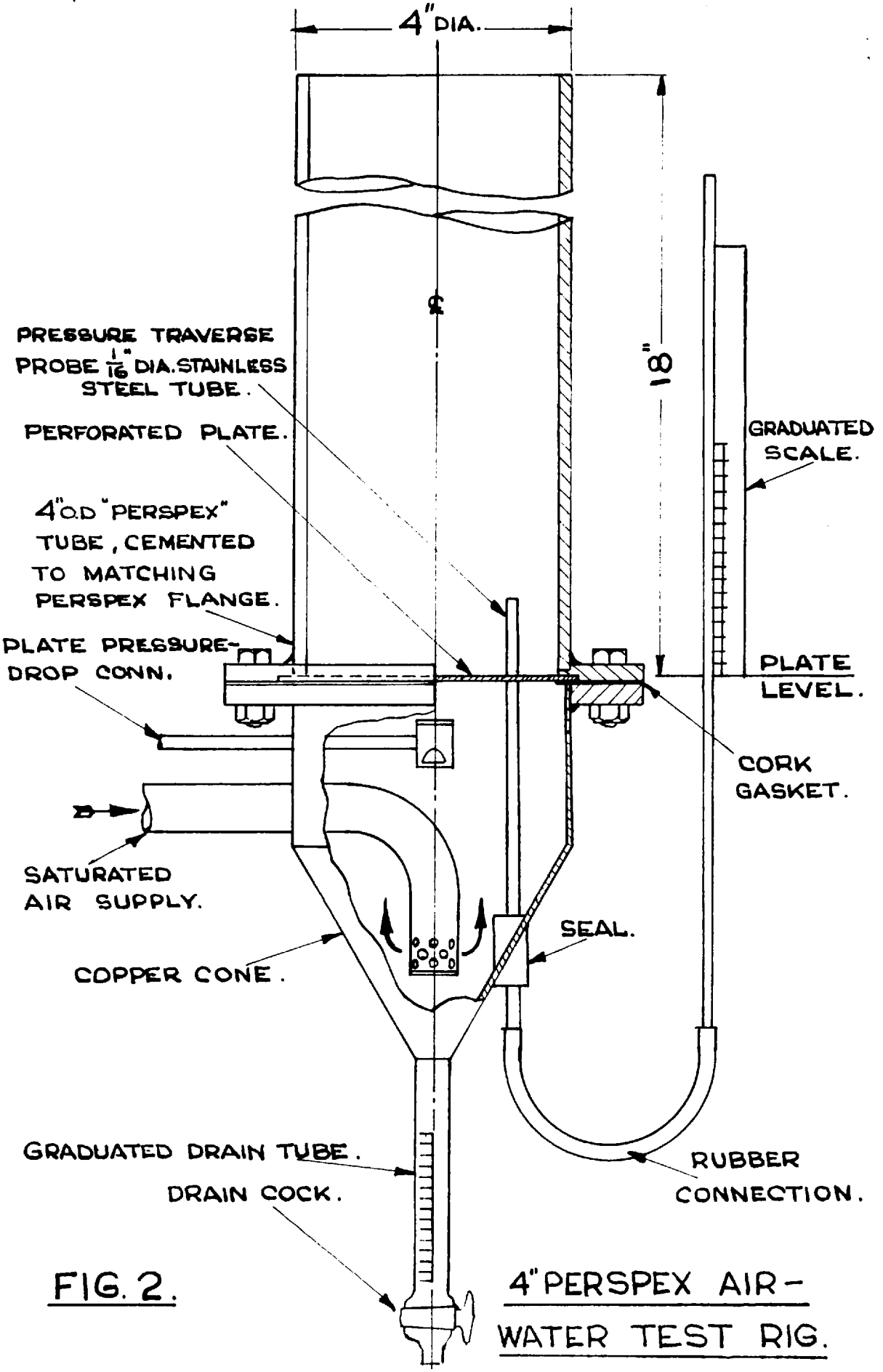
The isotope used for this purpose must meet the requirements laid down by the foregoing analysis of errors in the method. Caesium 137 provides an almost mono energetic source of high energy gamma rays and has a suitable half life of 30 years. The strength of the isotope depends on a balance between three factors, the amount of shielding required, the need to eliminate the effect of changes in the background count and the time taken to record the set number of counts. The optimum source strength is one that requires the minimum amount of shielding to make the apparatus comply with Safety Regulations, is strong enough to make the counting process independent of the background count and yields suitable count times. A simple calculation shows that for the physical system to be used in the determination of dispersion densities, a one millicurie source would give count times of approximately 100 seconds when timing 50,000 counts. This was judged to be a reasonable period for the minimisation of errors in the timing device.

3. Details of Experimental Rigs.

3.1. 4" Diameter Air-Water Column Simulator.

The preceding discussion of methods available for plate hold-up determination showed that some doubt exists as to the reliability of methods based on static pressure measurements in the dispersion. Since the great bulk of previous work has been correlated in terms of hold-up data and contact times based on these methods, it is important to determine the relationships between these measurements and the true liquid hold-up. The hydrodynamics of air-water systems, in this regard, can be safely assumed to be similar to actual distilling mixtures and advantage taken of the simplicity and ease of operation of an air-water rig. Constructional details of the 4" column simulator are shown in Figure 2

The basic column assembly consists of an 18" length of flanged, 4" bore Perspex tube bolted to a 24 gauge brass air distributor cover, the 1/16" thick perforated insert, suitably gasketted being fitted between the connecting flanges. The conical section of the bottom cover terminates in a 1" bore, glass measuring tube suitably calibrated to allow determination of weep rates and the total plate hold-up. Air supply from the mains is filtered and stepped down to 5 psig at a main reducing valve. Air, saturated by bubbling through water in a saturator, is passed to a 5 cubic feet capacity surge vessel that acts also as a knockout drum for entrained liquid. Flow measurement is by a metric size



10.6.62.
WPM/2.

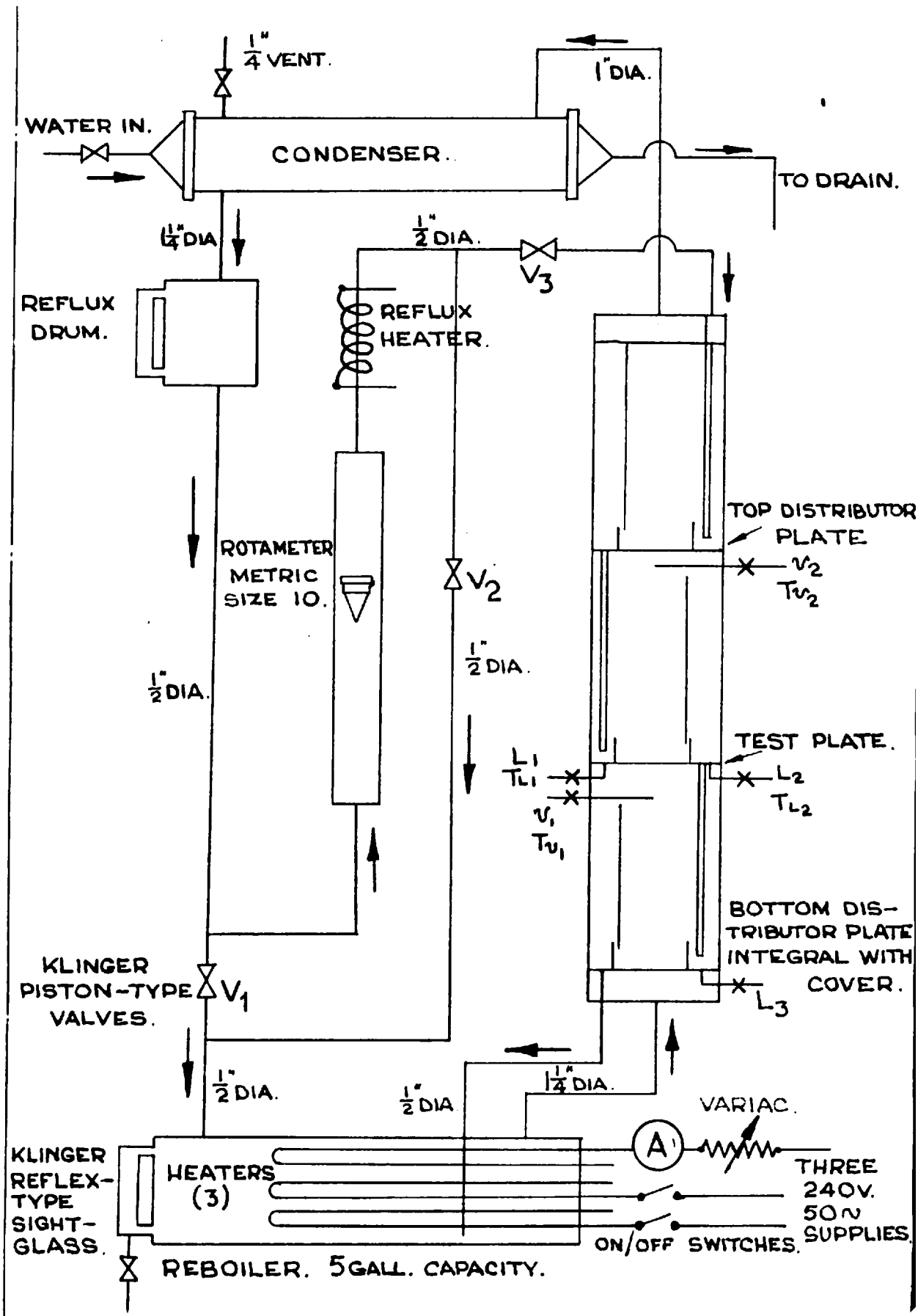
FIG. 2.

4" PERSPEX AIR-WATER TEST RIG.

35 Rotameter and is controlled by a needle valve in the line. Air enters the bottom distributor cover through a ½" bore copper tube, the end being blanked off to cause air to discharge through several 1/8" peripheral holes. A length of 1/16" diameter stainless tubing is used for the vertical static pressure traverse and enters the column through a tight fitting rubber bung sealed into the bottom cover. The traverse is connected via rubber tubing to the measuring arm of a U-tube manometer mounted directly on a graduated scale. A pressure tapping below the bottom plate allows dry and wet plate pressure drops to be measured.

3.2. 4" Diameter Glass Distillation Column.

A line diagram showing the essential features of the 4" test rig is shown in Figure 3. (The basic column unit is a three plate column with 12" plate spacing assembled from three, 4" nominal bore sections of Q.V.F. glass pipe. Three is the minimum number of plates required to ensure representative behaviour of the test plate providing a distributor plate for vapour and liquid above and below it. Since visual observation of all phases of test plate behaviour is required, the masking effects of the Q.V.F. coupling flanges must be avoided. The test plate is screwed to a brass ring expanded against the column wall in the middle of one of the glass sections so that visual observation from plate level to top of the dispersion is possible. Liquid and vapour leakage past the plate is prevented by the insertion

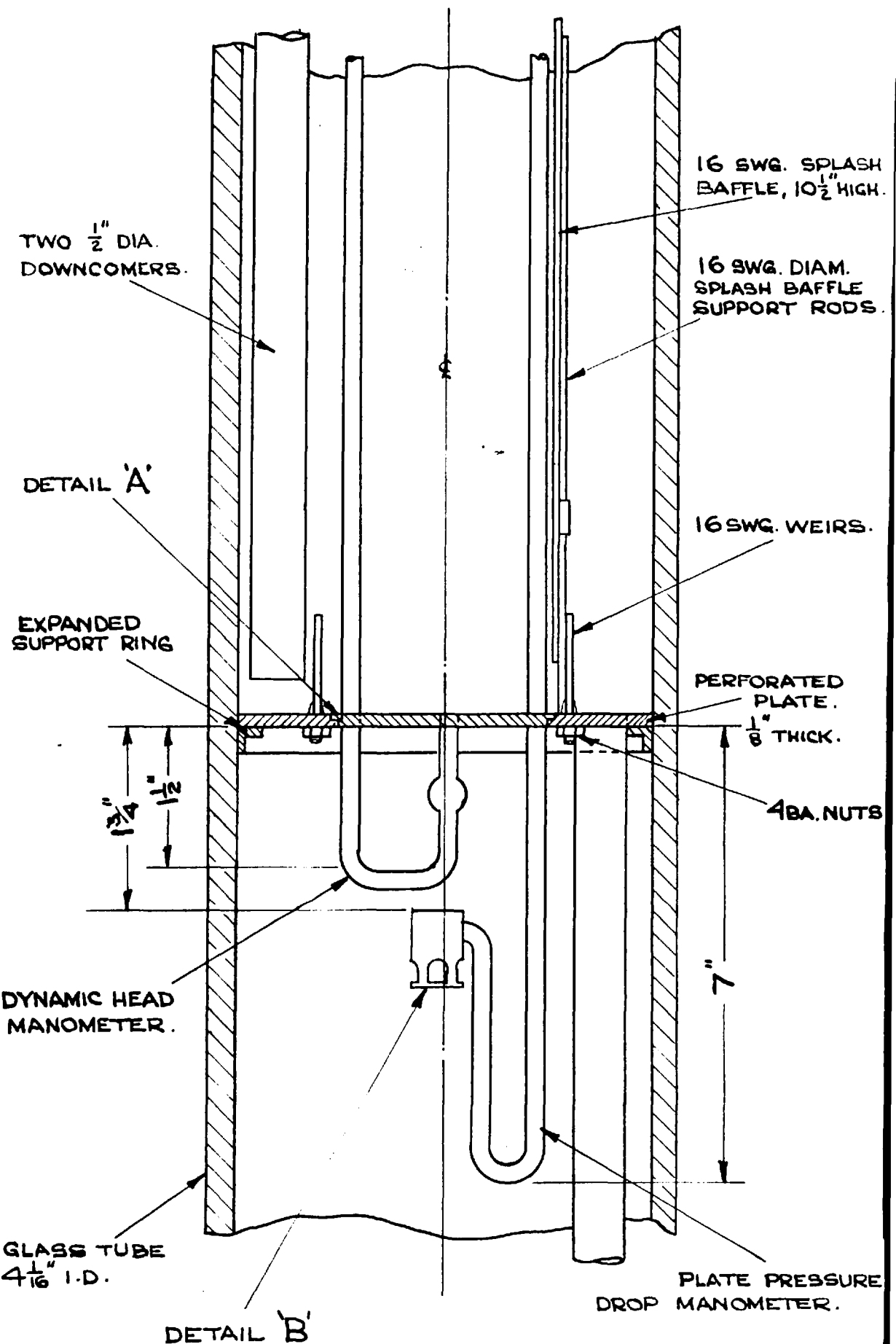


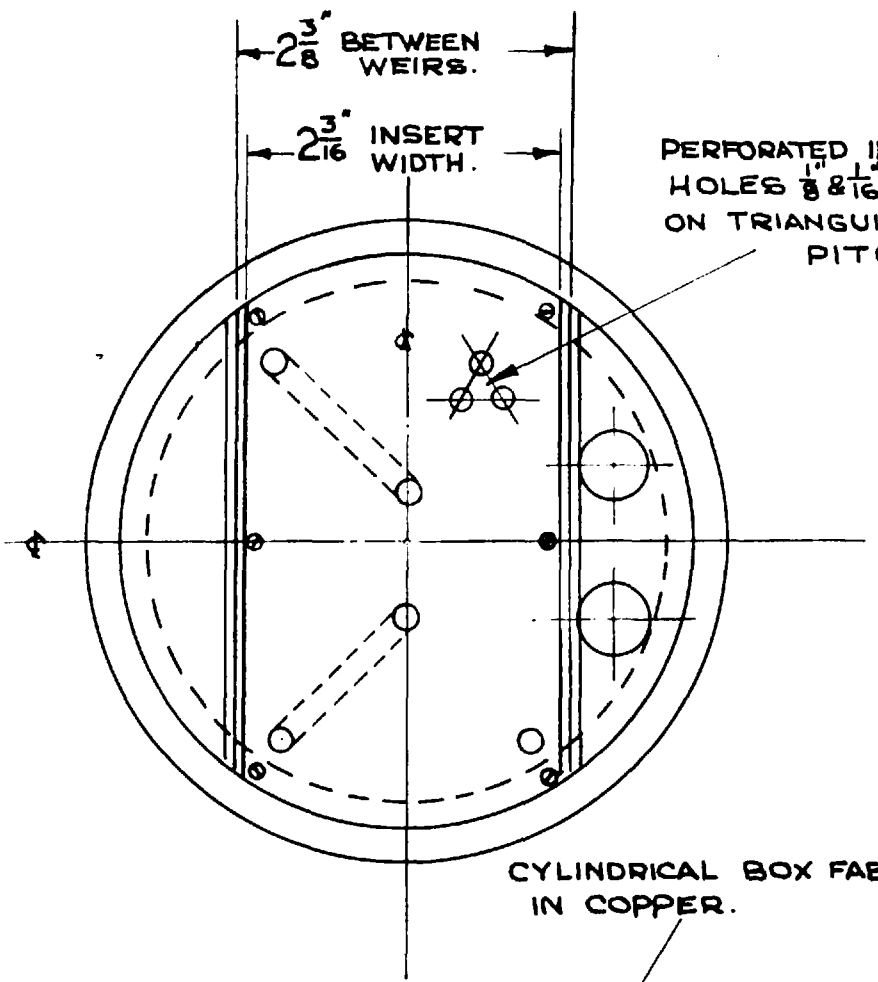
FH. 12.6.62. WPM/3.

FIG. 3. LINE DIAGRAM of 4" DISTILLATION COLUMN.

of PTFE tape between the expanding ring and the column walls. The test plate contains a removeable perforated section that allows changes of hole size and pitch to be made and the chord weirs are also interchangeable. Details of the plate assembly are given in Figure 4.

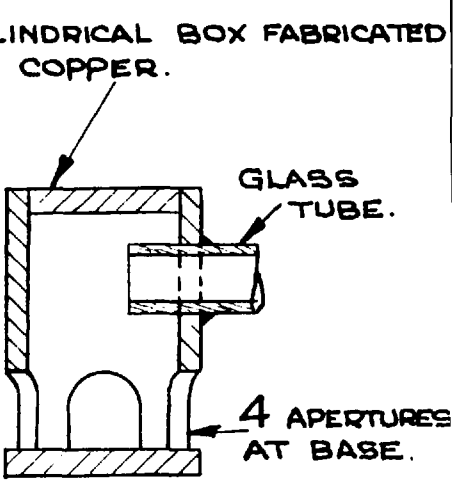
Two, 1/8" bore glass manometers used in the estimation of the dynamic head of the dispersion are sealed with Araldite to the plate. One leg of each manometer is flush with the plate and the other projects into the vapour space above it, a capacity bulb and capillary section being incorporated to damp out fluctuations. Total and dry plate pressure drops are measured by an internal U-tube manometer connecting the vapour spaces above and below the plate, using the plate liquid as the manometric fluid. To simulate conditions at the centre of a larger distillation plate, a splash baffle is fitted at the outlet weir. This is a full width underflow baffle that projects well into the vapour space above the plate, allows the dispersion to build up against it and ensures that only clear liquid flows over the weir. Liquid flow around the weirs and splash baffle is prevented by asbestos paper sealing at the column walls. A central baffle at right angles to the weirs is fitted in order that oscillations set up at right angles to the direction of liquid flow may be damped out. Again this is necessary in order that the operation of a large column may be simulated there being evidence to show that such oscillations do not occur in large columns.







DETAIL A
JOINT SEAL of PERFORATED INSERT.



DETAIL B
ENTRAINMENT TRAP.

FIG. 4.
PLATE ASSEMBLY DETAILS.

The boil up rate is controlled by a combination of switches and a Variac controlling three, 2.7 Kw Tubalox immersion heaters. The immersion heater was originally supplied as a three phase, 8.1 Kw unit with three heating elements delta connected but has been modified to operate as three single phase heaters. In this way, only one heater element need be controlled by a Variac, the others being switched in or out as required. The column vapour rate at total reflux is obtained from the rotameter reading in the reflux line, operation at any desired reflux ratio being obtained by passing liquid to the reboiler through valve V_1. The reflux piping is also designed to allow measurement of dry plate pressure drops. The rotameter is still used to measure column vapour rate with liquid return to the reboiler via valve V_2 instead of flowing back to the column through valve V_3. Reflux piping is of $\frac{1}{2}$" copper tubing using Instantor type couplings, Klinger piston type valves being used. Constant reflux rate is obtained by provision of a $3\frac{1}{2}$" diameter reflux drum at the condenser discharge, a large bore connection allows entrained vapour and non condensables to be vented back to the condenser.

3/8" brass spacer rings placed between the Q.V.F. sections allow thermocouple probes and vapour and liquid sampling probes to be inserted into the test section, the positioning of the probes being shown on the line diagram. Copper-constantan thermocouples are provided for temperature measurement using a conventional Potentiometer circuit.

3.3. Gamma Ray Traverse System and Ancillary Counting Equipment.

The complete traverse system is shown in Figure 5. Its main components are two, 1" diameter steel guide rods, a cross piece fabricated from $\frac{1}{2}$" thick light alloy sheet to which the scintillation counter shield and the source container are bolted, and two base legs made from $1\frac{1}{4}$" x 1/8" mild steel Tee sections. The cross piece is raised or lowered by the screw action of the feed rod, threaded 5/8" BSF with 26 TPI, and can be levelled by the three levelling screws in the base. The traverse system is of such dimensions that it can be used with columns up to 6" diameter and can traverse over a vertical distance of 18".

The lead shielding for the one millicurie Cs 137 source, details of which are shown in Figure 6, is in the form of a $3\frac{3}{4}$" diameter lead cylinder with a protective outer shell of brass of 1/8" wall thickness. This was fabricated by blocking off one end of a 4" O.D. brass tube section and pouring in molten lead using a central, suitably shaped brass tube to act both as a $\frac{1}{4}$" collimation tube and as a holder of the source pellet. The assembly is completed by a brass, screwed end plug to enclose the source, whilst for safety in storage and transit, a $\frac{1}{4}$" lead plug is provided to block off the collimation hole. The Cs 137 source, type CDCM1 from the Radiochemicals Centre, Amersham, is in the form of a 10 mm. diameter monel cylinder and sits in the centre of the lead castle with a minimum of 1 7/8" of shielding around it. This

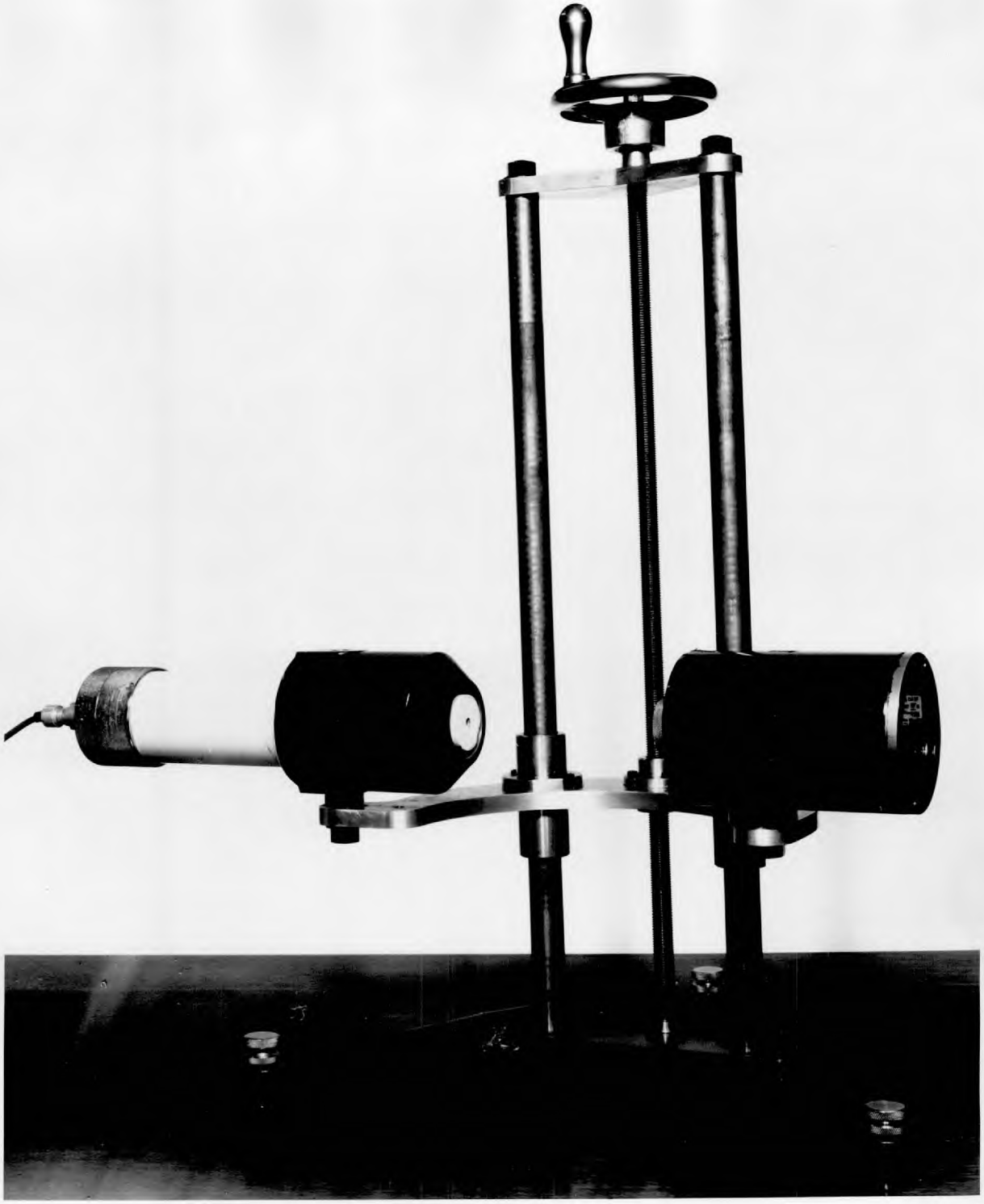


Figure 5 Gamma Ray Traverse System

thickness of shielding is sufficient to bring the dose rate well below the figure of 2.5 m rads per hour at 5 cms stipulated by the Imperial College Code of Practice against Radiation Hazards.

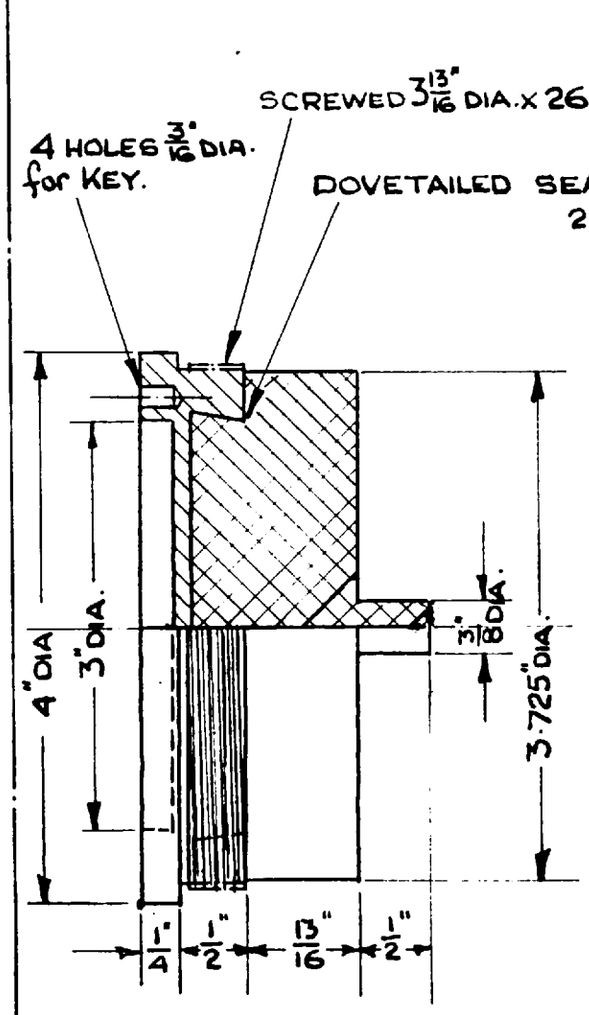
The essential requirement for the traverse system, if consistent results are to be obtained, is that the collimation holes of the source and counter are always in the same position relative to each other. Before the Cs 137 pellet was loaded, the source and counter collimators were lined up by passing a piece of $\frac{1}{4}$" steel rod through each collimation hole. The bosses of both source and counter shields were dowelled and matching holes drilled in the cross piece so that they must always be perfectly aligned. Suitable holes in the traverse support table ensure that the traverse system is always in the same position relative to the column.

It is apparent from the order of counting times likely to be encountered, approximately 500 per second, that a scintillation counter must be used, the Geiger-Muller tube not being effective at such high count rates. A Labgear Type D4133 Directional Scintillation Counter with an external shield and $2\frac{1}{4}$" long collimating block drilled with a $\frac{1}{4}$" hole was available. Photons emitted by gamma ray excitation of a thulium activated sodium iodide crystals are fed to the photo cathode of an eleven stage, inbuilt photo multiplier tube operating at 850 volts from the EHT supply.

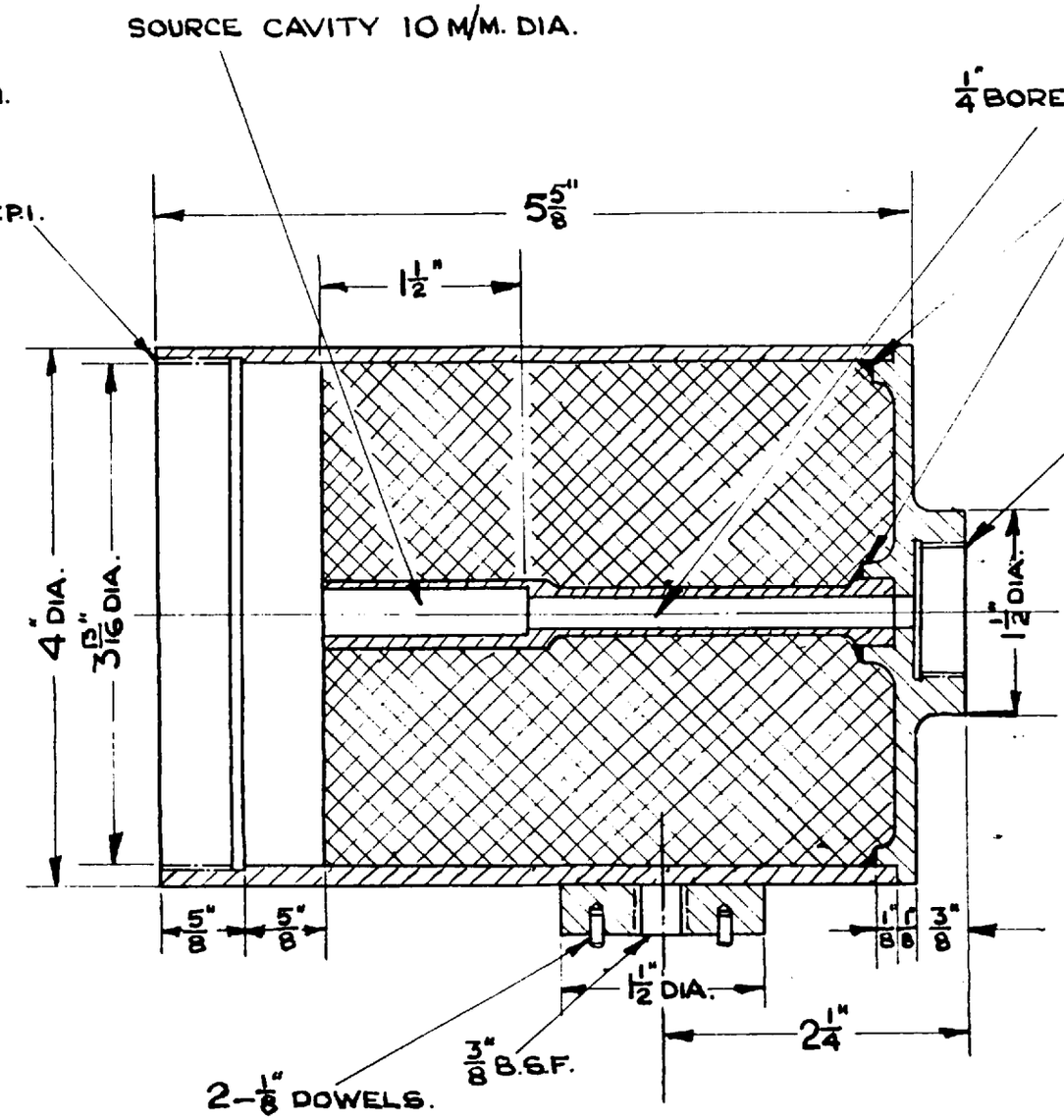
To achieve the greatest accuracy in gamma ray counting, the EHT supply to the scintillation counter must be very stable.

The photo multiplier tube in the counter has eleven stages so that the overall gain may vary with the eleventh power of the applied voltage. Of the commercially available EHT units, the Dynatron Type N103 Power Unit yields the most stable output. It is of the HF oscillator type with feedback amplification and for a ±10% mains variation, the variation in output is only ±0.05%. The presence of ripple and spurious pulses are reduced to such a level that a discriminator need not be used. Linear amplification of the pulses received from the photo multiplier tube is achieved with a Dynatron 1008 amplifier and these are fed directly to a Phillips GM4810 Electronic Counter. This counter has no inbuilt timing device so count times have to be determined manually using a stopwatch, a possible source of error in the method.

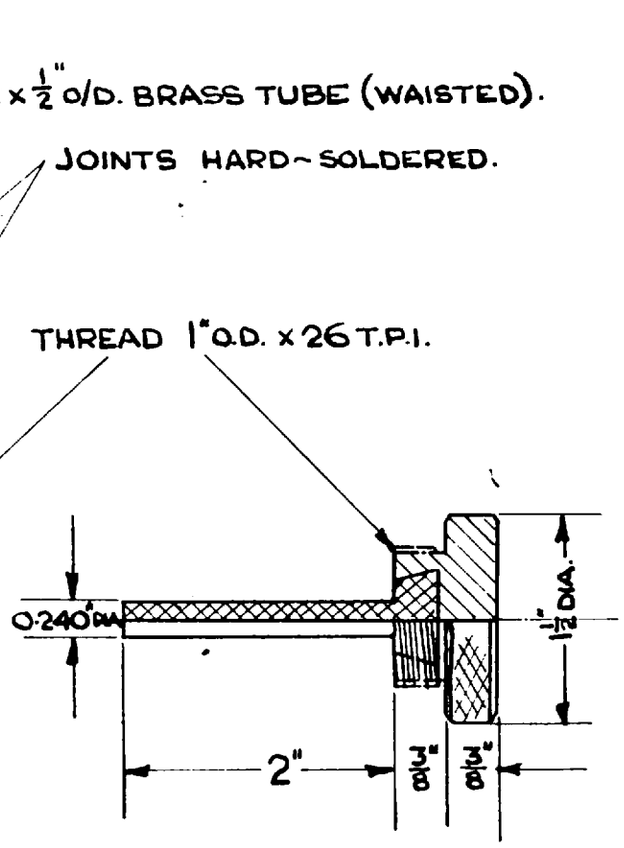
FIG. 6. LEAD SHIELDING for 1 MILLICURIE Cs.137. SOURCE.



END CAP for BODY.



BODY.



BLANKING PLUG for COLLIMATING HOLE.

BRASS SHOWN THUS:-

LEAD

SCALE:- 3/4 FULL SIZE.

15/5/62.
WPM/6.

4. Experimental Programme.

The traverse system was located in its fixed position relative to the column with the beam of gamma radiation passing along the column centre line. A downward traverse near the plate located zero traverse height as the point at which there was a significant increase in count rate through the empty column, this being the point at which the bottom of the collimated beam was at plate level. Heights above this datum were measured by a cathetometer sighted on the traverse cross piece. The count rate, the time in seconds taken to record 50,000 counts was determined for the condition of the column empty and when filled with liquid at several heights above the plate. With the column empty, the mean count rate was 98 seconds with an average deviation of 0.3% whilst for the column filled with liquid, a mean of 175.8 seconds was found, the average deviation being 0.5%. The straight line calibration curve shown in Figure 7 was then constructed on semi logarithmic paper through the points (t = 98 secs, $\rho = 0$) and (t = 175.8 secs, $\rho = 1$).

The selected perforated insert and weirs were fitted into the test plate ensuring that there were good seals between both the weirs and splash baffle and the column walls and that the plate was level. The boil up rate was adjusted to the desired value and the reflux rate regulated to maintain a constant level in the reflux drum. At constant reflux drum level, the boil up rate at total reflux was obtained directly from the reflux

rotameter reading and at partial reflux the liquid return to the column was similarly obtained. The column came to hydrodynamic equilibrium fairly quickly. Equilibrium was taken to have been reached when the reflux drum level, rotameter and manometer readings were steady. There were occasional fluctuations in the mains voltage so that regulation of the boil up rate was necessary to maintain constant hydrodynamic conditions.

As previously discussed, the traverse system was zeroed at plate level and a vertical traverse made in the dispersion. Readings were taken at 0.5 to 1 cm. intervals in the regions of greatest change in the profile shape and at 2.3 cm. intervals in the constant density region. The profiles were plotted as volume fraction liquid in the dispersion against height above the plate, the area under the curve, determined using a planimeter, was evaluated as the static head of liquid on the plate. Simultaneous with the determination of the dispersion density profiles, the dynamic head and total plate pressure drops were measured. Dry plate pressure drops were determined in a separate series of runs with the downcomers blocked and the column traced with hot water to prevent undue condensation on the plate.

Dispersion density profiles and other plate hydraulic data for the 80% normal - 20% iso pentane mixture were obtained for the range of perating and design variables given below.

(1) Hole sizes 1/16" and 1/8" diameter.

(2) Hole pitch/hole diameter ratios of 2 and 3 (23 and 10% free area respectively)

(3) Weir heights of 2, 3 and 4 cms.

(4) Column F factors from 0.4 to 1.1 corresponding to superficial vapour velocities of 0.9 and 2.4 feet per second.

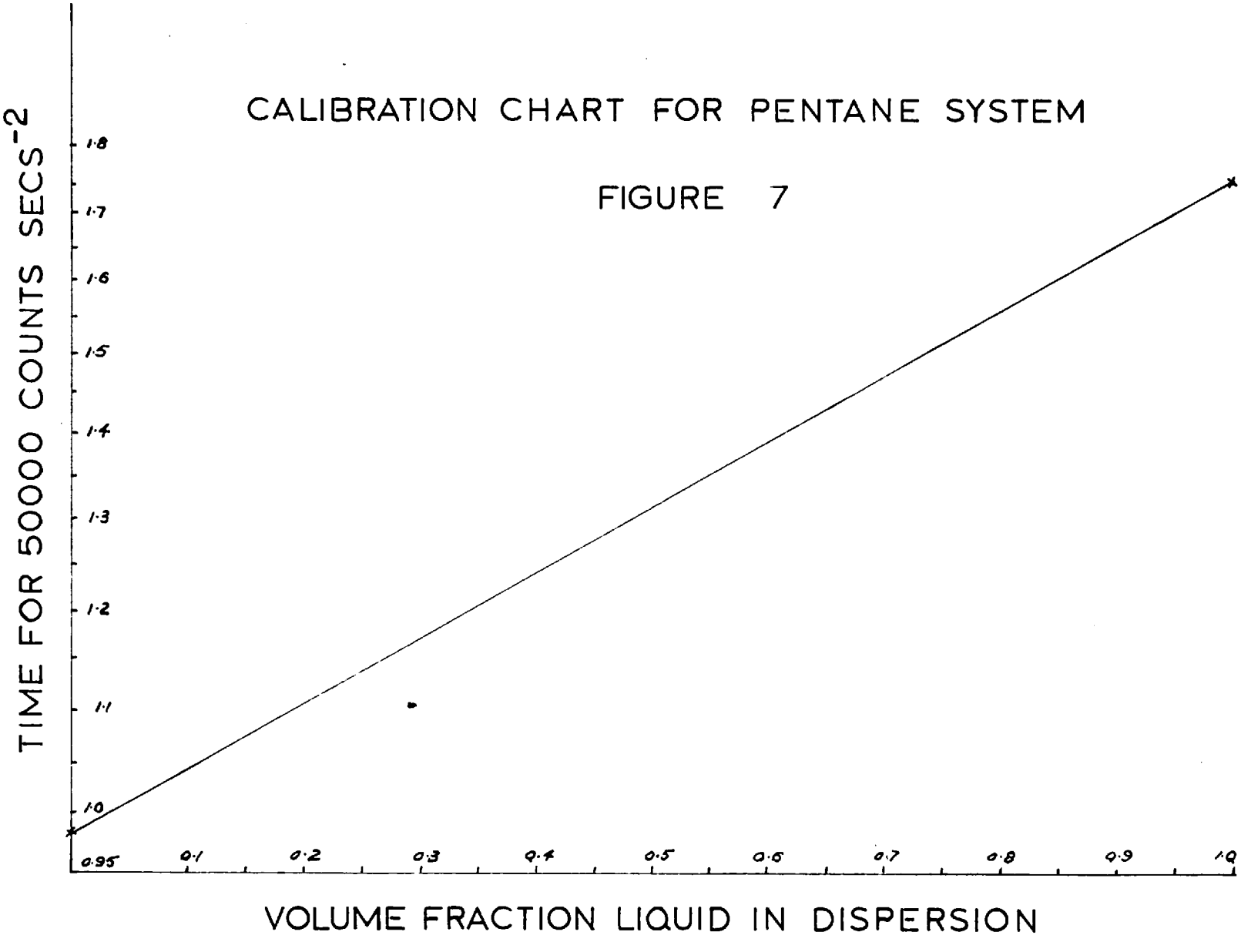
The perforated plates used had the following characteristics:

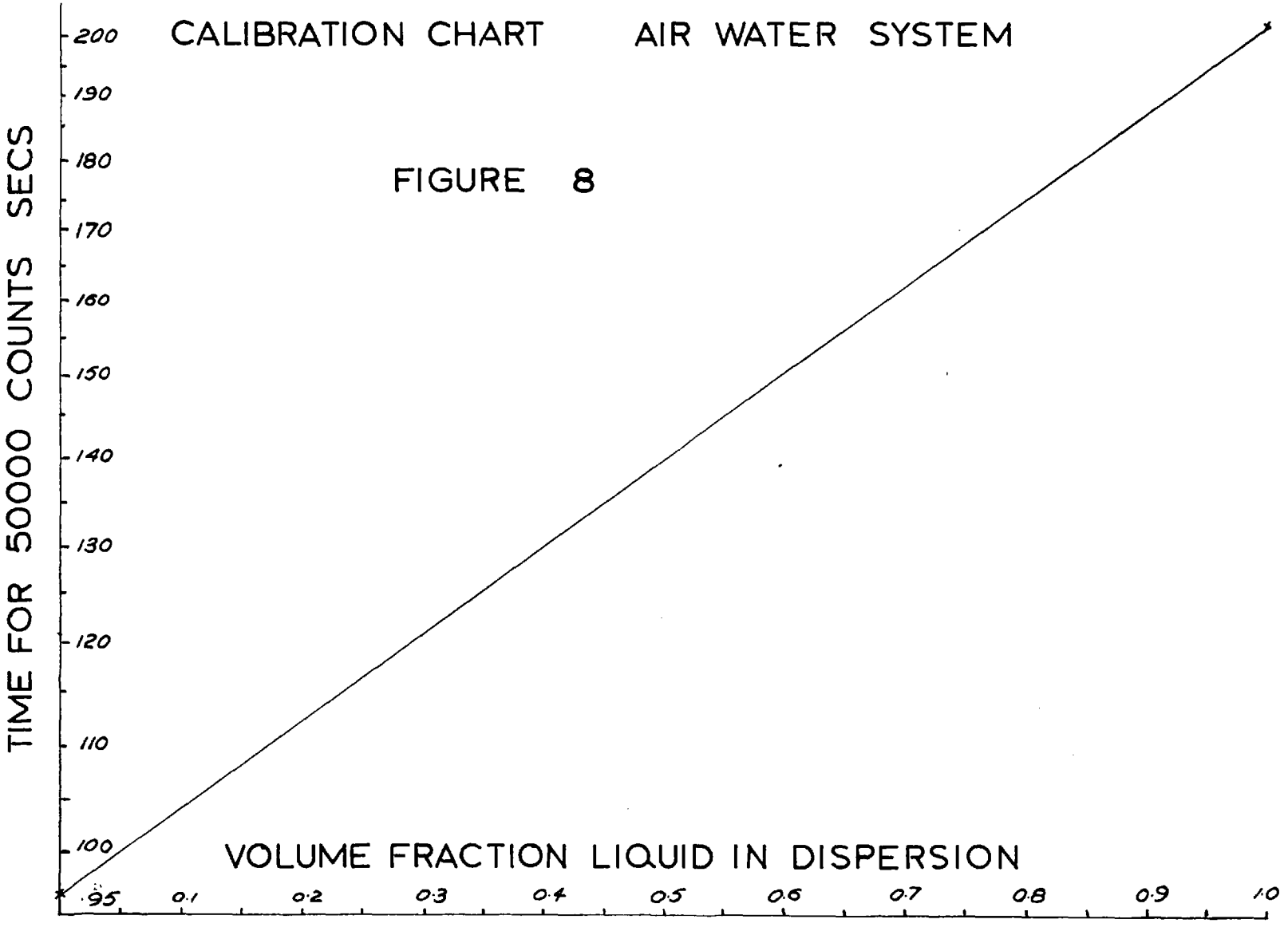
Insert No.	Hole Size	Triangular Pitch	No. of Holes	% Free Area
	ins.	ins.		
1	1/16	1/8	303	23
2	1/16	3/16	151	10
3	1/8	1/4	76	23
4	1/8	3/8	38	10

The plate thickness was constant at 3/32" for all inserts whilst the free area of the plates was calculated from the hole size and pitch relationship.

Evaluation of pressure probe traverses as a measure of dispersion density profiles was performed in the 4" air-water simulator. Even using pre-saturated air, some entrainment and evaporation losses occurred during the time taken to complete the static pressure and simultaneous gamma ray traverses. Calibration of the rig showed losses of approximately 1 ml/minute and constant liquid hold-up on the plate was achieved by appropriate additions at one minute intervals. The column air rate was set at the predetermined level and a known amount of liquid distributed over the plate. Drainage of the plate at the end of the run gave the actual liquid hold-up and acted as a check on its constancy over the run. The variation of dynamic pressure in the dispersion was determined directly from the probe manometer reading, correcting

for capillarity effects and was compared with the static pressure profile obtained by integration of the density profile curve. Pressure profiles were obtained at column air rates of 1.5 and 2.9 feet per second for liquid hold ups corresponding to static heads of 4 and 8 cms of water. The air distributor plate used was a 1/16" brass plate with 514, 1/25" perforations on 1/8" pitch, the free area being 5%.


CALIBRATION CHART FOR PENTANE SYSTEM
FIGURE 7
TIME FOR 50000 COUNTS SECS^{-2}
1·8
1·7
1·6
1·5
1·4
1·3
1·2
1·1
1·0
0·95
0·1
0·2
0·3
0·4
0·5
0·6
0·7
0·8
0·9
1·0
VOLUME FRACTION LIQUID IN DISPERSION


CALIBRATION CHART AIR WATER SYSTEM
FIGURE 8
TIME FOR 50000 COUNTS SECS
200
190
180
170
160
150
140
130
120
110
100
VOLUME FRACTION LIQUID IN DISPERSION
·95
0·1
0·2
0·3
0·4
0·5
0·6
0·7
0·8
0·9
1·0

EXPERIMENTAL RESULTS

5.1 Validity of the Radio Isotope Density Measuring Technique

The conditions necessary for the gamma ray absorption technique to yield true values of dispersion density have been discussed in Section 2.4. A preliminary check on the reliability of the counting equipment was made by comparing the actual liquid path length, the column internal diameter, with that calculated from the relationship

$$\ln t = \ln t_0 + \mu \rho D)$$

For the calibration points ($t_0 = 96.5$ secs, $\rho = 0$) and ($t = 203$ secs, $\rho = 1$) and a value of μ, the mass absorption coefficient of water of 0.085 $cms^2/gram$, the calculated path length is 8.72 cms, The column internal diameter is 8.7 cms, the measurements checking to 2.3%. It can be inferred from this that the collimation system has minimised scattering errors and that the electronic counting equipment is reliable. Thus any error in the measurements of vapour-liquid dispersion densities can only be due to time fluctuations in the density.

The error due to these fluctuations for the range of variables studied in the 4" distillation column was evaluated using the 4" air-water column simulator. This apparatus allowed dispersions of known liquid hold ups to be produced, the hold up being measured by draining the plate, and comparison made with the result obtained by integration of the experimentally measured density profile.

Detailed experimental data are given in Appendix A as runs A1, A2, A3 and A4, the pertinent results being given in Table 1.

TABLE 1

Run	Column Air Velocity ft/sec	Liquid Holdup by Draining Plate	Liquid Holdup Calc. from Density Profile	% Error
A1	1.2	125 mls	118 mls	-5.6%
A2	1.0	450 mls	430 mls	-4.6%
A3	2.9	200 mls	192 mls	-4.0%
A4	2.5	500 mls	490 mls	-2.0%

Over the range of vapour rates and liquid hold ups studied, the maximum deviation of the time average dispersion density from the true value is -5.6% demonstrating the reliability of the technique. Another independent check comes from the information gathered on the performance of dynamic head manometers as a means of estimation of plate hold up. Typical experimental data are plotted in Figure 9 showing a comparison of the static head, calculated from the density profiles, with the actual dynamic head manometer readings. As discussed more fully at a later stage, the divergence of the curves at higher vapour rates is considered to be due to kinetic effects associated with the bubble streams rising from the adjacent plate orifices. At low hole velocities this effect is at a minimum and the manometers are fairly accurate indicators of the liquid hold up, the co-incidence of the curves at these low vapour rates providing an additional pointer to the validity of the experimentally determined density profiles .

5.2 Evaluation of Pressure Probe Measurements for Liquid Hold Up Determination

The veracity of liquid hold up data predicted by measurements of hydrostatic pressure within the dispersion has been questioned in Section 2.3.2 and the experimental program was designed to test the validity of measurements of this type by comparison with static heads determined by the gamma ray absorption technique.

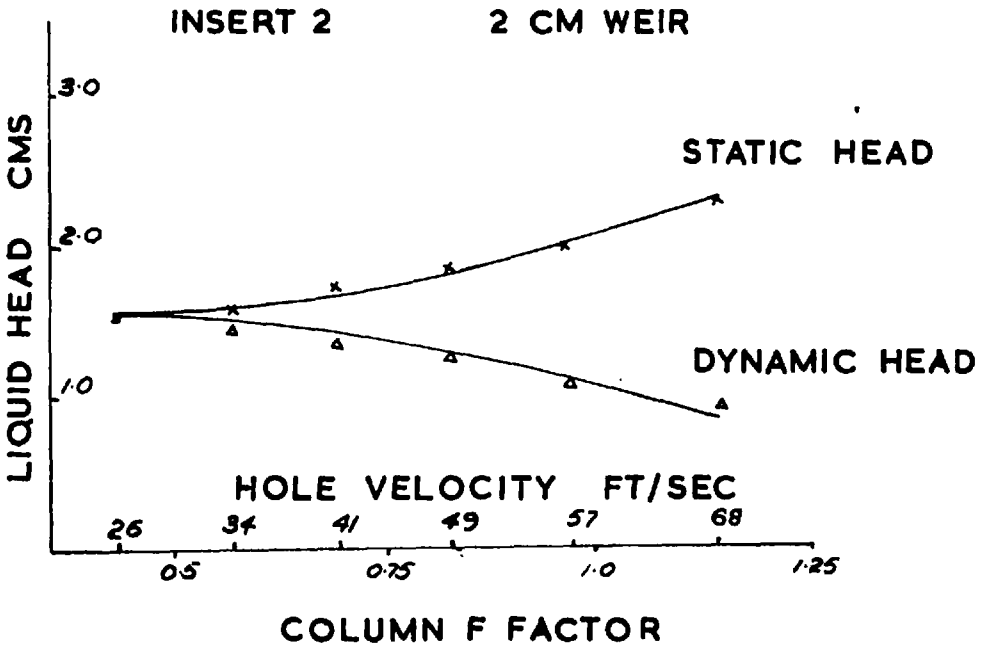
5.2.1 Plate Manometer Measurements

Figure 9 shows typical variation of the static head, due to the liquid hold up in the dispersion, and the plate manometer reading, the dynamic head, as a function of hole vapour velocity. At low hole velocities, the static and dynamic head curves co-incide, but with increasing hole velocity the curves diverge, the plate manometer reading being less than the static head of liquid above it. Both the hole velocity at which the divergence commences and the magnitude of the divergence of the two curves depend on the % free area of the plate.

As can be seen from Figure 10, a plot of $\log (h_s - h_d)$ against $\log(\rho v_h^2)$, two distinct curves are obtained for the two different % free area plates used. The divergence between static and dynamic heads is substantially independent of hole size and weir height and is determined only by the hole velocity and the hole diameter/hole pitch ratio. Both these lines have a slope of unity so that the divergence appears to be a purely kinetic effect associated with the vapour flow through the plate holes. On this basis one would

FIGURE 9

EFFECT OF HOLE VELOCITY ON DIVERGENCE OF STATIC HEAD FROM DYNAMIC HEAD



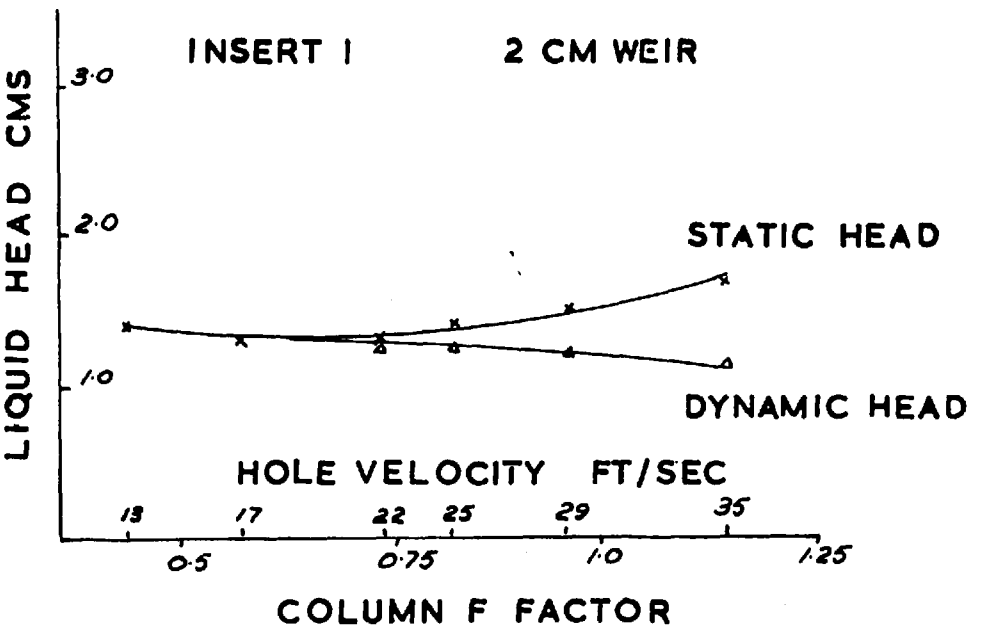
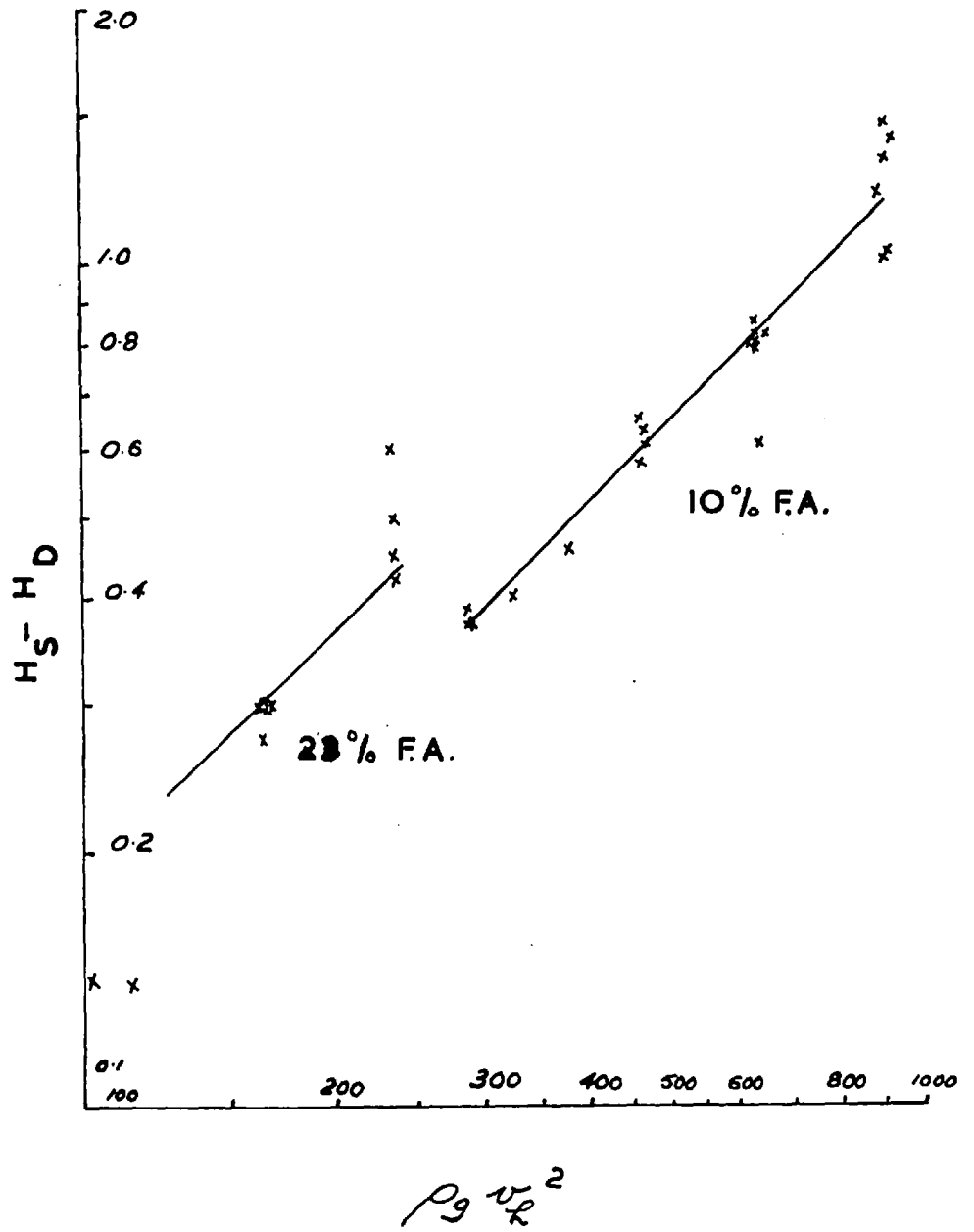


FIGURE 10

VARIATION OF $H_S - H_D$ WITH $\rho_G V_H^2$



expect an effect of hole pitch as the closer the holes to the manometer, the greater the effect at a given hole velocity and the lower the hole velocity at which the static and dynamic heads start to diverge.

The induction zone surrounding a jet is a well known phenomenon (58) and Alexander et al (/) measured the static pressure in the induced stream surrounding a confined jet. The results showed that the static pressure is a minimum in the plane of the orifice and requires a finite distance downstream of the orifice to rise to a steady value. By analogy with this confined jet, a rapidly moving bubble stream could be assumed to cause a similar effect. Due to frictional and inertial resistance between the bubble stream and the surrounding liquid, there is a momentum transfer between the rising bubbles and the liquid surrounding the bubble stream. A vertical velocity component is induced in the liquid and the resulting buoyancy force acts to reduce the static pressure in the vicinity of the bubble stream below that due to the liquid hold up in the dispersion. The magnitude of this effect is dependent on the hole vapour velocity. At low hole velocities the effect is small and cannot be detected experimentally, but with increasing vapour rate, the hydrostatic pressure in the "induction zone" decreases continuously, resulting in decreasing plate manometer readings even though the liquid hold up may be actually increasing. The hydrostatic pressure readings on the induction zone of a jet increases with radial distance from the jet boundary. The closer the first circle of holes are to the plate manometer, the greater

will be the kinetic effect at a given hole velocity and the lower the hole velocity at which the divergence becomes apparent. Early experimental results on the air-water system showed that blocking off the first circle of holes around the manometer results in a positive shift in the dynamic head curves. Fairly small bore tubes are generally used for plate manometers so as to minimise disturbances of the vapour flow and capillarity correction must be made to determine the true dynamic head. For the pentane system studied the capillarity correction was of the order of 0.3 cms. The use of published dynamic head values in any correction should be made with some caution as one can never be certain that such corrections have been made.

It can be seen that plate manometer readings are unreliable as a measure of the liquid hold up on sieve plates. The dynamic heads so measured are not the static heads due to the liquid hold up in the dispersion differing from them by an amount dependent on column operating and design variables and on the details of the manometer installation. Because of this correlations of plate efficiency data based on dynamic head and dispersion height measurements should be viewed with some caution. Unless a low hole velocity is used or the plate has a low % free area, the dynamic head is not a true measure of the liquid hold up. Only with a fixed column geometry and a fixed hole velocity can plate performance be characterised using these dynamic head measurements as for example in the work of Planck (60) who successfully correlated efficiencies in liquid phase controlling systems using the term ($h_d/h_f - h_d$).

5.2.2 Pressure Probe Traverse Measurements

Several workers (24) have attempted to determine the liquid hold up on an operating plate by integration of a dispersion density profile based on a vertical pressure probe traverse in the dispersion. Such a method would be valid if the pressure probe reading accurately determined the variation of static head due to the liquid hold up with height in the dispersion. In the induction zone near to the plate the probe readings would be expected to be less than the true static head due to the effects discussed in Section 5.2.1. The curves of hydrostatic pressure (i.e. the pressure probe readings) and the true static head due to the liquid hold up would be expected to converge with increasing height above the plate as the induction effect falls off and the individual jets lose their identity in the turbulent region developing above the plate.

From an application of the Navier Stokes Equation to a two phase, fully developed turbulent flow it can be shown that

$$\bar{p} + \rho_L \left\{ \left(\overline{u_x'^2} \right) - \left(\overline{u_x'^2} \right)_f \right\} = g \left\{ h_s - (h_s)_f \right\}$$

where $\bar{p}$ = mean hydrostatic pressure at a point x above the plate

$\overline{u_x'}$ = mean value of the turbulent fluctuating velocity component at the point x.

$\left(\overline{u_x'}\right)_f$ = mean value of the turbulent fluctuating velocity component at the top of the dispersion.

h_s = true static pressure due to the liquid in the dispersion at the point x.

$(h_s)_f$ = true static pressure due to the liquid in the dispersion at the top of the dispersion.

ρ_L = liquid density

The derivation of this relationship is given in Appendix A.

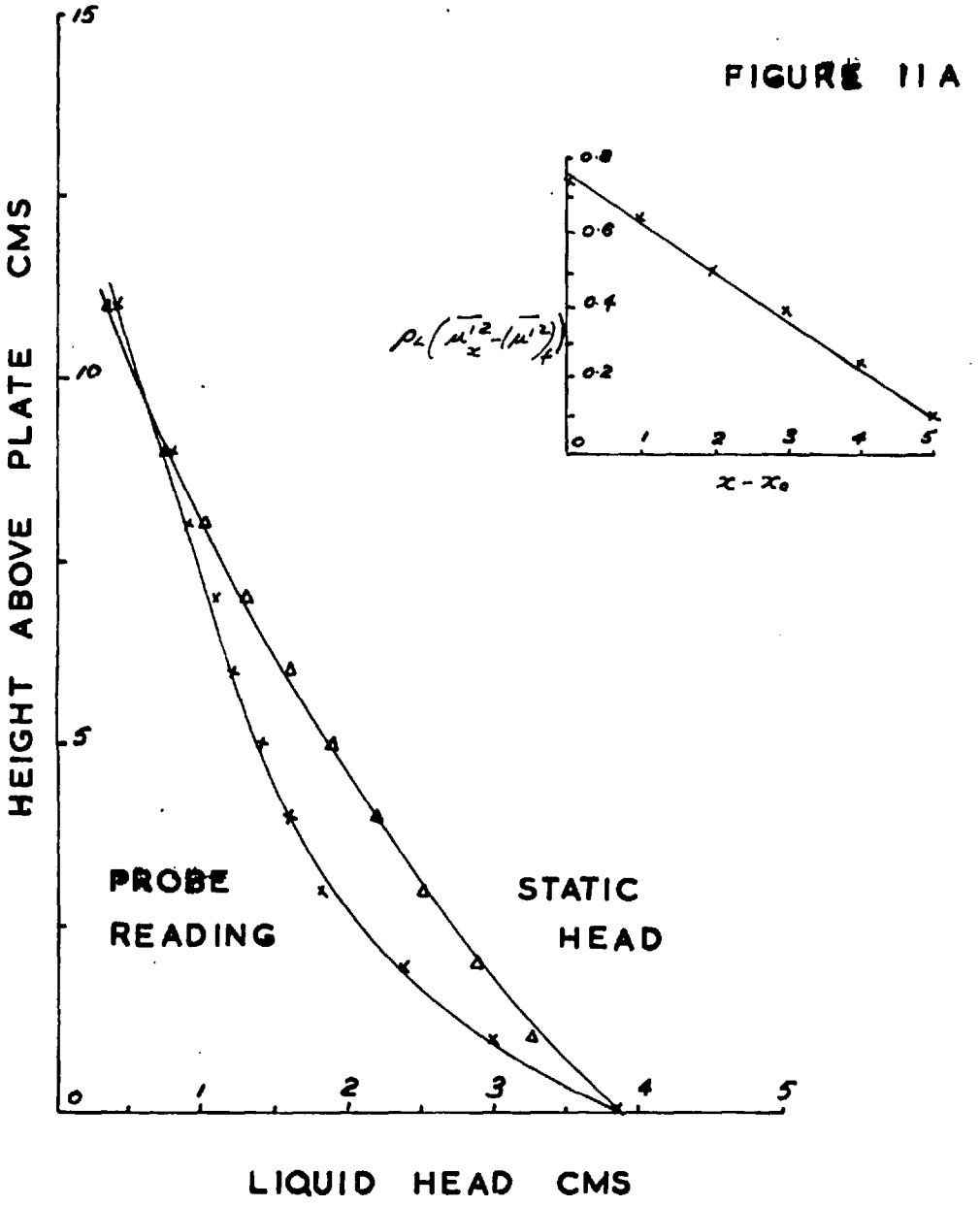
The significance of this result is that the mean hydrostatic pressure, the pressure probe reading, at any point in the dispersion is less than the static head due to the liquid hold up in the dispersion by an amount determined by the difference in the intensity of turbulent fluctuations between the point of measurement and the top of the dispersion.

In order to test the validity of this result, the air-water column simulator shown in Figure 2 was used to compare the pressure probe traverse measurements with the static head profile determined by the gamma ray absorption technique. Results of a typical pressure probe and gamma ray traverse are shown in Figure 11 whilst further data is tabulated in Appendix A as Runs B1, B2 and B3. Data was obtained at hole velocities such that there was negligible effect of the induction zone near the plate as verified by co-incidence of the two curves at plate level. Thus any divergence of the pressure probe reading from the true static head is due solely to the intensity of the turbulent fluctuations at that level above the plate.

At plate level the vapour jets are discreet entities and the probe is sufficiently distant from the jets that the liquid motion immediately around it is unaffected by them. The turbulent

FIGURE 11

COMPARISON OF PRESSURE PROBE READING WITH TRUE STATIC HEAD



fluctuations induced by the jets spread with increasing height above the plate and at a certain level they fill the whole column cross section giving rise to a region of homogeneous turbulence in which there is a continuous decay of the energy containing eddies with height above the plate. In the region between the plate and the level at which the flow pattern becomes one of homogeneous turbulence, that is, in the so-called turbulence generating region, the intensity of the turbulent fluctuations in the neighbourhood of the probe increases with increasing height above the plate. Thus the divergence of the pressure probe readings from the true static pressure increases until a maximum is reached at a level corresponding to the onset of fully developed turbulent flow. For the curves shown, the maximum occurs at a level of 3 cms above the plate, a level that co-incides with the commencement of the constant density region of the dispersion density probe reading.

The maximum deviation of the pressure probe reading from the true static head would be expected to be equivalent to one velocity head based on the value of the hole velocity. For a hole velocity of 40.5 ft/sec, the velocity head is of the order of 1.0 cms of water whereas the maximum deviation has the value of 0.75 cms of water. This energy loss is accounted for by viscous dissipation of energy in the turbulent eddies developing in this zone.

For the case of the turbulence produced downstream of the turbulence producing meshes commonly used in wind tunnels, the decay of the total kinetic energy of the turbulent fluctuations in

the region of fully developed turbulence follows the simple law (6)

$$\mu_x'^{-2} \propto (x - x_o)$$

where x corresponds to the distance above the perforated plate and x_o is an arbitrary distance that may be fixed, in this case, at the level corresponding to the onset of fully developed turbulence. Figure 11(a), a plot of the intensity of the turbulent fluctuations with increasing distance downstream of the plate shows a linear decay law in the fully developed turbulent region rather than the relationship given above. This decay law applies to the turbulence produced by the flow of air or liquid on passing through a mesh and it appears that the turbulence produced downstream of a mesh in a two phase system does not follow the same decay law.

The fact that the pressure probe reading is not the true static head due to the liquid hold up in the dispersion and differs from it by an amount dependent on the intensity of turbulent fluctuations invalidates attempts to measure liquid hold ups using this technique. Kafarov and Vigdorov (45) in a similar set of measurements found a discrepancy between the pressure probe readings and the true static head of liquid and attempted to explain it on the basis of a buoyancy effect caused by a gas-liquid frictional resistance. Their results are also complicated by induction effects near the plate as negative dispersion densities were calculated for this region at high gas rates.

In view of these results, in any situation in which a pressure probe is introduced into a turbulent dispersion account must be taken of the intensity of turbulent fluctuations in the flow in determining the significance of the probe readings. Pressure probe readings appear to be of more value in determining the intensity of the turbulent fluctuations than for the determination of liquid hold up.

6 Liquid Hold up on Sieve Plates

6.1 Dispersion Density Profiles

A typical series of dispersion density profiles is shown in Figure 12. The shape of the profile shows a gradual transition from clear liquid near the plate to a liquid-vapour dispersion of almost constant density above it. The increased kinetic energy of the vapour stream resulting from increased boil up rate, progressively shifts more liquid from near the plate into the dispersion, increasing the extent of the constant density region.

The shape of the profiles is not greatly altered by changes in hole size or weir height as shown in Figures 13 and 14 but decreasing the % free area from 23% to 10% makes the constant density region more pronounced. The profile in such cases, at higher vapour rates, tends to an almost vertical straight line showing no sharp distinction between clear liquid and dispersion. The shape of the profile and hence the liquid hold up is only slightly affected by changes in reflux rate. For the several design variables studied, the effect of reducing the L/V ratio from 1.0 to 0.5 at a constant column F factor of 0.8, is an average decrease in hold up of only 10% as can be seen from Figure 15.

The magnitude of the density in the constant density region is independent of the boil up rate and is characteristic of the plate, being determined by such design factors as hole size, % free area and weir height. By considering the perforated plates used in these studies to be analogous to the turbulence producing grids used in

FIGURE 12 DISPERSION DENSITY PROFILES

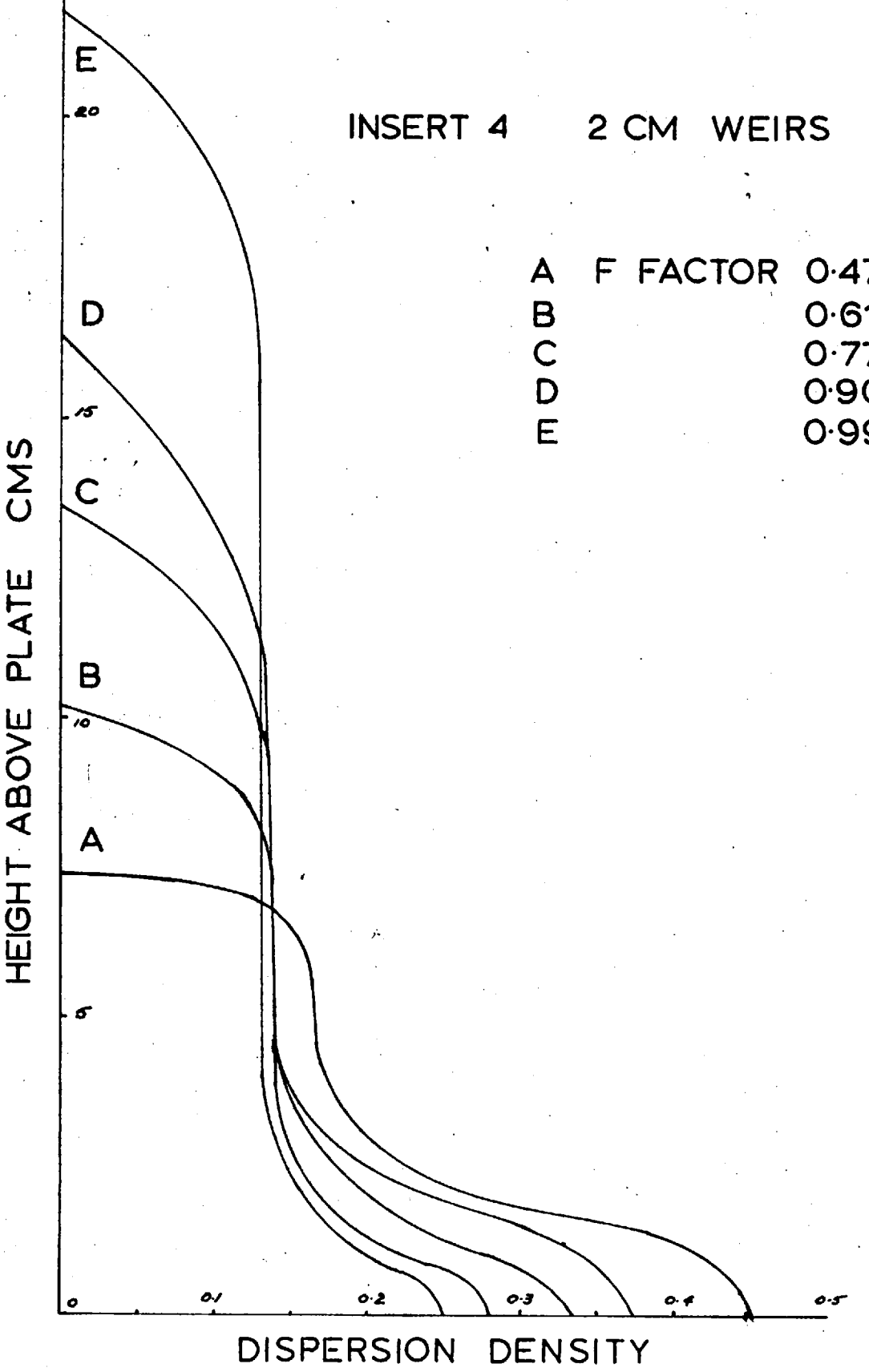


FIGURE 13 EFFECT OF WEIR HEIGHT

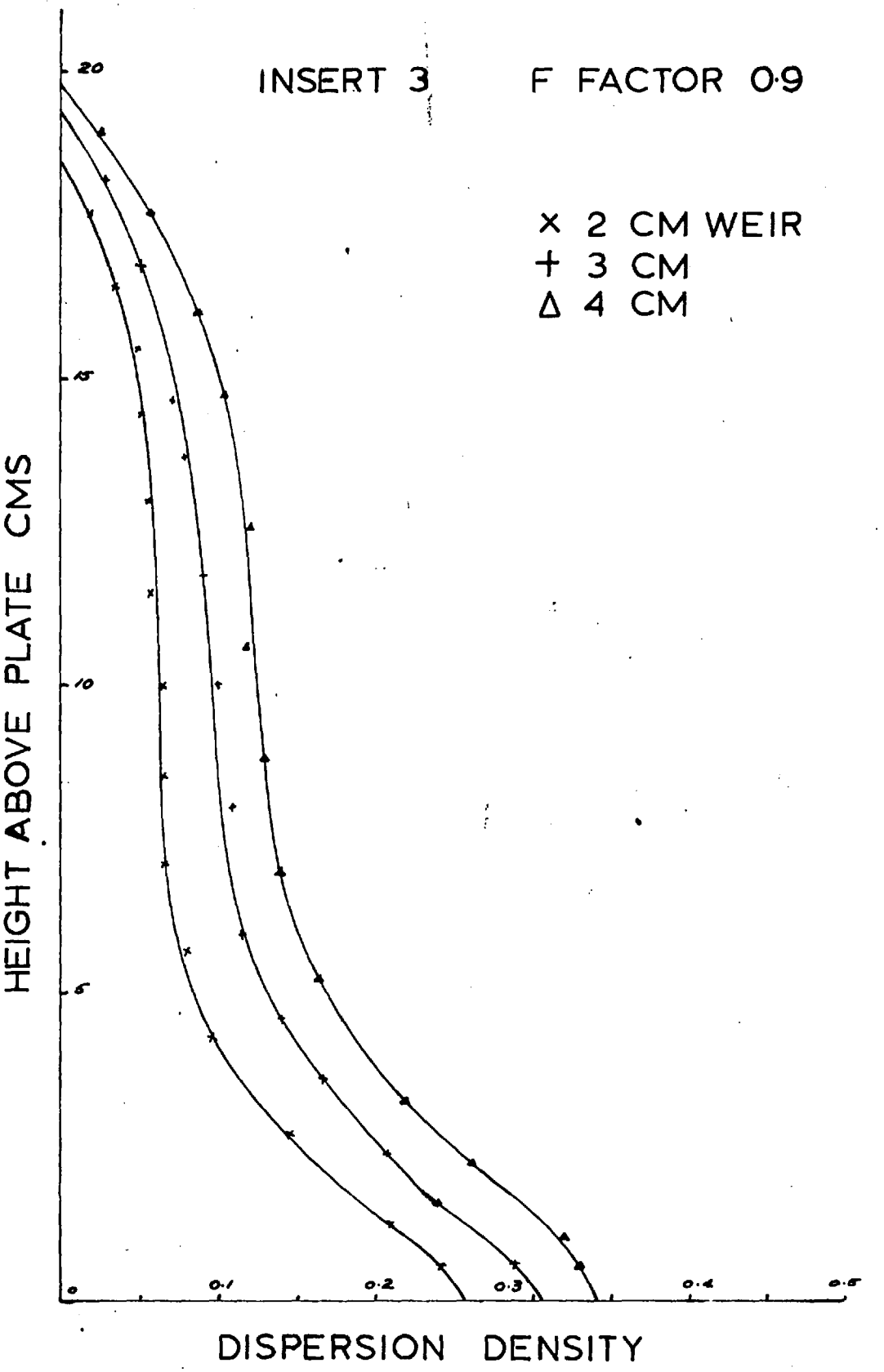


FIGURE 14

EFFECT OF HOLE SIZE AND % FREE AREA

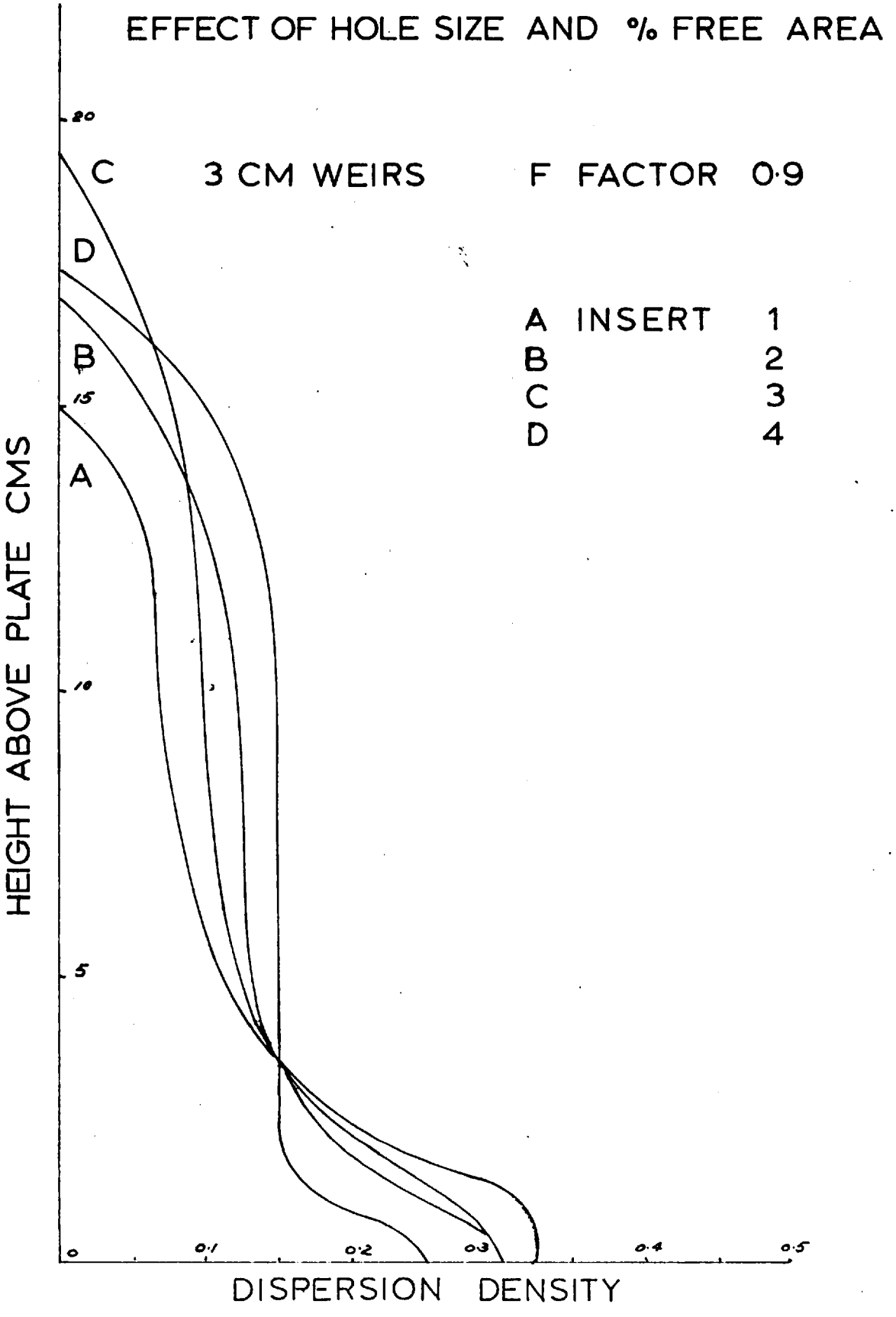
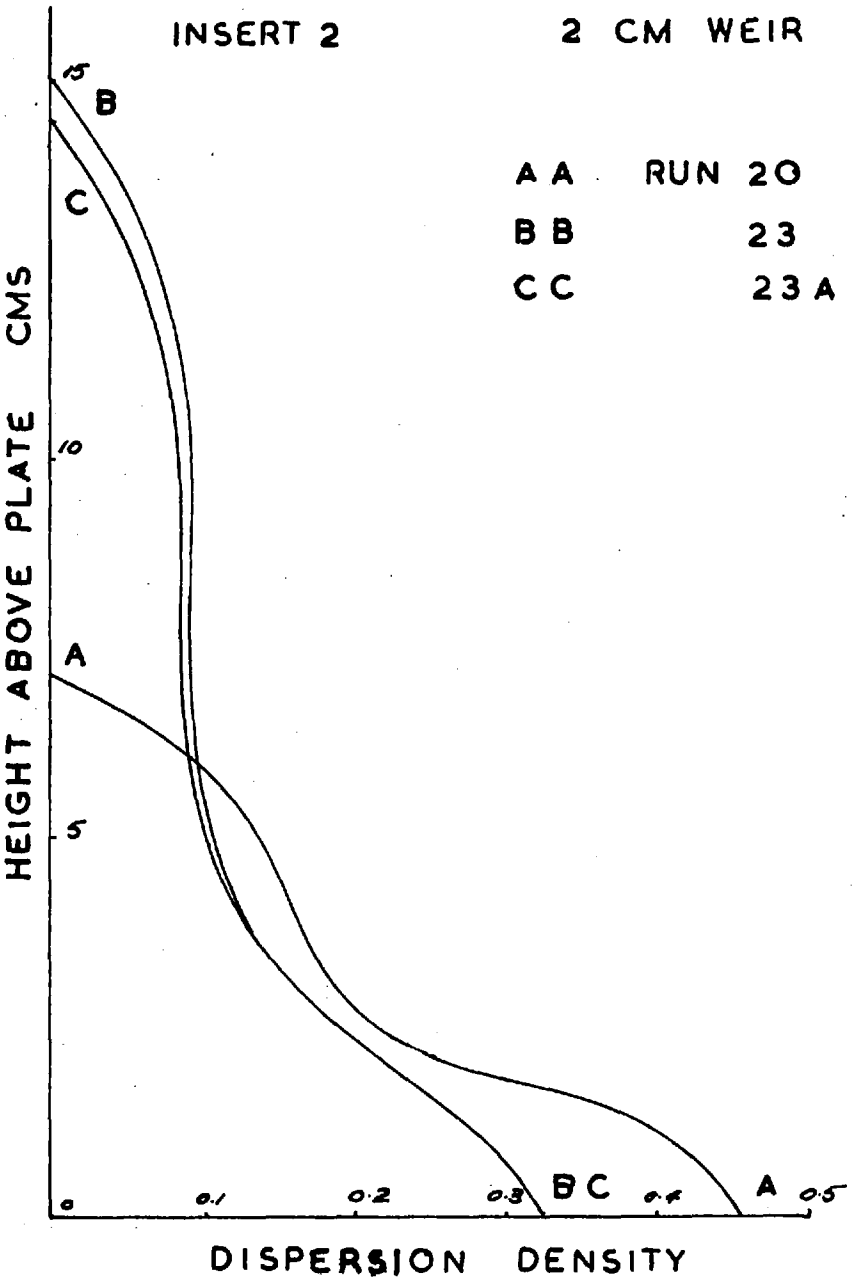


FIGURE 15

EFFECT OF LIQUID RATE



wind tunnels, the constant density region of the profile corresponds to the region of homogeneous turbulence formed behind such grids, Batchelor (6) has shown for the single phase region of homogeneous turbulence produced downstream of these grids, that the turbulence pattern is determined by factors such as the mesh size and the mean velocity of flow through the grid. Application of these results, in a qualitative fashion, to the profile data obtained in this work explains the effect of hole size and % free area, the first corresponds to the size of the mesh openings and the second to the thickness of the grid bars. It also appears reasonable, for the two phase system found in this work, that the weir height would be a factor determining the turbulence level above the plate. In general, at constant F factor in the column, the dispersion density increases with increasing weir heigh and decreasing % free area whilst, other parameters being equal, dispersions formed on plates with $\frac{1}{8}$" holes are more dense than those on similar plates with 1/16" holes. Hence the shape of the dispersion density profile, and thus the liquid hold up on the plate, may be reasonably assumed to result from the attainment of a dynamic equilibrium between the turbulence pattern set up above the plate and the liquid flow onto the plate.

6.2 Variation of Liquid Hold up with Design and Operating Variables

As well as providing data on the variation of point dispersion density with height above the plate determination of an experimental

dispersion density profile allows the calculation of the total liquid hold up on the plate. The variation of the liquid hold up for several design and operating variables at a weir height of 4 cms is shown in Figure 16. The liquid hold up is seen to be relatively constant over most of the range of vapour rates above the weep point and may even decrease slightly, as was the case with the higher % free area plates. At F factors above 0.9, the hold up tends to increase sharply due, possibly, to some effect of the splash baffle causing a retention of liquid on the plate.

Consideration of the experimental data has shown that the hole size, hole velocity and weir height are the design parameters determining the liquid hold up. Typical variation of the liquid hold up for these several design variables at a column F factor of 0.9 is given in Table 2.

Table 2

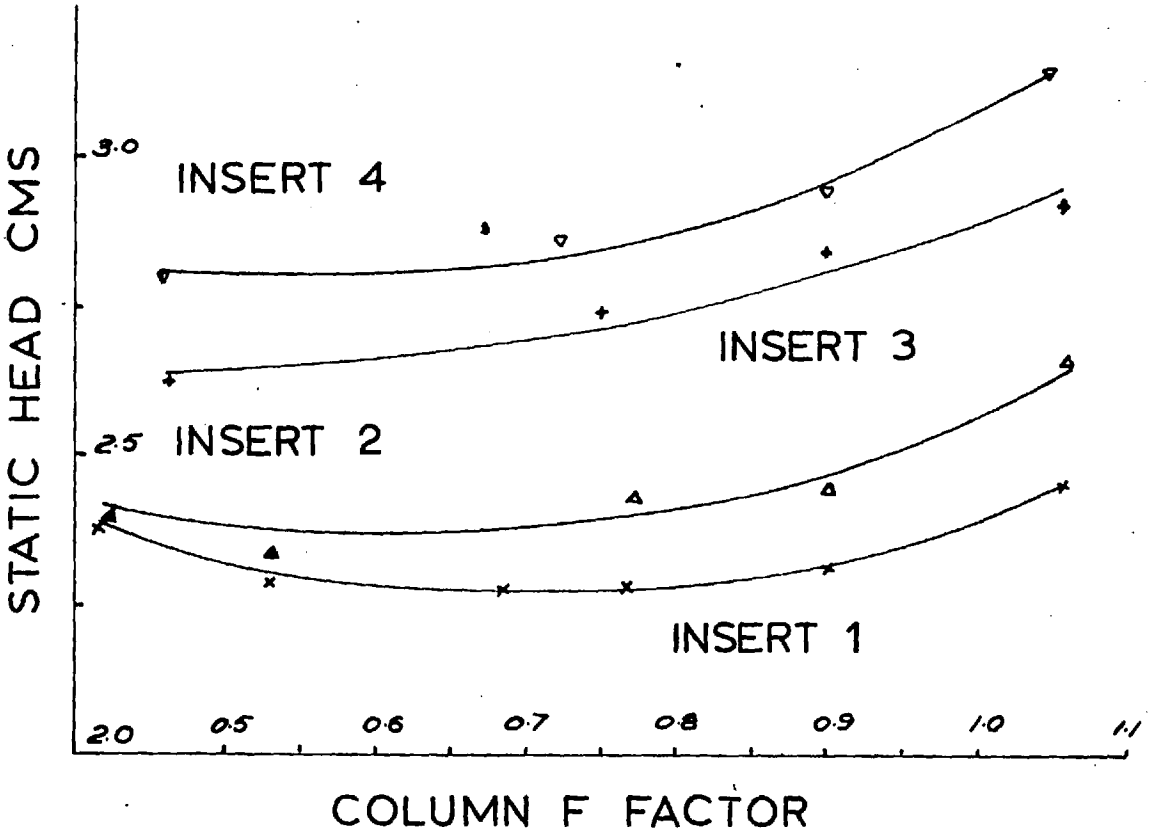
Measured Liquid Hold up at Column F factor of 0.9

% Free Area	23%		10%	
Hole Velocity	29		58	
Hole Size	1/16"	1/8"	1/16"	1/8"
Result	Static Head expressed as cms pentane			
2 cm Weirs	1.5	1.6	1.97	2.15
3 cm Weirs	1.87	2.25	2.27	2.6
4 cm Weirs	2.25	2.80	2.42	2.96

FIGURE 16

EFFECT OF DESIGN VARIABLES ON STATIC HEAD

4 CM WEIRS



For a given hole size, weir height and the same hole velocity the total hold up is independent of the % free area of the insert. The distribution of the hold up between clear liquid and the dispersion, however, is dependent on the % free area of the plate. The higher % free area inserts show the highest percentage hold up in the dispersion. For $\frac{1}{8}$" holes and 2 cm weirs, for example, at a hole velocity of 30 ft/sec, the static heads on 23% and 10% free area inserts are 1.8 and 1.85 cms respectively whilst the corresponding values for % liquid hold up in the foam are 92% and 70%. There is a distinct effect of hole size, inserts with $\frac{1}{8}$" holes giving rise to higher hold ups for the same weir height and hole velocity than those with 1/16" holes. Comparison of hold up values for the two hole sizes at constant orifice Reynolds number still show this effect of hole size. More detailed knowledge of the mechanism of formation of these dispersions and the variation of the turbulence pattern both in the clear liquid and in the dispersion, as a result of changes in the several design variables, is needed before any explanation of the results can be given.

6.3 Distribution of Liquid between Bubbling Zone and the Dispersion

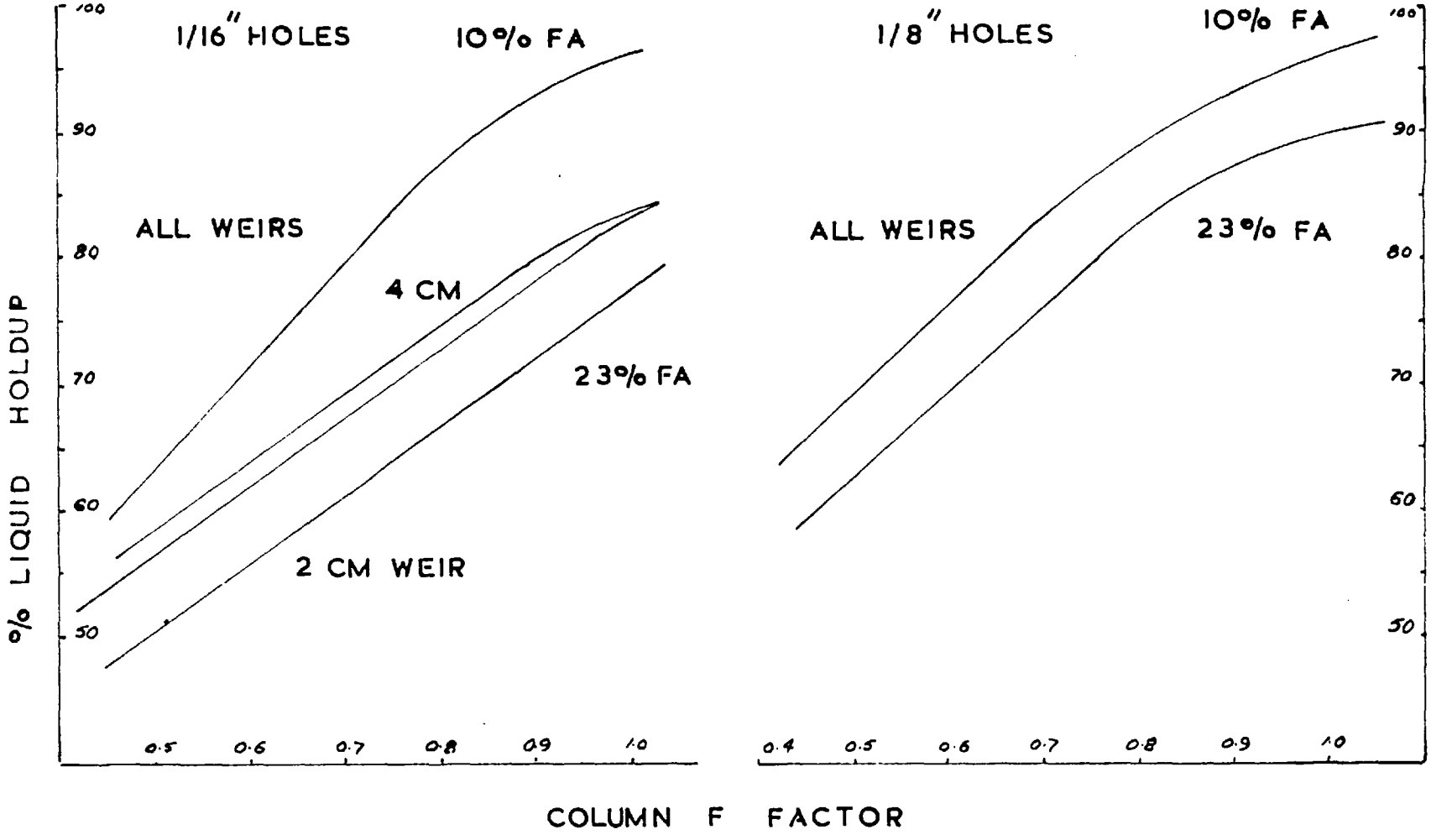
The column design was such as to allow a usual estimate of the clear liquid height on the tray to be made. This measurement corresponded to that detected by the gamma ray traverse, the profile at this point showing a change in density from that of the aerated

liquid near the plate to that corresponding to the dispersion forming region. The area under a profile above this height can be considered to be a measure of the liquid hold up in the dispersion whilst the area below it is that due to the 'clear liquid' near the plate.

The distributions obtained in this manner are plotted in Figure 17. As would be expected , the same variables that determine the total liquid hold up also determine the distribution of liquid on the plate. Larger hole sizes and higher hole velocities are seen to give the higher percentage hold up in the dispersion whilst increasing the weir height gives greater dispersion hold ups in the case of 1/16" holes but has no effect for $\frac{1}{8}$" holes.

The range of hole velocities studied, from 13 to 60 ft/sec, covers the normal industrial operating range and the fact that on sieve plates over most of this range, 75 - 90% of the liquid hold up is in the dispersion is not widely appreciated. On this basis one would expect a significant part of the total mass transfer to occur in the dispersion since published variations of plate efficiency data with vapour velocity show only a slight decrease with increasing vapour rate (20). Gerster (30) predicted that 90% of the liquid is held up in the dispersion but his conclusion that 90% of the mass transfer also occurs in the dispersion has yet to be shown experimentally.

FIGURE 17 % LIQUID HOLDUP IN THE DISPERSION



7. Plate Pressure Drop Studies

In industrial sieve plate design practice, the column diameter is determined as a function of the plate spacing using empirical capacity charts, the design values chosen being those that result in the column of lowest first cost. The plate geometry, hole size and pitch, and the weir height are determined primarily by the allowable pressure drop over the column, some account being taken of corrosion and the tendency of the system to foul the plates in choosing the hole size. If the column functions satisfactorily from the hydrodynamic viewpoint, its performance as a fractionating device is assumed also to be satisfactory. Whether it is justifiable to fix the plate geometry and weir height to satisfy pressure drop limitations without taking into account their effect on plate efficiency is discussed in Part B of this thesis; however an examination of the available methods of plate pressure drop calculation is of intrinsic interest.

7.1. Evaluation of Available Calculation Methods

It was first thought that the total plate pressure drop was a simple addition of the dry plate pressure drop and the static head on the plate.

$$h_T = h_{DP} + h_S$$

Subsequent experimental work showed that this simple relationship did not hold and a residual pressure drop, h_R, had to be included to make the equation balance

$$h_T = h_{DP} + h_S + h_R$$

The static head was known only for plates with no liquid cross flow and in order to apply this relationship to an operating colunn, the static head had to be estimated from the liquid head at the weirs using an experimentally determined, "aeration factor", such that

$$h_S = \beta h_W$$

giving

$$h_T = h_{DP} + \beta h_W + h_R$$

Dry Plate Pressure Drop

The dry plate pressure drop is normally calculated for the true average vapour velocity through the plate perforations using equations based on the simple orifice equation for flow through a sharp edged circular orifice.

$$h_{DP} = \frac{v_h^2 \rho g}{2g\, c^2}$$

where h_{DP} = dry plate pressure drop lb/ft^2

v_h = hole velocity ft/sec

ρ_g = vapour density lb/ft^2

g = acceleration due to gravity ft/sec^2

c = orifice coefficient

This form has been used directly by Foss and Gerster[22] whilst Kamei et al[46] have expressed it in the form

$$h_{DP} = 0.187 \frac{v_h^2}{c^2} \frac{\rho_g}{\rho_L}$$

where h_{DP} = dry plate pressure drop in ins. of liquid on the plate

and ρ_L = liquid density lb/ft^3

These equations apply to a single orifice and correction factors have been introduced to take into account the effect of neighbouring holes present on a perforated plate. Kolodzie and Van Winkle[50] determine the velocity of approach factor as the ratio of the total free area of perforations to the column cross sectional area as:

$$h_{DP} = \frac{v_h^2 \rho_g}{2g\ c^2} \left\{ 1 - \left(\frac{A_h}{A_c}\right)^2 \right\}$$

Hughmark and O'Connell[40] make allowance for the velocity of approach on the basis of the fraction free area of active plate, a term based on the hole diameter and pitch ratio only:

$$h_{DP} = \frac{0.003\ F_h^2\ (1 - f^2)}{c^2}$$

where $F_h = v_h(\rho_g)^{\frac{1}{2}}$

f = fraction free area of active plate

h_{DP} = dry plate pressure drop, ins. of water.

This equation can be readily shown to be based on the simple orifice equation, the numerical factor 0.003 (1 x 12/2g x 62.4) being the conversion factor to express pressure drop in inches of water.

The value of the orifice coefficient used in equations of this form influence greatly the calculation of dry plate pressure drop. In a given design situation, the use of this basic equation with the authors' recommended orifice coefficients give values that differ by up to 12%. Apart from Kolodzie and Van Winkle, other

authors are vague as to the source and reliability of their orifice coefficients. The most comprehensive and reliable source of orifice coefficients is the excellent experimental data presented by Kolodzie and Van Winkle and extended by Smith and Van Winkle[70]. The coefficients are presented as functions of the hole pitch/hole diameter ratio, hole diameter/plate thickness ratio, and the orifice Reynold's Number. To simulate conditions existing in columns where the presence of weir boxes and downcomers limit the perforated area, orifice coefficients are presented for various perforated area/total column cross sectional area ratios for the range of variables of industrial interest. Kolodzie and Van Winkle claim prediction to within 5% of the data obtained by Hunt et al[41] and to within 10% of that presented by Mayfield et al[54] in a 6'6" diameter column. For these reasons it is recommended that dry plate pressure drops should be calculated using the equation and orifice coefficients presented by these authors.

The relationship between plate pressure drop and hole velocity can be expressed in the alternative form

$$h_{DP} = k\, v_h^{\,n}$$

the values of the constant k and the exponent n being determined empirically from experimental data. The pressure loss through a sharp edged orifice is generally accepted to be proportional to the hole velocity to the 1.8 power. Arnold et al[3] confirm this for a 0.029" (24 SWG) thick insert whilst Jones and Pyle[44] found an exponent of 1.9 for a plate 1/16" thick. The constant k

has a value depending on the % free area of the plate, the hole size and the method of insert fabrication. There appears to be no real advantage in using relationships of this kind since reliable orifice coefficients are available and there are only limited published values for the constant K.

In industrial columns, it is argued, the perforated plates would have to be reasonably thick to provide adequate mechanical strength so that the plate orifice would approximate to a short tube rather than a sharp edged orifice. By considering the dry plate pressure drop to be composed of the entrance and exit loss from a short tube, Hunt et al correlated a wide range of experimental data for several gas-liquid systems at a plate thickness/hole diameter ratio of unity as

$$h_{DP} = 1.14 \frac{v_h^2}{2g} \left\{ 0.4 \left(1.25 - \frac{A_h}{A_A}\right) + \left(1 - \frac{A_h}{A_A}\right)^2 \right\}$$

where h_{DP} = dry plate pressure drop, feet of vapour

A_A = cross sectional area of column available for vapour flow ft^2

A_h = total hole cross sectional area.

The application of this correlation to column design should be treated with some caution. Dry plate pressure drops calculated in this way are up to 30% less than those measured experimentally by Mayfield et al in a large column notwithstanding the fact that both Hunt and Mayfield used plates with the same T/D_h ratio. Hunt's data was obtained for carefully drilled and reamed holes

and the other authors used plates either punched or rough drilled. From this one can conclude either that Hunt's physical model is invalid and/or that the fabricating technique affects the pressure drop across the plate. Since Kolodzie and Van Winkle can predict both Hunt's data to within 5% and Mayfield's data to 10%, the difference in fabrication methods has a minor effect and the validity of Hunt's physical model is open to doubt.

Pressure Drop Associated with Liquid on the Tray

Early workers in attempting to analyse the components making up the total plate pressure drop found that the total plate pressure drop did not increase in the same proportion as an increase in weir height. This led to the popular misconception that the head due to an aerated liquid is less than that of the equivalent amount of clear liquid[19]. Such workers failed to realise that the liquid hold up in a plate is determined as much by the momentum and turbulence patterns produced by the vapour flow as by the weir height and is not simply equivalent to a liquid depth equal to the weir height plus weir crest.

The aeration factors proposed by the several workers have been discussed in some detail in Section 2.3. and their applicability to the estimation of the static liquid head on an operating plate in Section 7.2.2. Suffice to say at this stage that they give reasonable estimates of the liquid hold up on a plate but that there is some confusion in the literature as to their use in calculating total plate pressure drops.

Kemp and Pyle's[47] aeration factor

$$\beta = \frac{h_{T_1} - h_{T_2}}{h_{W_1} - h_{W_2}}$$

gives the relationship between the change in liquid hold up and the change in weir height causing it, assuming a constant residual pressure drop. Mayfield's[54] aeration factor

$$\beta' = \frac{h_T - h_{DP}}{h_W}$$

gives the ratio of the liquid hold up plus residual pressure drop to the head at the weir and is numerically different from that of Kemp and Pyle.

The correct form of the equations for calculation of the total pressure drop using these aeration factors is

$$h_T = h_{DP} + \beta h_W + h_R$$

and

$$h_T = h_{DP} + \beta' h_W$$

The effective head correlation presented by Hughmark and O'Connell[40] is based on Mayfield's aeration factor and the author's use of a residual pressure drop term is superfluous. Equations of this type appear to be quite successful in estimating the total plate pressure drop and are commonly used in industrial design.

An equation of the form

$$h_T = R(h_{DP} + h_W)$$

has been proposed by Arnold et al[3], the term R has no physical

significance and was determined empirically from experimental data. As data on the variation of R with design variables are limited, there is no advantage in using an equation of this type in preference to those already discussed.

Even with accurately known amounts of liquid on the plate, the sum of the dry plate pressure drops and the true static head does not equal the total plate pressure drop. The value of the residual pressure drop, introduced to make up this deficit, has been found to be relatively independent of the liquid hold up, hole size and pitch, vapour rate and the nature of the gas-liquid system studied. A constant value of approximately 0.5 inches of water has been found by most investigators and confirmed by the experimental work associated with this thesis.

It is generally assumed that this residual pressure drop represents the energy needed to form bubbles, to create and maintain interfacial surface in the dispersion and to produce turbulent mixing in the dispersion. Garner et al[23] attempted to calculate the energy required for interface formation and estimated it to be of the order of a few millimeters of water. No satisfactory correlation has yet been found for the residual pressure drop in terms of these energy requirements.

The fact that no satisfactory correlation has been found for this term is not surprising if one realises that such a term has no physical significance. The energy requirements to form new surfaces appear to be minor components of this term which is, in

reality, a correction factor needed to take into account the inaccuracy of the concept of plate pressure drop as the sum of the dry plate pressure drop and the liquid head on the plate. The dry plate pressure drop is measured (or calculated) on the time average vapour velocity through the holes. No account is made of the fact that the bubbling process is cyclic, the vapour flow through each hole being intermittent, or that, at a given instant, not every hole is bubbling. It is also tacitly assumed that the pressure drop across the plate under bubbling conditions is calculable by the same relationships as apply to the free flow of vapour through the plate perforations.

Brown[7] has suggested the following equation for the estimation of plate pressure drops

$$h_T = h_p + h_s$$

where h_p is an empirical term, determined experimentally as $(h_T - h_s)$, to replace the sum of h_{DP} calculated on the time average vapour flow and the residual pressure drop. Using dimensional analysis, the functional groups determining this term were found and their coefficients obtained empirically from experimental data on air-water and several other gas-liquid systems in both 6" and two foot square columns as

$$Eu = 9.29\ (1 + 10000/Reg)^{0.87}\ (We)^{0.11}\ (F_R)^{0.24}\ \left(\frac{\mu_L}{\mu_g}\right)^{0.08}$$
$$\left(\frac{\rho_L}{\rho_g}\right)^{-0.32}\ \left(\frac{D_h\ f_p}{V_h}\right)^{-0.36}$$

where $Eu = \rho_L (h_T - h_s) / \frac{\rho_g V_h^2}{2 g_c}$

$We = / \frac{D_h \rho_g V_h^2}{2 g_c}$

$F_R = \frac{D_h \cdot g}{V_h^2}$

(The terms have the units assigned to them in the Nomenclature)

This method of estimating total plate pressure drop is of limited practical use, the uncertainty in the estimation of h_s for an operating column would be greater than the accuracy gained by using h_p values (if available) rather than the $(h_{DP} + h_R)$ approximation to them. If care is taken in choosing the method of estimation of the dry plate loss and if the published aeration factors are applicable to the system being handled, then the normal method of estimation based on summing the component parts appears satisfactory for most industrial purposes.

7.2. Analysis of Pressure Drop Experimental Data

Experimental data relating to total and dry plate pressure drops are tabulated in Appendix A, Tables 16, 17, 18 and 19 and represented graphically in Figure 18.

7.2.1. Dry Plate Pressure Drop Measurements

Dry plate pressure drop data was determined experimentally with pentane vapour flowing up the column, the downcomers being blocked off and reflux being returned directly to the reboiler. Difficulties inherent in measuring dry plate pressure drops due to condensation of the pentane vapour on the plate were overcome by fitting two 250 watt Pope radiant heaters to the column at plate level. Before start up the column and plate were pre-heated to prevent condensation on the walls or the plate and once a constant column temperature had been reached only occasional heating was necessary to keep the plate dry.

The dry plate pressure drop data for both 10 and 23% free area inserts and for both hole sizes in the range of hole velocities from 15 to 55 ft/sec are correlated by the relationship

$$h_{DP} = 7.43 \times 10^{-3} \, v_h^{1.8}$$

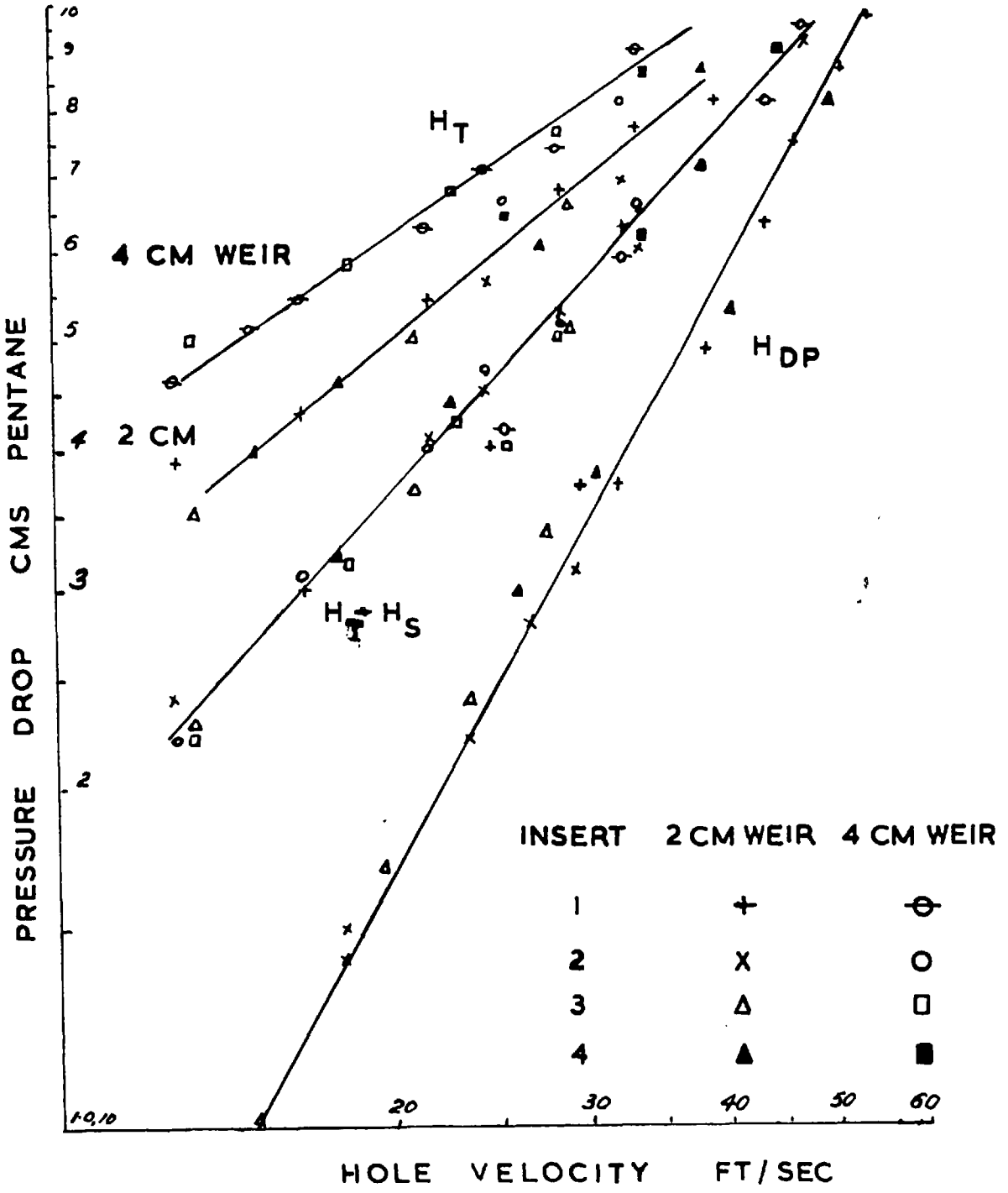
where h_{DP} = dry plate pressure drop in cms of pentane

v_h = hole velocity in ft/sec

The average deviation of experimental points from this relationship is 5.5% with a maximum deviation of 15%. The velocity term exponent of 1.8 shows that for these inserts, the holes behave as sharp edge orifices even though the plate thickness/hole diameter

FIGURE 18

PRESSURE DROP DATA



ratio for these inserts corresponds ostensibly to the range of applicability of the short tube model proposed by Hunt et al.

The equations, discussed in Section 7.1., used by other workers to predict dry plate pressure drops were used to calculate the dry plate pressure drop for a hole velocity of 20 ft/sec. A comparison of the calculated result and the measured value is given in Table 3.

Table 3

Author	Calculated h_{DP}	Measured h_{DP}	% Error
Kolodzie and Van Winkle	1.7 cms	1.65 cms	3%
Kamei et al	1.85	1.65	12
Jones and Pyle	1.95	1.65	18
Mukhlenor and Tarat[56]	1.98	1.65	20
Hughmark and O'Connell	1.78	1.65	8
Hunt et al	1.4	1.65	-15

Apart from the equation due to Hunt et al based on the analogy of the plate orifice to a short tube, the equations given by the other five authors differ only in values used for the orifice coefficient. As previously stated, the orifice coefficient data presented by Kolodzie and Van Winkle are the most reliable and were obtained using a wide range of gases and for perforated area/column cross sectional area ratios corresponding to those in actual distillation columns. It is not surprising, therefore, that the use of these orifice coefficients predicts very closely the measured dry

plate pressure drop. The other authors are vague as to the source and reliability of their orifice coefficients and the use of their equations is not recommended. The equation developed by Hunt et al on the analogy between a plate orifice and a short tube predicts a value 15% less than the measured value. Since this equation predicts values up to 30% less than those measured by Mayfield et al in a 6'6" diameter column with relatively thick plates, the physical model on which the equation is based is open to question and the equation is not recommended for use in column design.

7.2.2. Comparison with Previous Methods of Correlation

Arnold et al have correlated total pressure drop data in the form

$$h_T = R\ (h_{DP} + h_w)$$

The data obtained from this present work yield values of h of 1.13 and 0.93 for 2 and 4 cm weirs respectively compared with those given by Arnold et al of 1.15 and 1.03. There is no advantage in using a correlation of this type as the factor R has no physical significance and there is little data available on its variation with operating and design variables.

Another common method of correlating total plate pressure drop data is in terms of an aeration factor, the relationship.

$$\beta = \frac{h_{T_1} - h_{T_2}}{h_{W_1} - h_{W_2}}$$

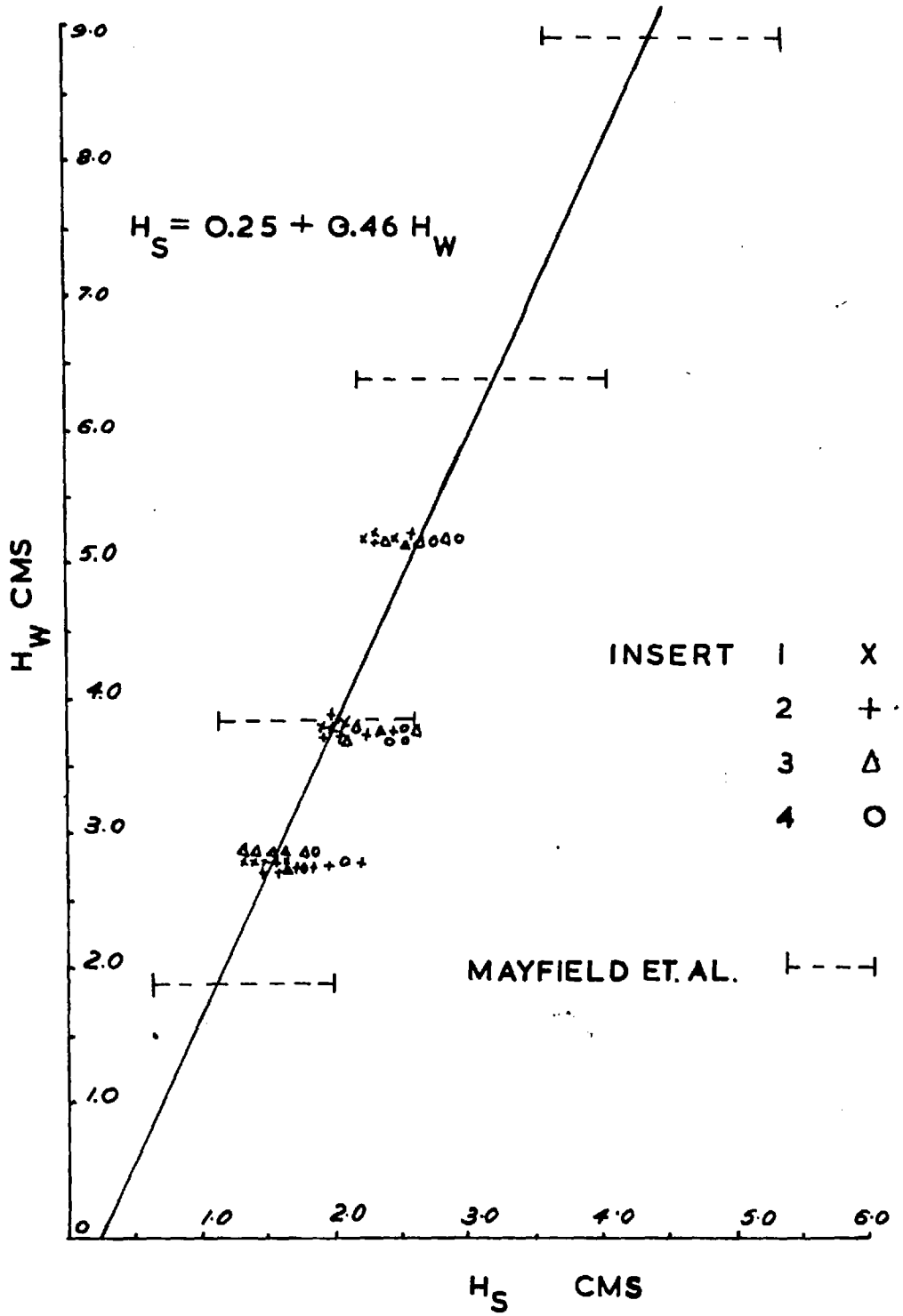
due to Kemp and Pyle being a correlation of this type. From the curves given in Figure 18, the difference in total plate pressure

drop between 2 and 4 cm weirs at the same vapour rate is substantially constant at 1.2 cms of pentane over the range of inserts and operating variables studied. The inlet weir heads were measured and found to be almost constant over the range of design and operating variables studied, and average values of 5.2 and 2.8 cms may be taken for the liquid head at 4 and 2 cm weirs respectively. For these parameters, the value of β remains approximately constant at a value of 0.5 for all the variables studied.

At constant gas rate $(h_{T_1} - h_{T_2})$ is a direct measure of $(h_{s_1} - h_{s_2})$ and reference to Figure 19 shows that, except for 10% free area plates at low weir settings, the great majority of the experimental liquid hold up data points for all inserts and for the three weir heights studied, fall close to a straight line of slope 0.46 when plotted as static head against head at the inlet weir. Some of the scatter at the high weir settings is undoubtedly due to scatter in the experimentally measured pressure drops; however the scatter at low weir settings appears to be due to the fact that the liquid hold up in the dispersion is determined largely by the vapour flow pattern above the plate and is relatively unaffected by the head at the weir for these low weir settings. This same feature has been noted by Mayfield et al and by Kirschbaum[49]; however for the range of weir heights encountered in distillation practice it would seem sufficient to use the simple linear relationship given between h_s and h_w. Thus the aeration factor due to Kemp and Pyle gives in fact a successful prediction

FIGURE 19

RELATIONSHIP BETWEEN H_S AND H_W



of the relation between the static head and the head at the inlet weir.

Mayfield et al define an aeration factor

$$\beta' = \frac{h_T - h_{DP}}{h_W}$$

Aeration factors, for the present work, calculated in this manner show a tendency to increase with increasing hole velocity. The aeration factor increases from 1.1 to 1.25 for 2 cm weirs and from 0.8 to 0.9 for 4 cm weirs for an increase in hole velocity from 15 to 35 ft/sec. This increase in aeration factor with increasing hole velocity was also found by Mayfield et al and Figure 20 shows a correlation of the present data with that due to Mayfield et al and the effective head data of Hughmark and O'Connell plotted as the ratio of effective head/weir height against weir height. The aeration factors for the pentane system are in reasonable agreement with those reported in the literature so that it appears that aeration factors based on air-water studies are applicable to hydrocarbon systems.

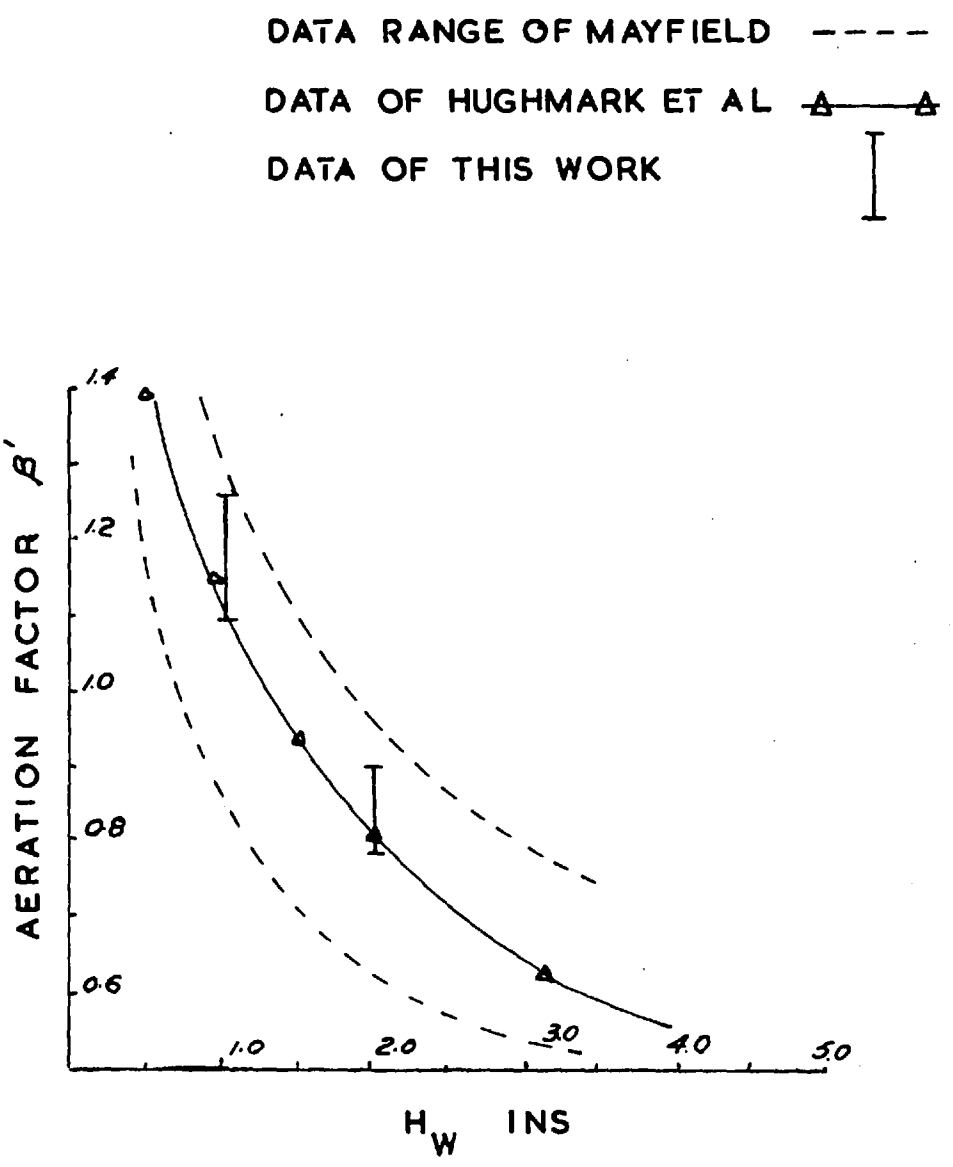
7.2.3. Estimation of Total Plate Pressure Drop

It appears logical to estimate the total plate pressure drop as the sum of the pressure drop due to the vapour flow through the plate and the dispersion formed above it and the static head due to the liquid hold up in the dispersion.

$$h_T = h_p + h_s$$

FIGURE 20

COMPARISON OF AERATION FACTORS WITH LITERATURE VALUES



As is stated in Section 7.1, there is no justification for assuming that the pressure drop across a perforated plate is the same for the case of vapour issuing as a bubble stream into a two phase dispersion as for the discharge of vapour in the form of a continuous jet into a single phase region as is the case in the normal method of measurement of dry plate pressure drops. Since values of h_T and h_s could be determined in this work by direct experimental means, a correlation for h_p could be obtained in terms of the design and operating variables studied.

For the range of hole velocities of 13 to 50 ft/sec, the true plate pressure drop (h_p) was found to be independent of hole size and pitch and weir height, the data for all weirs and inserts being correlated with an average deviation of 4.5% and a maximum deviation of 12% by the relationship

$$h_p = 0.145\ V_h^{1.08}$$

where h_p = true plate pressure drop (cms pentane)

V_h = hole velocity (ft/sec)

This correlation is purely empirical and is not based on any physical model; hence no prediction can be made of the effects of design and operating variables outside of those studied in this column.

An empirical relationship has been developed by Brown relating the true plate pressure drop to the hole velocity and the gas-liquid system properties. The equation is complicated and predicts values of h_p of greater magnitude than those experimentally

measured. At a hole velocity of 16.8 ft/sec, the predicted value of h_p of 4.1 cms of pentane is 30% greater than the measured value of 3.0 cms. Brown's equation contains a term involving the frequency of the pressure fluctuations under the plate and the discrepancy is most probably due to differences in this frequency for the two experimental rigs. Brown's test rig was of square cross section with no distributor plate under the test plate, the air from the blower discharging directly into the air chamber below the plate so that differences in pressure fluctuations are quite probable.

Since there are no correlations available for the true plate pressure drop for the range of design variables encountered in normal industrial design, alternative methods of estimating the contribution of the plate to the total pressure drop must be sought. Some success has been achieved in the past in correlating total plate pressure drop in terms of the dry plate pressure drop based on the true average gas flow through the dry plate and the static head of liquid on the plate by the inclusion of a residual pressure drop term. As previously stated in Section 7.1. this residual pressure drop term has no physical significance and is purely a correction factor to allow for the inaccuracy in the assumption that the plate pressure drop calculated on the true average gas flow through the dry plate corresponds to the true plate pressure drop. The veracity of this statement is borne out by the fact that the experimental residual heads tend to increase

slightly with increasing hole velocity, are independent of hole size and weir height and have the same value for a wide variety of vapour-liquid systems, the measured residual heads of the order of 2 cms of pentane corresponding to the figure of 0.5 inches of water quoted by Hunt et al and other workers. On this basis, for the accuracy required of technical calculations, the contribution of the plate (h_p) to the total pressure drop can be estimated as the sum of the dry plate drop based on the true average gas flow and a residual head that may be assumed constant at 0.5 inches of water.

The best estimate of the static head of liquid on the plate is given by the relationship

$$h_s = \beta h_w + C$$

where β is the aeration factor defined by Kemp and Pyle and, as shown in Section 7.2.2., has an approximately constant value of 0.46 over the range of variables studied. The method of correlation adopted by Mayfield et al, in effect relates the sum of the terms (h_s + h) to the head at the weir and the relationship between h_w and h_s may be deduced from this data by taking the residual pressure drop to have a constant value of 0.5 inches of water. The spread of values obtained when the data presented in Mayfield et al's Figure 10 is plotted as in the form of h_w against h_s is shown in Figure 19. The line representing the relationship between h_w and h_s found in this work lies almost in the middle of the range of values obtained from Mayfield's data. Thus the

experimental linear relationship

$$h_s = 0.25 + 0.46\ h_w$$

is just as successful a correlation of Mayfield et al's data as that proposed by these authors. The fact that the relationship between h_w and h_s determined for a hydrocarbon system in a 4" diameter column is in general agreement with the results obtained on the air-water system in a large diameter column encourages the view that this simple linear relationship may have general applicability in industrial column design.

The main drawback in the use of these aeration factors to predict liquid hold ups is that a means of predicting the head over the weir is required. Most workers assume that the standard Francis Weir formula modified by a velocity of approach correction can be used for this purpose. The splash baffle fitted at the outlet weir in this column modifies the flow upstream of the weir so that the Francis formula would not be expected to apply; nevertheless the measured liquid head over the outlet weir appears to be in reasonable agreement with that calculated from the Francis formula.

Successful correlation of the present data has been obtained in terms of the head at the inlet weir rather than the more usual head at the outlet weir. For the inlet weir head, the Francis formula predicts values 30-40% of the measured values. If the liquid hold up in the dispersion is determined by the dynamic equilibrium between the liquid flow onto the plate and the liquid

and vapour flow pattern set up above the plate then the measured head of the inlet weir is more likely to bear a direct relationship to the liquid hold up than a head calculated from the Francis formula that is completely independent of any consideration of the vapour flow through the plate.

As a rule values of the head at the inlet weir are not available; hence one must use weir heads calculated from the Francis formula.

Thus it appears that the most useful form of a relationship to predict total plate pressure drop is

$$h_T = h_p + h_s$$

where $h_p = h_{DP} + \frac{1.25}{\rho_L}$

and $h_s = 0.25 + 0.46\ h_w$

the liquid head terms being expressed as cms of liquid.

The use of these relationships allows the successful prediction of the experimental total pressure drop data, the average deviation of results being 6% with a maximum deviation, apart from one suspect value, of 12%.

PART II

PLATE EFFICIENCY STUDIES

8. The Concept of Plate Efficiency and its Relation to Column Design Variables

Reasonably reliable methods are available for determining the number of theoretical plates required to effect a given separation (68) A theoretical plate is defined as one on which the liquid is completely mixed and the entering vapour reaches equilibrium with the plate liquid. Such conditions are never achieved on an actual plate and from a design viewpoint it is important to have a measure of the departure from ideality.

The most commonly used plate performance factor is the Murphree Plate Efficiency (52) defined in terms of vapour compositions as

$$E_{OG} = \frac{y_n - y_{n-1}}{y_n^* - y_{n-1}}$$

where Yn and Yn-1 are the average compositions of the vapour leaving plates n and n-1 respectively and Y_n^* is the composition of vapour in equilibrium with the liquid Xn leaving the plate. This relationship is only satisfactory if the liquid and vapour are completely mixed and since, in practice, concentration gradients can exist in the liquid and vapour streams, the efficiency at a point on the plate is defined as

$$E_{PG} = \frac{y_L - y_e}{y_L^* - y_e}$$

where Y_L and Y_e are the compositions of the vapour leaving and entering a small area of plate in which both the liquid and vapour are assumed completely mixed and Y_L^* is the vapour composition in equilibrium with the liquid in this small area. Equations have been presented by

several authors (21), (25), relating point efficiency to the overall plate efficiency; however successful prediction of the overall plate efficiency from the point efficiency requires knowledge of plate mixing parameters and the effect on these parameters of changes in column operating and design variables.

Having defined a plate performance factor suitable for use in column design calculations, a means of estimating the value of this performance factor as a function of system properties and design variables is required. At best, the column designer has access to plate efficiency data gained from past operating experience for a given type of system in a given type of column. Failing this, empirical or semi-quantitative correlations have to be used to predict plate efficiency. These range from the correlations for hydrocarbon systems due to Drickamer and Bradford (18) and O'Connell(57) based solely on the molal viscosity and relative volatility of the feed being independent of fluid flowrates and type of contacting device used, to the equation derived by Geddes (26) from consideration of the mass transfer from a single spherical bubble. Both type of relationship appear to correlate previous experimental data, the agreement in the case of Geddes' relationship is generally assumed to be due to a fortuitous cancellation of errors whilst O'Connell's correlation apparently results from the choice of data from similar types of system in similarly designed columns.

Other workers have adopted a different approach in determining the variation of overall plate efficiency as a function of design

and operating variables. Data of this type has been presented by Umholtz and Van Winkle (72) and Manning et al (53) for the octane-toluene system in 3 inch and 5 feet diameter columns respectively. Both sets of data show that the plate efficiency first increases with vapour rate until weepage stops and then remains reasonably constant over a wide range of vapour rates. The fall off in efficiency at higher rates is considered to be due to vapour channelling and entrainment caused by degeneration of the dispersion into a spray regime. The plate efficiency increased with increasing weir height due to an increase of liquid hold-up on the plate and there was little effect of reflux ratio. This latter result is in accord with the experimental result presented in Part I of this thesis that the reflux ratio has little effect on either the total liquid hold-up or the distribution of liquid between the bubbling zone and the vapour-liquid dispersion. These results have been obtained for a particular system in columns of a particular design but are useful to the column designer in showing the trend of variation of plate efficiency with design and operating variables.

A more fundamental approach has been made by Gerster et al (31) using the relationships, first proposed by Whitman (76), governing the transfer of material across a vapour-liquid interface, these relationships are based on the assumptions that the rate of mass transfer is controlled by molecular diffusion through thin films on opposite sides of the interface and that there is no resistance to mass transfer at the interface. Using these relationships, the point

efficiency has been related to the separate vapour and liquid film transfer units by the expressions.

$$N_{P_G} = -E_{P_G}\left(1 - \frac{1}{E_{P_G}}\right)$$

where

$$\frac{1}{N_{P_G}} = \frac{1}{N_G} + \frac{m G_m / L_m}{N_L}$$

in which E_{P_G} = point efficiency based on vapour phase concentration differences

N_{P_G} = overall number of mass transfer units

N_G = number of gas phase transfer units

N_L = number of liquid phase transfer units

m = slope of the equilibrium line

L_m = flow rate of liquid (lb mole/hr ft^2)

G_m = flow rate of vapour -do-

these relationships apply to a small region on the plate where the vertical liquid concentration is constant and for plug flow of the vapour. If the liquid is completely mixed, then the point efficiency is identical with the overall plate efficiency. For cases in which liquid mixing effects are important, these authors have developed empirical relationships between point and overall point efficiencies based on the eddy diffusivity model.

The value of this approach is that by choosing systems in which the bulk of the resistance to mass transfer lies in one of the phases, the variation of both vapour and liquid phase mass transfer rates with design and operating variables can be determined experimentally.

Use is made of the following relationships.

$$N_{G} = k'_{G}\, a\, t_{G} = k'_{G}\, a \cdot \frac{\phi}{v_{A}}$$

where k'_{G} = mass transfer coefficient lb/moles/hr.ft^2(unit concentration difference)

a = interfacial area ft^2/ft^3 of vapour hold-up

t_{G} = average time of contact of vapour with liuqid

ϕ = vapour hold-up ft^3/ft^2 of bubbling area

and v_{A} = vapour velocity based on bubbling area ft/sec

Working with air-water systems, the number of vapour phase and liquid phase mass transfer units can be obtained from runs involving the humidification of air and the desorption of oxygen from water respectively (29) (30).

The results of these studies show that the number of vapour phase transfer units increases slightly with increasing vapour rate, is dependent on weir height and liquid flow rate and increases with increasing height of the vapour-liuqid dispersion. The number of liquid phase transfer units was seen to decrease with increasing vapour rate and with increasing dispersion height. There is considerable evidence from the work of Mukhlenov (55) and Pozin (64) that in gas film controlling processes, the number of vapour phase transfer units bears a direct relationship to dispersion parameters and shows a continuous increase with increasing column vapour rate.

The fact that the number of vapour and liquid phase mass transfer units depends on dispersion parameters encourages the view that a

more detailed investigation of the nature of such dispersions would allow further elucidation of the variables affecting plate efficiency.

8.1 Experimental Determination of Plate Efficiency Data

Plate efficiency studies were performed using the 4" diameter distillation column described previously in Section 3.2 for the range of operating and design variables used in the hydrodynamic studies except that the plate efficiency studies were confined to inserts with $\frac{1}{8}$ inch holes. Runs were performed only at total reflux since under these conditions the liquid leaving a plate had the same composition as the vapour entering the plate. Only liquid sampling was necessary in this case, thus eliminating errors arising from attempts at vapour sampling.

A trial run showed that, provided the boil-up and reflux rate could be maintained constant for a period in excess of fifty minutes, the column settled down to a steady state. During this settling down period, the dispersion density profile was measured using the gamma ray technique and a visual estimate was made of the clear liquid depth on the plate. At the end of the fifty minute period, the sample lines were flushed out and liquid samples were cooled to prevent flashing by passing them through coolers around which chilled water circulated. The samples were collected in pre-cooled glass vials and stored at $-15^{\circ}C$ until analysed.

Vapour phase chromatography was used to determine the mole fraction of iso pentane in the iso-pentane - normal pentane system used in this study. Originally, the analyses were performed on a Gas Chromatography Limited unit fitted with a flame ionisation detector

using hydrogen as the carrier gas and a 12 foot column packed with squalane on a kieselguhr support. However the detector saturated on the injection of samples greater than 0.5 microlitres and considerable difficulties were experienced in getting such small quantities into a syringe without partial vaporisation occurring and attendant unreliability in the analysis. This difficulty was overcome by using a Perkin Elmer Chromatograph fitted with a Katharometer detector. Using a 6 foot silicone oil column, quantities of up to five microlitres could be injected without saturating the unit. With such highly volatile mixtures care had to be taken to prevent partial vaporisation of the sample before injection into the carrier stream. The technique finally found to be reliable involved chilling both syringe and sample vial to -15°C and avoiding all unnecessary contact with the fingers on filling the syringe, an insulated block being used to hold the sample vial during the filling operation.

Equilibrium data for the pentane-iso pentane was calculated from the total pressure measurements of Redlick and Kister (67) and checked with data provided by the Koninklijke/Shell Laboratorium, Amsterdam.

8.2 Discussion of Experimental Plate Efficiency Results

The experimental data and values of parameters affecting the plate efficiency calculated from these results are presented in Tables 20, 21 and 22 in Appendix B.

Figure 21 shows a plot of overall plate efficiency against the superficial vapour velocity based on the plate bubbling area, the manner of correlation adopted by most other workers. The curves increase with increasing vapour rate and with increasing liquid hold up on the plate, the effect of decreasing % free area and increasing weir height being to increase the plate liquid hold up.

Figure 22 shows that the overall plate efficiency data correlates better in terms of hole velocity than in terms of superficial vapour velocity. It is interesting to note that, apart from the data presented by Hellums et al (36) for the n octane-toluene system in a 6 inch diameter column, other workers obtained correlation in terms of the superficial velocity. This previous work thus appears to indicate the physical mechanism of vapour-liquid contacting, the interfacial area of contact and the vapour-liquid contact time are determined by the column superficial velocity rather than the hole velocity.

The results of the hydrodynamic studies in the present work are much more readily correlated in terms of hole velocity rather than superficial velocity, and in particular the total liquid hold-up

FIGURE 22

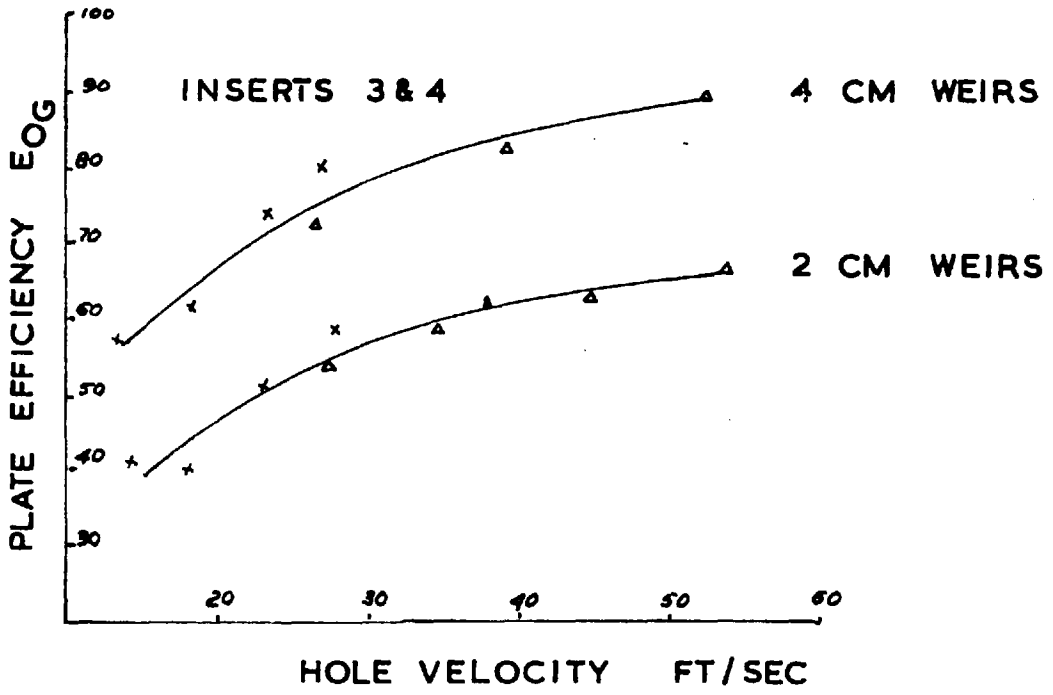
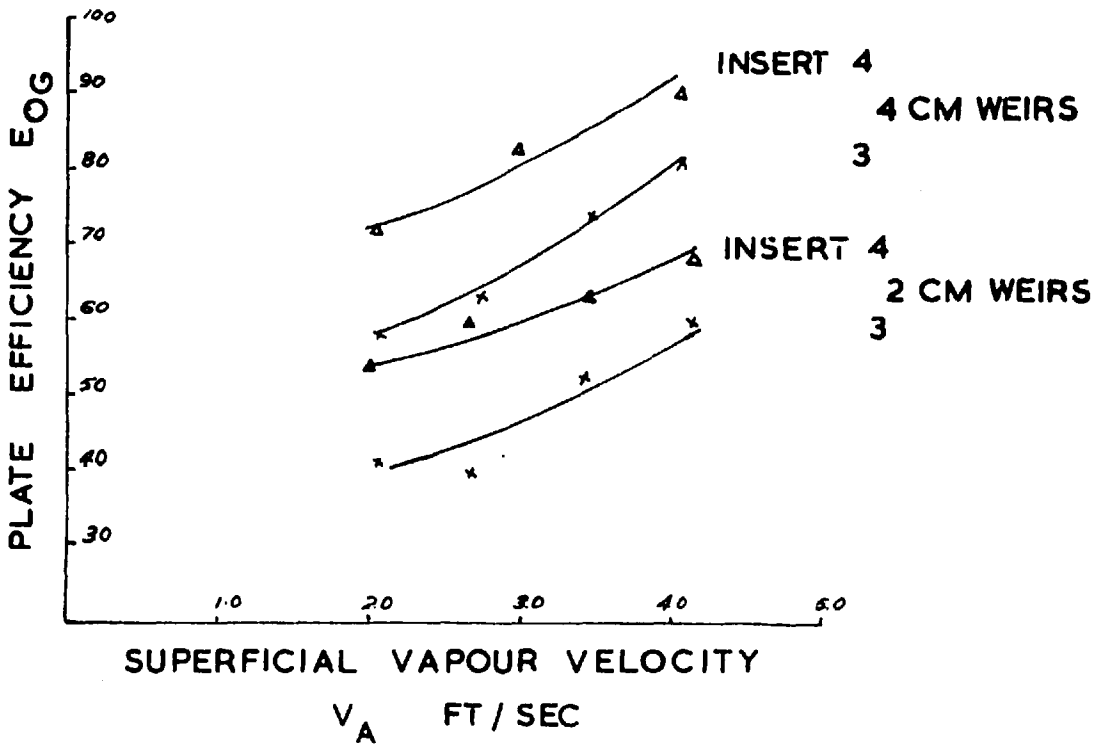


FIGURE 21



shows no effect of % free area when plotted against hole velocity. It is not surprising therefore that better correlation of the plate efficiencies is also obtained in terms of hole velocity, in agreement with the findings of Hellums et al (36).

Correlation of the plate efficiency data against hole velocity has eliminated the effect of % free area but distinct curves for each weir height studied are obtained. Again the effect of weir height is to increase the overall plate efficiency and the liquid hold up on the plate. The shape of the curves, showing a sharp initial increase followed by a region in which the increase in plate efficiency with increasing hole velocity is less pronounced, is best explained by consideration of the effect of free area. The liquid hold-up tends to show a more pronounced increase with vapour rate for the 23% free area plates, and since the results for these plates are in the lower hole velocity range this may be connected with the corresponding faster change of plate efficiency in this region.

It seems at first surprising that plate efficiencies should increase with vapour rate rather than decrease, since it is commonly held that the predominant effect of increasing vapour velocity is a reduction in contact time.

The average vapour contact time has been calculated from the relationship

$$t_G = \phi / v_A$$

where ϕ = vapour hold up (ft^3/ft^2 of plate bubbling area)

and v_A = superficial vapour velocity based on plate bubbling area (ft/sec)

From this work the value of the average vapour contact time increased with increasing vapour rate, a fact in direct contradiction to the generally accepted view. In this work, the increase in the height of dispersion above the plate with increasing vapour rate more than counterbalances the fact that the vapour passes through the dispersion at a faster rate. The numerical value of vapour contact time is greater for the 23% free area inserts than for the 10% free area inserts at the same hole velocity which seems to indicate that contact time is not the predominant factor and other effects are equally important.

Attempts were made to relate the number of vapour phase transfer units, N_G, evaluated as $- \ln(1 - Eo_G)$, to the vapour contact time as was done in the A.I.Ch.E. research programme. Correlation in terms of N_G was not as successful as for overall plate efficiency. This would indicate that liquid mixing effects on the plate are significant and it appears that the generally held view that there is complete liquid mixing in small columns does not hold in this case. Since the project was not set up to perform plate mixing studies, a detailed study of the mass transfer process

was not possible; nevertheless general conclusions can be drawn about the relationship between the overall plate efficiency and the nature of the hydrodynamic regime on the plate.

Figure 22 shows that the overall plate efficiency is determined by the hole velocity and the weir height, parameters that have been shown in the prior hydrodynamics study, to determine the total liquid hold up on the plate and the distribution of the hold up between clear liquid in the bubbling zone near the plate and the vapour-liquid dispersed region above it. Attempts to correlate the overall plate efficiency in terms of the total liquid hold up on the plate were not successful but a reasonable correlation of plate efficiency with the amount of liquid held up in the vapour-liquid dispersed region was obtained. This method of correlation, as shown in Figure 25, results in a single curve for both % free area inserts and for both weir heights, the scatter probably being due to the reliance on a visual estimate of the clear liquid depth. This result shows that mass transfer in the dispersion is important but it still has to be shown that it is predominant.

Figure 24 shows that the height of clear liquid in the bubbling zone decreases with increasing hole velocity. A qualitative estimate of the contribution to the total mass transfer occurring in the bubbling zone may be made by assuming the following relationship

$$(N_G)_L = (k_G{}^1)_L a_L (t_G)_L$$

FIGURE 24

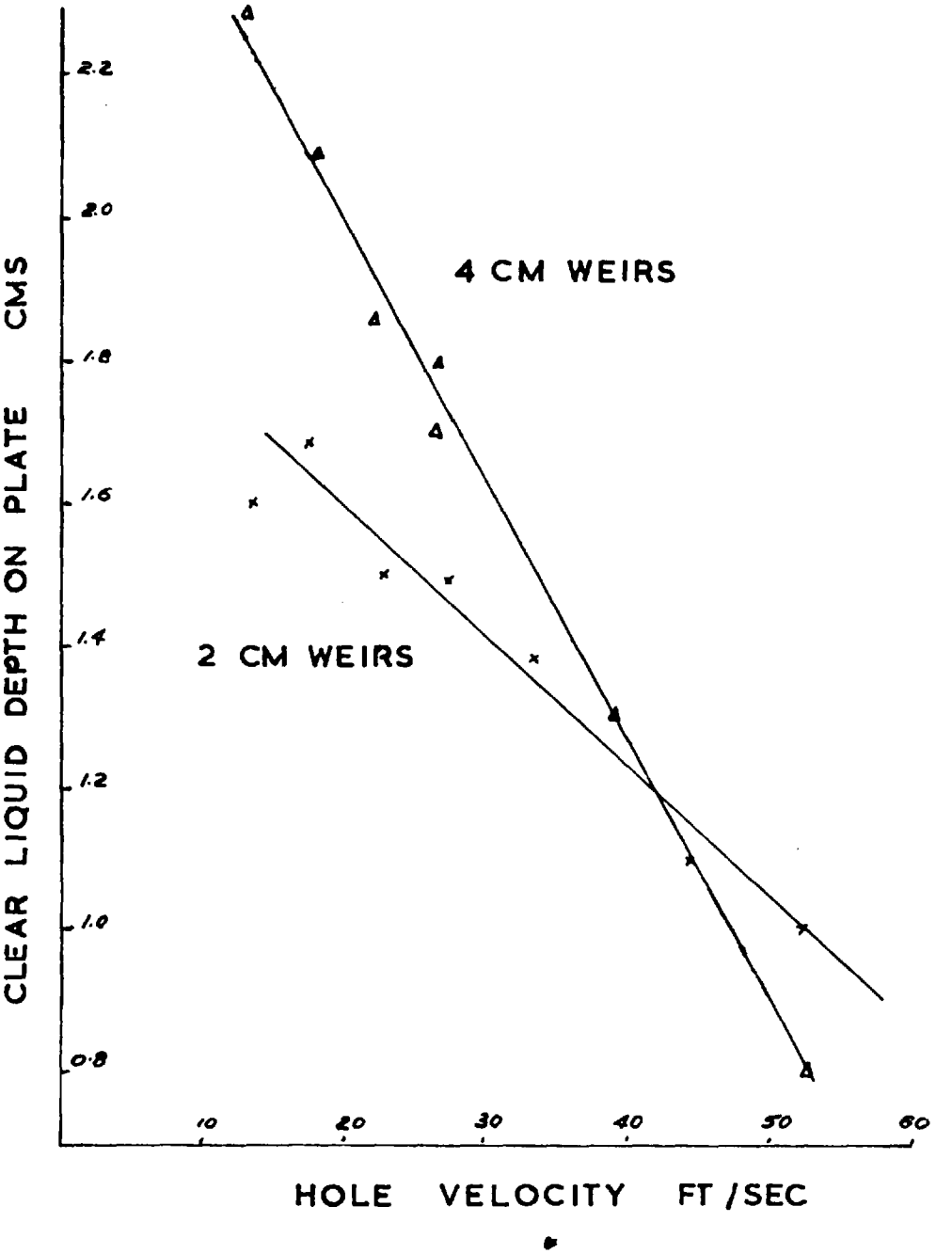
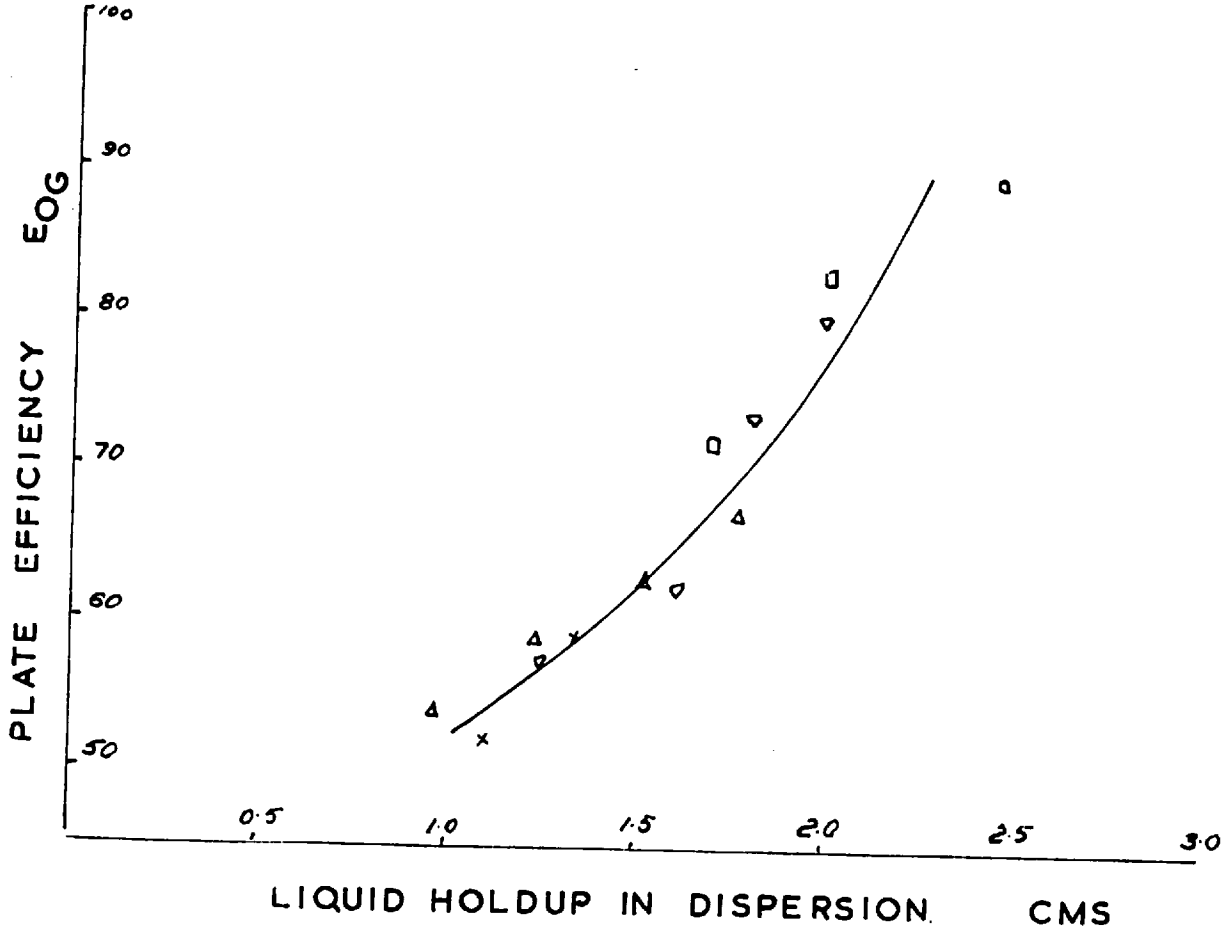

CLEAR LIQUID DEPTH ON PLATE CMS
2.2
2.0
1.8
1.6
1.4
1.2
1.0
0.8
4 CM WEIRS
2 CM WEIRS
10
20
30
40
50
60
HOLE VELOCITY FT/SEC

FIGURE 25


PLATE EFFICIENCY E_{OG}
100
90
80
70
60
50
0·5
1·0
1·5
2·0
2·5
3·0
LIQUID HOLDUP IN DISPERSION CMS

the subscript L referring to values of the several parameters in hte clear liquid of the bubbling zone as distinct from those in the vapour-liquid dispersed region.

To a first approximation the Chilton-Colburn analogy of heat and mass transfer can be applied to the turbulent mass transfer from a bubble stream so that the mass transfer coefficient $(k_G{}^1)_L$ may be taken as proportional to the vapour phase Reynolds Number ot the 0.8 power (*12*). Using the chain bubbling concpet of Van Krevelen and Hoftyzer (*73*), the bubble stream may be considered to be a chain of tightly packed bubbles stretching from the plate floor to the clear liquid surface. The total bubble interfacial area, a_L, at constant bubble size, would then be proportional to the depth of clear liquid in the tray. The average residence time in the bubbling zone is approximately the clear liquid height divided by the hole velocity, the bubbles being assumed to rise at a rate comparable with the time average vapour flow through the holes.

For the range of hole velocities and clear liquid depths given in Figure 24, the $(k_G)_L$ term would nearly treble as the vapour velocity varied from 15 to 50 ft/sec, the total bubble interfacial area would decrease by a factor of two approximately, whilst the vapour contact time would be decreased by a factor of 10. Thus even allowing for large inaccuracy in an approach of this type, the contribution of the bubbling zone would be expected to decrease rather than increase with increasing hole velocity. Thus at higher vapour

rates the major contribution to the total mass transfer process occurring on sieve plates would seem to occur in the vapour-liquid dispersed region rather than in the bubbling zone of clear liquid near the plate.

9. General Conclusions and Recommendations for Future Work

This thesis has been concerned with exploratory work connected with a new approach to plate performance studies, an approach, it is hoped, that will ultimately allow more confident design of fractionating columns by providing the necessary means of predicting plate efficiencies in terms of the hydrodynamic design parameters. Much time has been spent in designing and building apparatus and in developing experimental techniques; nevertheless the exploratory 4" column studies have yielded interesting results that allow broad conclusions to be drawn.

The plate pressure drop studies seem close to providing a more accurate design procedure; however the method of predicting static heads on the plate requires further study. The fact that the method proposed is in agreement with the data of Mayfield et al, obtained on a large column, is encouraging but further testing in the pilot plant column is required.

The dispersion density profiles show, in quantitative fashion, the two distinct hydrodynamic regions existing on sieve plates, the clear liquid in the bubbling zone near the plate and the vapour-liquid dispersed region of constant density above it. The experimental profiles confirm the view that differences exist between the dispersions formed in the air-water and light hydrocarbon systems and care should therefore be taken in extrapolating data obtained on the

air-water system to hydrocarbon systems. The dispersion density profiles also provide a reliable method of defining the height of dispersion above the plate.

The results of the plate efficiency studies showed that the overall plate efficiency could be related to the vapour-liquid dispersion parameters. The overall plate efficiency was shown to increase with increasing amounts of liquid hold up in the dispersed region and with increasing hole velocity. The hydrodynamic studies using the gamma ray absorption technique showed that these variables are determined by the column vapour rate, the % free area of the plate and the weir height. Since the higher % free area inserts give the higher percentage hold up in the dispersed region, it would be better to achieve high hole velocities by using these high % free area plates and operating at higher column superficial velocities rather than reducing the % free area of the plates.

Thus columns would appear to operate most efficiently and economically at high vapour rates hence the need to extend the experimental programme to the flooding region and to examine the mechanism of flooding in order that the column operating range might be extended.

Future experimental work should be based on the 16" diameter pilot plant column. Not only will this work be proof against the general criticism of small column results but it would enable the

influence of such factors as the height of the inlet weir and the location of splash baffles to be determined. The use of the larger column will also allow plate mixing studies to be performed.

Further elucidation of the mass transfer process occurring on sieve plates will be difficult unless a satisfactory means of interfacial area measurement can be developed. High speed cine analysis of the phenomena occurring in the middle of the dispersion rather than at the walls may yield information on interfacial areas and may also provide a model for the physical mechanism of vapour-liquid contacting in the vapour-liquid dispersed region. The wall effects will have to be eliminated and this appears feasible using a system of light probes or a tracer technique.

When a proper understanding of the influence of hydrodynamic parameters on plate efficiency has been achieved, and only when this has been achieved, should the work be extended to other systems so that the influence of system physical properties on plate efficiency may be determined.

PART III

16" PILOT PLANT DISTILLATION COLUMN

INTRODUCTION

The trend in commercial practice to towers of large diameter has accentuated the problems of maldistribution of liquid and vapour and its effect on plate efficiency. It was considered essential to work on as large a scale as possible, within the limits set by the College services and the financial resources available so that these effects might be investigated and plate mixing studies performed. A large unit would also be proof against general criticism of plate efficiency and hydraulic data obtained in small laboratory columns.

Maximum flexibility of operation was an essential requirement. The vapour rate had to be varied easily over the operational range from weeping to flooding, operation at partial reflux was desired and the column had to be capable of operating either as a stripping or a rectification column. Methods had to be found to change both the weir height and the plate geometry without dismantling the entire column and provision made for liquid and vapour sampling and thermocouple points. Although the great majority of these requirements were met, limitations as regards services, location and the necessity to keep to a limited but not ungenerous budget necessitated compromise solutions to many problems.

Feasibility Studies and Selection of General Process Conditions.

Investigation of the Departmental services showed that neither steam nor cooling water were available in the quantities necessary to operate a column, of minimum size of 12" diameter, up to the flood point. This was assumed to be at a superficial vapour

velocity of approximately six feet per second for a conventionally designed tower. The only alternative method for supplying the energy requirements appeared to be the use of a heat-pump cycle using a suitable refrigerant. The cycle would operate by condensing the refrigerant in the column reboiler, so vaporising the reboiler charge, expanding the liquid refrigerant to a lower pressure and temperature and using this cooled refrigerant as the coolant in the column condenser, the vaporised refrigerant then being recycled to the compressor. The heat energy for the distillation process, in this case, is supplied as electrical energy to the compressor motor.

The boiling point of the pentane system to be studied is 98°F, giving a condensing temperature of 91°F allowing for a 7°F temperature drop over the column. For a 25°F temperature difference across both the reboiler and condenser, the suction and delivery temperatures for the saturated refrigerant are 66°F (65 psig) and 123°F (164 psig). Between these limits, the refrigerant duty of the 5 x 4 Vee Block compressor, kindly loaned by Messrs J. & E. Hall Ltd., was 7.65×10^5 BTU/hr corresponding to a column boil up of 5000 lb/hr of pentane. On the basis of a 15.5" I.D. column, the maximum superficial vapour velocity would be 5.4 feet/second. The main process conditions were fixed in this way and the column and ancillary equipment were sized accordingly.

(Note: Process design calculations and the more important column design details are given in the Appendix to this thesis)

Refrigerant Flow Sheet Description.

Freon 12 Compressor Unit.

The basic unit consists of a 5" bore x 4" stroke, eight cylinder reciprocating vee block compressor belt driven at 665 rpm from a 100 BHP Brooks spring motor. Manual unloading equipment is incorporated, allowing both capacity control and start up under light load. High and low pressure cut outs are fitted on delivery and suction lines whilst an oil differential pressure switch guards against failure of the forced lubrication system. Start up control is by an oil immersed, combined stator/rotor Allen West starter. All wiring is 200 amp Pyrotenax copper sheathed cabling, mains connection being through an air-break isolator. The compressor and motor are anchored to a 16" thick, re-inforced concrete base keyed directly to a concrete floor. The initial levelling of the unit was facilitated by grouping 6" x $2\frac{1}{2}$" x $\frac{1}{2}$" mild steel levelling plates into the "green" foundation block, the unit was lined up by insertion of shims between the base plate and the metal plates.

Heat Exchangers

The choice of the type of heat exchanger employed was dictated by space limitations in the site area. Shell and tube exchangers with heat transfer areas of the order of 300 square feet are bulky and free space is required for tube bundle removal. The type of secondary surface light alloy heat exchanger commonly used in cyrogenic plants was chosen for its compactness and light

weight. A general description of this type of unit is given by Lenfestey[51] while the actual constructional details are shown on Marston Excelsior Ltd. Drawing No.D1431-A bound with this thesis.

The detailed process design of the two exchangers is given in the Appendix. To reduce cost the exchangers had to be identical in every way and the units purchased had a 2.41 cubic feet plain corrugated matrix, with 28 rows of Freon corrugations and 29 rows of pentane corrugations, arranged for cross contra flow with five passes on the Freon side and one pass on the pentane side. Overall design coefficients of 170 and 185 over the column reboiler and condenser respectively were used in area calculations resulting in a matrix area of 315 square feet for estimated temperature differences of 20 and 18°F. The overall weight of each exchanger is 150 lbs.

By-Pass Condenser

A plot of the refrigerant cycle on a Mollier diagram shows that more heat is supplied at the reboiler than extracted at the column condenser. The easiest way to overcome this inbalance is to condense part of the compressor delivery in a subsidiary water cooled condenser, feeding the condensed Freon 12 into the delivery line immediately prior to the column reboiler. The cycle requires that 35 lb/min of Freon 12 be condensed and area calculations show that a 12 pass, Halls N.T. condenser with 46, 7/8" tubes, 3'9" long with a condensing area of 44 square feet

would provide ample condenser capacity.

Ancillary Equipment

To achieve maximum heat transfer in the column reboiler, the condensing Freon 12 must be removed as fast as it is condensed. A high pressure float regulating valve sited below reboiler level serves this purpose. In the column condenser, the Freon 12 evaporator, the reverse situation is desired. The unit is operated flooded on the Freon side by feeding from an overhead liquid Freon receiver. This 18" diameter x 5'0" high vessel serves also as a suction separator ensuring that no entrained liquid is carried over into the compressor.

Any tendency for the high pressure float valve to 'hunt' could result in unstable cycle conditions. The capacity built into the system at the suction separator should damp out any instability set up. The stability of the refrigerant cycle is determined primarily by the operation of the by-pass condenser and a control system to maintain a constant column pressure by regulating the water flow to the by-pass condenser is the easiest way of achieving a balanced cycle. The control system fitted comprises a Foxboro Indicating Narrow Band Proportional Pressure controller actuating a $\frac{1}{2}$" Foxboro diaphragm type, pneumatic control valve in the water inlet line to the condenser.

During operation, a small quantity of crankcase oil is carried over with the Freon and accumulates in the suction separator.

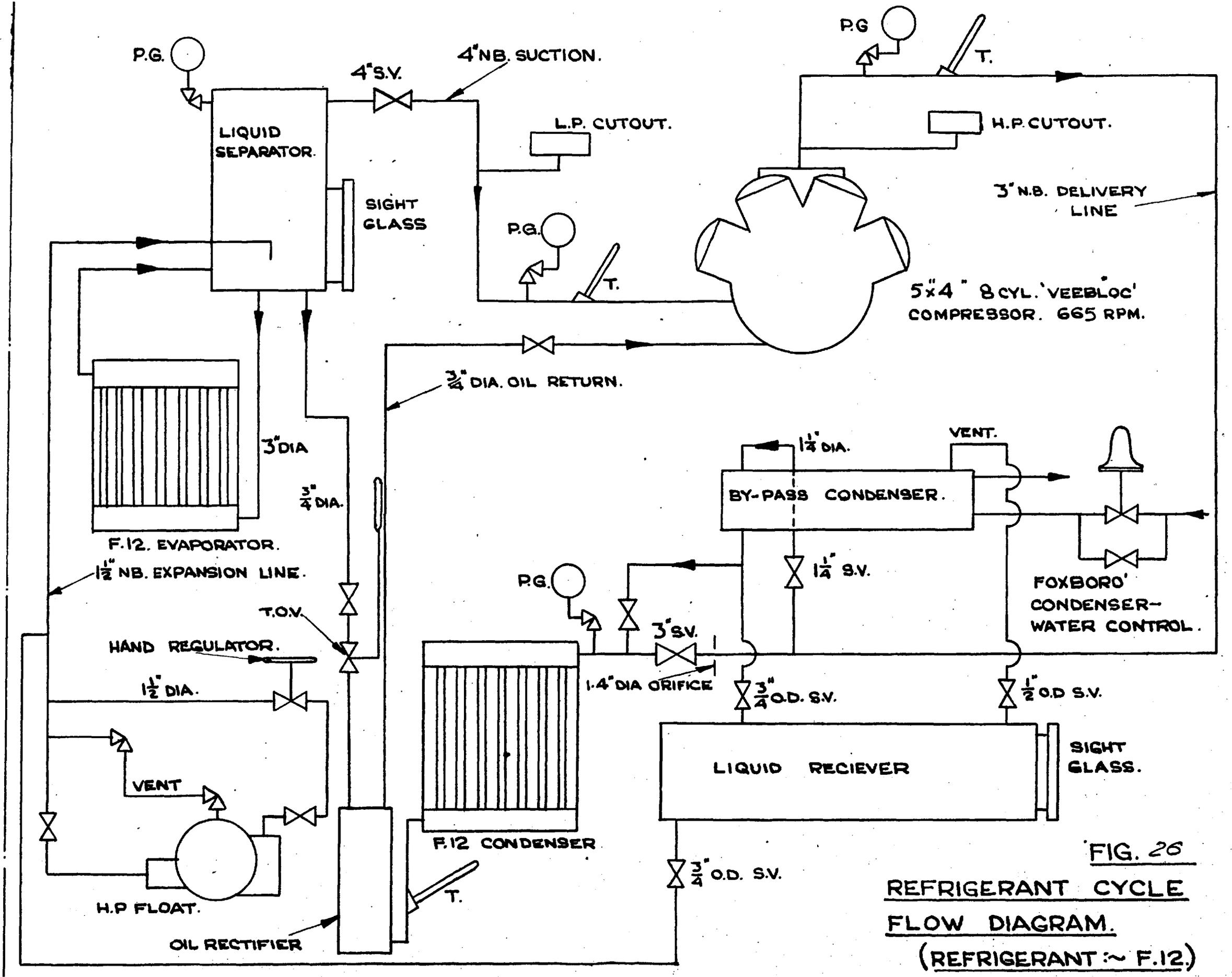


FIG. 26

REFRIGERANT CYCLE FLOW DIAGRAM.

(REFRIGERANT :~ F.12.)

17/1/62

A portion of the liquid hold up in the separator is bled off to an oil rectifier, a 6" diameter x 18" high tubular heat exchanger, the liquid Freon being evaporated off and the oil recycled to the compressor crankcase. A liquid Freon receiver of 400 lb capacity completes the refrigerant flowsheet.

Distillation Flowsheet Description.

Column Details.

The basic column unit is made up from four flanged sections of 16" O.D. x 15.5" I.D. mild steel pipe with dished end closures forming a three plate column of 11" overall length. Full details of the column sections, the size and positioning of external connections and the column internal details are given in Dore's Drawing No.3089. The partially vaporised charge from the reboiler enters the base of the column through a 6" diameter tangential inlet so as to separate entrained liquid from the vapour stream. A 6" deep Knitmesh de-entrainer pad below the bottom plate prevents any droplet mist being carried into the test section. Another de-entrainer above the top plate prevents carry over to the condenser.

The three sieve plates, on 18" plate spacing, are contained in a single section of the column so that only this section need be removed to allow the perforated inserts to be replaced. A $7\frac{1}{2}$" square hand-hole is provided above each plate to allow the weirs to be adjusted without dismantling the column. Two 2' x 2" wide glass viewing windows at 180° to each other, are provided for

visual observation of plate performance.

Variations in the refrigerant cycle heat duty are possible using the capacity control on the compressor but it is preferable to vary the vapour rate in the column by by-passing vapour around the column directly to the condenser. Since the total boil up is measured by the reflux rate at total reflux, either the flow through the column or through the by-pass needs to be metered. The direct metering of the flow through the column is not possible due to space limitations and a Type 150 Size 134 Gas Rotameter is installed in the by-pass line. Relative flow through the column and the by-pass are controlled by a gate valve in the by-pass line and an orifice line in the main vapour line to the condenser.

Plates and Downcomers

A conventional cross flow system is used, the plates being fitted with segmental downcomers to provide maximum perforated area. The column internal design is based on that developed in the 4" test rig. The fixed sections of the plate, i.e. the weir boxes, are bolted to a 7/8" x $\frac{1}{4}$" mild steel ring welded inside the column. The 1/8" thick perforated insert, made up from commercially available perforated sheet, is recessed into the support plate and fixed in position with Allen keys, the actual constructional details being shown on Dore's Drawing No.3090A. The column is fitted with 16 SWG inlet and outlet, chord weirs adjustable over the range of $\frac{1}{2}$" to 4". This is achieved by sliding the weir plate either up or down through a slot cut in the plate floor.

The necessary support above the plate is achieved by passing the weir between two sets of guide rails that serve also to seal the weir against the column wall. Splash baffles can be fitted to the outlet weir on each tray and these again are readily adjusted through the column handholes.

Reflux Piping

Condensed pentane is gravity fed to a 50 gallon feed tank set above the reflux pump. A direct connection between this tank and the main vapour line vents any vapour carry over back to the vapour space before the condenser. A Sigmund Centrifugal pump Type N-NE4, fitted with a 0.5 HP flame proof motor, capable of 16 g/m in against a 25' head, pumps reflux from the tank back to the column. To enable operation at partial reflux, provision exists to by-pass some of the reflux to the base of the column. Two Metric Size 47 Rotameters, calibrated in lb/min of pentane, are fitted directly into the reflux and by-pass lines. All valves in the reflux circuit are 1½" Teflon packed gate valves, and 'Klingerite' gasketting is used both in the reflux lines and the main column assembly. Two, 50 gallon storage tanks on the operating platform can feed by gravity either the reflux feed tank or the base of the column.

Column Layout and Site Details

The only location available within the Department was a basement laboratory with maximum headroom of 15'. The major disadvantage of the low headroom was partially counterbalanced

CONTROL PANEL.

SIGNAL TO FOXBORO' CONTROL VALVE ON BY-PASS CONDENSER.

$\frac{3}{8}$"

P.G

P.G

F.12 DELIVERY

F-12 SUCTION.

D.P CELL RECORDER

PRESSURE CONTROLLER

$\frac{1}{2}$" VENTS

50 GALL. STORAGE TANKS

REFLUX ROTAMETERS METRIC SIZE 47.

$\frac{1}{2}$" VENT.

SIGHT GLASSES.

50 GALL. FEED TANK.

$\frac{1}{2}$" DRAIN

SIGMUND N-NE4 16 G.P.M., 0.5 H.P., CENTRIFUGAL PUMP.

$\frac{1}{2}$" FILLING POINT

$\frac{1}{2}$" VENT.

4"

16" DIA. M.S. DISTILLATION COLUMN.

ORIFICE PLATE

4"

GAS ROTA-METER. TYPE. 150. SIZE. 134.

COLUMN CONDENSER.

6"

3"

COLUMN REBOILER.

$\frac{1}{2}$" DRAIN POINT.

$1\frac{1}{2}$"

FIG. 27

FLOW DIAGRAM for 16" Diam. DISTILLATION COLUMN.

18/7/62.

by the solid foundation available for the compressor block and adequate escape ways through existing windows and doors. A corner of the laboratory, 11' x 9½' in floor area was portioned off with a 4" pottery-block wall to form a flameproof enclosure. Within this enclosure the column and support structure was erected in accordance with Dores Drawing No.3101/CES. The rather cramped layout was made necessary by the need to allow unhindered access to the main laboratory doors that were within the site area. As can be seen from the column layout, the main operating panel, pump starter, reflux rotameters and the by-pass control system, are grouped together for ease of operation.

The rig received considerable attention from the London County Council Petroleum Inspector and certain building alterations were made to comply with the relevant sections of the Petroleum Act. All windows had to be reglazed with ¼" wired safety glass and 3" sills provided at each door to contain any spillage of pentane. An extraction system capable of 12 air changes per hour was installed, the high level air intake being fitted with a flame cowling. Column and storage tank vents are led to atmosphere and the ends covered with flame arrestor meshes. Three escape ways are provided in various parts of the enclosure and Dry Powder fire extinguishers and a supply of sand are located within the enclosure. All electrical installations within the enclosure satisfied the relevant Buxton Group requirements. The main compressor motor and starter were located outside the

flameproof area to avoid the necessity to provide flameproof equipment.

Experimental Facilities

The column is set up to allow the accumulation of experimental data necessary to investigate the hydrodynamic characteristics of sieve trays and plate efficiencies for the various types of vapour-liquid contacting on the plate. Liquid and vapour sampling paints are located as shown in Figure 27. Liquid sampling on the plates and at the bottom of the downcomers is through 1/8" bore sample lines let directly into the plate floor. Liquid samples from the top of the downcomers are obtained from an overflow pot placed in the liquid path in the downcomer. Samples are chilled using a "solid CO_2-alcohol freezing mixture to prevent flashing of the low boiling components. For efficiency measurements at total reflux only liquid sampling is necessary; however specially designed vapour sampling probes are fitted to allow plate efficiency measurements at partial reflux. Vapour and liquid temperatures are measured by using a conventional Potentiometer circuit. A Foxboro Differential Pressure Cell, calibrated in the range 0-10" W.G. is connected across the test plate and yields a continuous record of total plate pressure drop on a Foxboro Circular Chart Recorder. A modified traverse system is under construction to allow both vertical and horizontal dispersion density traverses to be made using the same gamma ray technique as on the 4" column.

Provision is also made to use light grids to illuminate the centre of the plate to allow high speed cine investigation of the nature of the dispersion.

10.1 Performance Proving Trial on Pilot Plant Column

A trial run was performed on the pilot plant column to check the stability of operation and the limit of plant performance.

Some difficulty was at first experienced in bringing the column to a steady state at high throughputs. The compressor has to be started under light load and the heat pump duty increased by bringing in several banks of cylinders in discrete steps. The step change in heat pump duty that occurred when a bank of cylinders was brought in was sufficient to vaporise most of the reboiler charge and the compressor cut out in the automatic high pressure switch. Successful run up to maximum boil up rate was obtained by by-passing vapour around the high pressure float valve until the compressor was fully loaded on all cylinders. The heat pump duty was then slowly increased by carefully closing the by pass valve so that violent fluctuations in the reboiler level were avoided. In this way the plant was brought up to maximum capacity and operation at a steady state was possible. The column pressure control system operated satisfactorily and it was found that if the reflux pump delivery valve was adjusted to maintain a constant level in the reflux drum, the column soon settled down to a steady state taking about $1\frac{1}{2}$ hours from the time the Freon by-pass valve was fully closed.

The boil up rate at maximum capacity was 8000 lb/hr of the n pentane-iso pentane mixture corresponding to a column superficial velocity of 8 ft/sec and a hole velocity of 85 ft/sec. Suction and

delivery pressures were 32 and 154 psig respectively. The heat exchangers were designed to give a boil up rate of 7,600 lb/hour. Since the design rate has been exceeded and the value of delivery pressure is close to the design value, the overall design coefficients used are reliable, the low suction pressure being most likely due to inefficient purging of non condensable gases from the condenser matrix. The low value of suction pressure has increased the heat pump duty, mechanical power requirements being correspondingly increased, leading to higher boil up rates than predicted.

The run was carried out at total reflux, using 4 cm weirs and a splash-baffle. The plate was similar to Insert No 4 of the 4 inch column, having $\frac{1}{4}$ inch holes on $\frac{3}{8}$ inch pitch. Liquid samples were taken, and the measured plate efficiency was 45%. This value is much lower than would have been expected from the 4 inch column results, but it would be extremely unwise to attempt to draw any conclusions from this single measurement. Errors are easily possible, and in particular it is felt that some vaporisation of the liquid may have occurred in the sampling lines; a more efficient method of cooling these is highly desirable. In any case the vapour velocity was much higher than those employed in the 4 inch column tests, so that direct comparison of results is not possible. A high gas flow rate was deliberately used to ascertain the limiting capacity of the system, and the trial should simply be considered as a demonstration that the plant can be run under stable conditions, and fulfills the design conditions.

NOMENCLATURE

a	interfacial area ft^2/ft^3 of vapour hold up
A	cross sectional area of column available for vapour flow ft^2
A_h	total free area of plate perforations ft^2
C	orifice coefficient
Eo	overall plate efficiency
E_{pG}	point efficiency
f	fraction free area of active plate
f_p	frequency of pressure fluctuations in the chamber under the plate $secs^{-1}$
Fh	hole F factor $(v_h \rho_g^{\frac{1}{2}})$
Fs	column F factor $(v_s \rho_g^{\frac{1}{2}})$
g	acceleration due to gravity ft/sec^2
Gm	molal flow rate of vapour 16 moles/hr ft^2
h_D	dynamic head of liquid on the plate cms of liquid
h_{DP}	dry plate pressure drop " " "
h_R	residual pressure drop " " "
hs	static head of liquid on the tray " " "
hT	total plate pressure drop " " "
hw	weir height + weir crest " " "
k'_G	mass transfer coefficient 16 moles/hr ft^2 (unit conc. diff.)
Lm	molal liquid rate 16 moles/hr ft^2
m	slope of the equilibrium line

N_P overall no of vapour phase mass transfer units

N_G no of vapour phase mass transfer units

NL " " liquid " " " "

ϵ_G average time of contact of vapour with liquid (secs)

v_A vapour velocity based on plate bubbling area ft/sec

v_h vapour velocity through the holes ft/sec

vs superficial vapour velocity in the column ft/sec

β aeration factor due to Kemp and Lyle

β' aeration factor due to Mayfield

ρ_g vapour density $16/ft^3$

ρ_L liquid density $16/ft^3$

σ surface tension dyne/cm

μ_L liquid viscosity centipoise

μ_g vapour viscosity "

ϕ vapour hold up in the dispersion ft^3/ft^2 of bubbling area

BIBLIOGRAPHY

(1) Alexander L.G. et al — Chem.Eng.Prog.Symp. Series No 10 93 1954

(2) Andrews S.P. — Proc.Int.Symp.on Distillation Brighton England May 1959

(3) Arnold D.S. et al — Chem.Eng.Prog. 48 633 1952

(4) Ashley W. — Refrig.Eng. 43 89 1942

(5) Baker F. — ibid 61 986 1953

(6) Batchelor G.K. — "Theory of Homogeneous Turbulence" Camb.Uni.Press 1959 p 134

(7) Brown R.S. — Ph.D. Thesis Univ. of California (Berkeley) 1958

(8) Calderbank P.H. — Trans.Inst.Chem.Eng.Lond. 36 442 1958

(9) Calderbank P.H. et al — Proc.Int.Symposium on Distillation Brighton England May 1959

(10) Calderbank P.H. and Rennie J. — Trans.Inst.Chem.Eng.Lond. 40 3 1962

(11) Cameron J.F. — "Radio Isotopes in Scientific Research" Pergamon Press London 1958

(12) Chilton T.H. and Colburn A.P. — Ind.Eng.Chem. 26 1183 1934

(13) Clark N.O. — J.Sci.Inst. 23 256 1946

(14) Clark N.O. and Blackman V. — Trans.Farad.Soc. 44 1 1948

(15) Crozier R.A. — Ph.D. Thesis Univ.of Michigan 1956

(16) Danckwerts P.V. — Chem.Eng.Sci. 2 1 1953

(17) Davies J.A. — Ind.Eng.Chem. 39 778 1947

(18) Drickamer H.G. and Bradford J.R. — Trans.Am.Inst.Chem.Eng. 39 319 1943

(19) Eduljee H.E. — Brit.Chem.Eng. 3 14 1958

(20) Ellis S.R.M. and Bennet R.J. — J.Inst.Pet. 46 19 1960

(21) Foss A.S. et al — A.I.Ch.E.Journal 4 231 1958

(22) Foss A.S. and Gerster J.A. — Chem.Eng.Prog. 52 28 1956

(23) Garner F.H. et al — Trans.Inst.Chem.Eng.Lond 31 168 1953

(24) Garner F.H. and Freshwater D.C. — ibid 33 205 1955

(25) Gautreaux M.F. and O'Connell H.E. — Chem.Eng.Prog. 51 232 1955

(26) Geddes R.L. — Trans.Am.Inst.Chem.Eng. 42 79 1946

(27) Gerster J.A. — Univ.of Delaware, Communication to ABCM/BCPMA Distillation Panel May 1958

(28) Gerster J.A. et al — "Tray Efficiencies on Distillation Columns" Univ.of Delaware 1958

(29) Gerster J.A. et al — Chem.Eng.Prog. 47 523 1951

(30) Gerster J.A. et al — ibid 47 621 1951

(31) Gerster J.A. et al — ibid 45 716 1949

(32) Gibson E.J. et al — Int.J.of App.Rad and Isotopes 2 129 1957

(33) Gilbert T.J. — Chem.Eng.Sci. 10 243 1959

(34) Grohse E.W. — A.I.Ch.E.Journal 1 358 1955

(35) Hay J.M. and Johnson A.I — A.I.Ch.E.Journal 6 465 1958

(36) Helluns J.D. et al — ibid 4 465 1958

(37) Helsby F.W. — Ph.D. Thesis Univ.of London (I.C.) 1958

(38) Holladay R. Refrig.Eng. 64 39 1956

(39) Hours R. "Mesure de la Concentration en Graz d'une Emulsion Gas Liquide par Absorption de Rayons Gamma" Rapport CEA No 521 1956

(40) Highmark G.A. and O'Connell H.E. Chem.Eng.Prog. 53 127 1957

(41) Hunt C.D. et al A.I.Ch.E. Journal 1 441 1955

(42) Hutchinson M.H. et al "Aerated Flow Principle Applied to Sieve Plates" Paper presented at the Los Angeles meeting of the A.I.Ch.E. May 1949

(43) Hiwa C.S. and Beckmann R.B. A.I.Ch.E. Journal 6 359 1960

(44) Jones J.B. and Pyle C. Chem.Eng.Prog. 51 424 1955

(45) Kafarov VV. and Vigdorov A.S. J.App.Chem.(USSR) 34 542 1961

(46) Kamei S. et al Chem.Eng.(Japan) 18 108 1954

(47) Kemp H.S. and Pyle C. Chem.Eng.Prog. 45 435 1949

(48) Kern D.Q. "Process Heat Transfer" McGraw Hill New York 1950

(49) Kirschbaum E. Chem.Ing.Tech. 72 283 1962

(50) Kolodzie P.A. and Van Winkle M. A.I.Ch.E.Journal 3 305 1957

(51) Lenfestey A.G. "Secondary Surface Heat Exchangers" Paper presented to the Low Temp. Group of the Phys.Soc. London Dec. 1959

(52) Lewis W.K. — Ind.Eng.Chem. 28 399 1936

(53) Manning E. et al — ibid 49 2051 1957

(54) Mayfield F.D. et al — ibid 44 2238 1952

(55) Mukhlenor I.P. — J.App.Chem. (USSR) 31 1328 1958

(56) Mukhlenor I.P. and Tarat E.Y. — ibid 32 2055 1959

(57) O'Connell H.E. — Trans.Am.Inst.Chem.Eng. 42 741 1946

(58) Pai Shih. I. — "Fluid Dynamics of Jets" Van Nostram and Co. Inc. N.Y. 1954

(59) Parry L. and Hodgson J. — J.Brit.Inst.Rad.Eng. 17 365 1957

(60) Planck C.A. — Ph.D. Thesis North Carolina State College 1957

(61) Platt W.A. — Ph.D. Thesis Univ.of London (I.C.) 1961

(62) Potter O. and Pattel S. — Refrig.Eng. 64 45 1956

(63) Pozin M.E. et al — J.App.Chem.(USSR) 27 9 1954

(64) Pozin M.E. and Kopylev J. — ibid 31 375 1958

(65) Pozin M.E. et al — ibid 30 43 1957

(66) Prince R.G.H. — Proc.Int.Symp.on Distillation Brighton England May 1959

(67) Redlich O and Kister A.T. — J.Amer.Chem.Soc. 71 505 1947

(68) Robinson C.S. and Gilliand E.R. — "Elements of Fractional Distillation" McGraw Hill N.Y. 1950

969) Rustin A. — Ph.D. Thesis Univ.of Birmingham 1961

(70) Smith P.L. and Van Winkle M. A.I.Ch.E. Journal 4 266 1958

(71) Trice V.G. and Rodgers W.A. ibid 2 205 1956

(72) Umholtz C.L. and Van Winkle M. Ind.Eng.Chem. 49 226 1957

(73) Van Krevelen D.W. and Hoftyzer H. Chem.Eng.Prog. 46 29 1950

(74) Vanokur Y.G. and Delman V.V. Khim.Prom. 7 619 1959

(75) Whitehouse W.J. and Putnam J.L. "Radio Active Isotopes" Oxford Univ.Press 1953

(76) Whitman W. Chem.and Met.Eng. 24 146 1923

(77) Witzig C.J. Refrig.Eng. 56 153 1948

(78) Yokota N. Chem.Eng.(Japan) 23 438 1959

(79) Zuiderweg F.J. and Harmens H. Chem.Eng.Sci. 9 89 1958

CHECK ON VALIDITY OF RADIO ISOTOPE TECHNIQUE FOR LIQUID HOLD UP DETERMINATION

Run No. A-1

System: Air-Water

Air Flow Rate: 1.02 feet/sec (superficial)

Column F factor: 1.07

Calibration points:

column empty	98 secs
column full of water	205 secs

Height above Plate	Time for 50000 counts	Dispersion density
cms.	secs.	Vol. fraction liquid
0.5	163	0.71
0.7	166	0.73
0.8	158	0.65
0.9	153	0.6
1.1	143	0.51
1.6	140	0.48
2.1	126.5	0.34
2.7	119	0.26
3.6	115	0.21
4.0	110.5	0.16
4.7	108	0.13
5.1	106	0.10
5.7	105	0.09
6.2	99.5	0.02
7.0	98.5	0.01

Liquid Hold Up by Integration of Density Profile	= 118 mls.
Actual Liquid Hold Up by Draining Dispersion	= 125 mls.
% Error in Radio Isotope Determination	= 5.6%

Run No. A-2

System: Air-Water

Air Flow Rate: 1 ft/sec (superficial)

Column F factor: 0.9

Calibration points:

* column empty	106 secs.
column full of water	250 secs.

Height above Plate cms.	Time for 50000 counts secs.	Dispersion density Vol. Fraction liquid
0.7	171.5	0.56
1.3	170	0.55
1.8	169	0.54
2.4	163	0.5
3.3	161.5	0.49
4.2	160	0.48
5.0	161.5	0.49
7.0	161.5	0.49
7.8	157	0.46
8.7	147	0.38
9.6	135	0.28
10.5	123	0.17
11.4	117	0.11
12.3	113	0.07
13.2	109	0.03
14.0	108	0.02

Liquid Hold Up by Integration of Density Profile = 430 mls.

Liquid Hold Up by Draining Dispersion = 450 mls.

% Error in Radio Isotope Technique = 4.6%

* Glass column

Run No. A-3

System: Air-Water

Air Flow Rate: 2.9 ft/sec (superficial)

Column F factor: 2.6

Calibration points:

column empty 98 secs.
column full of water 205 secs.

Height above Plate cms.	Time for 50000 counts secs.	Dispersion density Vol. fraction liquid
0.5	158.5	0.65
0.8	158.5	0.65
1.4	157.5	0.55
1.8	125.5	0.33
2.5	123	0.30
2.9	123	0.30
3.6	123	0.30
4.7	123	0.30
5.8	123	0.30
6.3	122	0.29
7.4	115	0.21
7.9	112	0.18
8.5	110	0.15
9.1	107.5	0.11
10.6	100	0.03
12.8	98.5	0.01

Liquid Hold Up by Integration of Density Profile = 192 mls.

Liquid Hold Up by Draining the Dispersion = 200 mls.

% Error in Radio Isotope Technique = 4%

Run No. A-4

System: Air-Water

Air Flow Rate: 2.5 ft/sec (superficial)

Column F factor: 2.24

Calibration points:

column empty	106 secs.
column full of water	250 secs.

Height above Plate cms.	Time for 50000 counts secs.	Dispersion Density Vol. fraction liquid
0.5	163	0.50
1.1	163	0.50
2.0	157	0.46
3.3	149.5	0.40
4.0	147	0.38
5.7	147	0.38
6.6	145	0.36
7.5	142.5	0.34
8.5	142.5	0.34
9.4	143.5	0.35
11.2	145.5	0.36
12.1	143.5	0.35
12.9	138	0.30
13.9	135.5	0.28
14.8	125	0.19
15.9	121	0.15
16.6	115.5	0.10
19.2	114	0.08
24.0	107	0.01

Liquid Hold Up by Integrating Density Profile = 490 mls

Liquid Hold Up by Draining Dispersion = 500 mls

% Error in Radio Isotope Technique = 2%

Table 1 Insert 1 1/16" holes on $\frac{1}{8}$" Triangular Patch 2cm Weirs

Run No.	1	2	3	4	5	6
Vapour Rate based on active area of plate (ft/sec)$\frac{1}{2}$	2.0	2.61	3.38	3.76	4.4	5.24
F_A (ρv^2)	0.90	1.16	1.51	1.67	1.96	2.33
Liquid Rate (gpm)	0.17	0.22	0.28	0.32	0.39	0.43
Clear liquid height (cms)	1.7	1.7	1.7	1.5	1.25	1.0
Dynamic head (cms)	1.4	1.3	1.25	1.25	1.2	1.1

	Height (cms)	Dispersion Density	Height (cms)	Dispersion Density	Height (cms)	Dispersion Density	Height (cms)	Dispersion Density	Height (cms)	Dispersion Density	Height (cms)	Dispersion Density
	0	0.4	0	0.355	0	0.335	0	0.32	0	0.31	0	0.3
DISPERSION	0.6	0.45	0.6	0.385	0.6	0.335	0.6	0.33	0.6	0.325	0.6	0.295
	1.1	0.38	1.1	0.335	1.1	0.305	1.1	0.295	1.1	0.285	1.1	0.265
DENSITY	1.6	0.27	1.6	0.335	1.6	0.225	1.6	0.225	1.6	0.22	1.7	0.205
	3.0	0.17	3.0	0.13	3.1	0.110	3.0	0.215	3.0	0.125	3.0	0.12
PROFILE	3.8	0.14	3.7	0.105	4.0	0.08	3.8	0.09	3.8	0.105	4.2	0.10
	4.6	0.12	4.4	0.095	4.6	0.07	4.8	0.08	4.9	0.08	5.5	0.078
DATA	5.3	0.10	5.1	0.09	5.6	0.075	5.7	0.075	6.0	0.075	6.7	0.06
	6.0	0.075	5.9	0.08	6.6	0.065	6.6	0.07	7.1	0.065	8.0	0.06
	6.8	0.035	6.6	0.075	6.9	0.065	7.4	0.065	8.2	0.065	9.3	0.055
	7.1	0.035	7.3	0.055	7.6	0.055	8.4	0.06	9.3	0.055	10.5	0.045
	7.4	0.005	8.0	0.055	8.3	0.05	9.3	0.06	10.4	0.06	11.8	0.05
			8.6	0.03	9.1	0.04	10.2	0.05	11.5	0.055	13.1	0.045
			9.3	0.025	9.8	0.035	11.1	0.035	12.6	0.05	14.4	0.045
			10.9	0.01	10.5	0.03	12.0	0.035	13.7	0.05	15.7	0.035
					11.2	0.025	12.9	0.025	15.1	0.02	17.5	0.015
							13.2	0.001				
Calculated Static Head (cms)	1.38		1.29		1.31		1.39		1.50		1.65	
% Liquid in Dispersion	47%		54%		58%		64%		72%		83%	

Table 2 Insert 1 1/16" holes on $\frac{1}{8}$" Triangular P tch 3cm Weirs

Run No.	7	8	9	10	11	12	13
Vapour Rate based on active area of plate (ft/sec)	1.73	1.98	2.6	3.38	3.78	4.4	5.25
F_A ($\rho v_s^{\frac{1}{2}}$)	0.77	0.88	1.15	1.5	1.68	1.95	2.33
Liquid Rate (gpm)	0.14	0.16	0.22	0.28	0.31	0.37	0.44
Clear liquid height (cms)	2.1	1.8	1.7	1.7	1.5	1.2	1.1
Dynamic head (cms)	2.1	2.0	1.9	1.75	1.7	1.6	1.5

DISPERSION DENSITY PROFILE DATA

Height (cms)	Dispersion Density	Height (cms)	Dispersion Density	Height (cms)	Dispersion Density	Height (cms)	Dispersion Density	Height (cms)	Dispersion Density	Height (cms)	Dispersion Density	Height (cms)	Dispersion Density
0	0.48	0	0.46	0.6	0.435	0.6	0.37	0.6	0.335	0.6	0.33	0.6	0.3
0.6	0.51	0.5	0.485	1.1	0.43	1.1	0.37	1.1	0.35	1.5	0.255	1.1	0.275
1.3	0.50	1.3	0.465	1.8	0.335	1.8	0.265	1.8	0.26	2.2	0.215	1.6	0.235
3.4	0.205	2.2	0.315	2.2	0.27	2.2	0.235	2.2	0.225	3.9	0.15	2.2	0.18
4.0	0.18	3.4	0.185	3.5	0.17	3.7	0.155	3.4	0.155	5.4	0.115	3.3	0.15
4.5	0.18	4.2	0.165	4.2	0.15	4.7	0.13	4.6	0.125	7.0	0.10	4.4	0.125
5.2	0.16	4.7	0.16	4.9	0.135	5.4	0.115	5.7	0.11	8.6	0.095	5.4	0.115
6.0	0.145	5.4	0.145	5.6	0.13	6.4	0.105	6.7	0.09	10.2	0.09	6.7	0.085
6.7	0.10	6.2	0.14	6.4	0.12	7.3	0.105	7.8	0.09	12.2	0.065	8.0	0.085
7.2	0.075	6.9	0.11	7.1	0.115	8.2	0.105	8.9	0.098	14.1	0.035	9.5	0.07
7.8	0.05	7.6	0.085	7.8	0.085	9.1	0.085	10.0	0.075			10.7	0.07
8.4	0.04	8.4	0.05	8.5	0.08	10.0	0.06	11.2	0.065			12.2	0.07
8.9	0.02	9.1	0.02	9.3	0.06	10.9	0.06	12.2	0.03			13.4	0.065
				10.1	0.025	11.8	0.025	13.0	0.015			14.7	0.055
				10.5	0.01							16.0	0.04
												17.1	0.03
												18.1	0.025

Calculated Static head (cms)	2.06	1.99	1.86	1.83	1.84	1.87	1.92
% Liquid in Dispersion	52	56.3	59.6	64.3	71.0	77.5	82

Table 3 Insert 1 1/16" holes on $\frac{1}{8}$" Triangular pitch 4 cm Weirs

Run No.	14	15	16	17	18	19
Vapour Rate based on active area of plate (ft/sec)	2.02	2.62	3.4	3.78	4.4	5.25
F_A ($\rho^{\frac{1}{2}}$)	0.9	1.2	1.5	1.68	1.95	2.33
Liquid Rate (gpm)	0.16	0.22	0.28	0.31	0.39	0.44
Clear liquid height (cms)	2.3	2.0	1.7	1.5	1.3	1.2
Dynamic head (cms)	2.5	2.4	2.25	2.15	2.1	1.9

	Height (cms)	Dispersion Density	Height (cms)	Dispersion Density	Height (cms)	Dispersion Density	Height (cms)	Dispersion Density	Height (cms)	Dispersion Density	Height (cms)	Dispersion Density
DISPERSION DENSITY PROFILE DATA	0.5	0.51	0.5	0.435	0.5	0.42	0.5	0.375	0.5	0.345	0.6	0.305
	1.4	0.48	1.3	0.435	1.3	0.37	1.4	0.355	1.4	0.29	1.4	0.27
	2.4	0.35	2.3	0.315	2.4	0.24	2.3	0.25	2.3	0.21	2.3	0.205
	3.4	0.245	3.2	0.225	3.5	0.20	3.3	0.195	3.2	0.185	3.2	0.16
	5.0	0.195	5.0	0.17	5.2	0.16	5.0	0.16	5.1	0.145	5.1	0.16
	6.1	0.175	6.1	0.145	6.4	0.145	6.2	0.145	6.1	0.145	6.1	0.14
	7.2	0.14	7.2	0.125	7.5	0.13	7.2	0.125	7.2	0.125	7.4	0.125
	8.3	0.075	8.2	0.10	8.6	0.11	8.3	0.11	8.3	0.09	8.7	0.105
	9.4	0.035	9.1	0.065	9.7	0.09	9.4	0.11	9.4	0.10	10.0	0.10
	10.1	0.02	10.2	0.038	10.9	0.07	10.5	0.075	10.5	0.095	11.2	0.085
			10.8	0.02	12.0	0.06	11.4	0.075	11.6	0.085	12.7	0.085
					12.9	0.03	12.5	0.05	13.1	0.07	14.1	0.085
					13.4	0.005	13.6	0.03	14.3	0.045	15.6	0.07
							14.1	0.015	15.2	0.03	17.1	0.05
									15.8	0.02	18.5	0.05
											19.6	0.03
											20.3	0.01

Calculated Static Head (cms)	2.42	2.29	2.27	2.25	2.25	2.4
% Liquid in Dispersion	53.6%	[illegible]	68%	74.6%	79.8%	84%

Table 4 Insert 2 1/16" holes on 3/16" Triangular Pitch 2cm Weirs

Run No.	20	21	22	23	24	25
Vapour Rate based on active area of plate (ft/sec)	1.98	2.61	3.16	3.78	4.4	5.25
F_A ($\rho^{1/2}$)	0.88	1.16	1.4	1.68	1.96	2.33
Liquid rate (gpm)	0.16	0.22	0.26	0.31	0.37	0.44
Clear liquid height (cms)	1.7	1.5	1.1	0.7	0.5	0.4
Dynamic head (cms)	1.55	1.45	1.35	1.25	1.05	0.95

	Height (cms)	Dispersion Density	Height (cms)	Dispersion Density	Height (cms)	Dispersion Density	Height (cms)	Dispersion Density	Height (cms)	Dispersion Density	Height (cms)	Dispersion Density
	0.4	0.45	0.6	0.39	0.6	0.36	0.6	0.305	0.6	0.31	0.6	0.24
DISPERSION	1.3	0.38	1.2	0.35	1.1	0.34	1.2	0.28	1.3	0.255	1.1	0.23
	2.8	0.165	2.8	0.16	2.9	0.16	2.9	0.165	2.7	0.175	2.6	0.16
DENSITY	3.7	0.145	3.7	0.125	3.7	0.13	3.9	0.135	4.1	0.125	4.4	0.12
	4.3	0.155	4.7	0.095	5.1	0.11	6.3	0.095	7.0	0.095	8.0	0.08
PROFILE	5.6	0.12	5.5	0.11	6.2	0.10	7.6	0.09	8.5	0.085	9.9	0.065
	6.5	0.04	6.4	0.11	7.4	0.10	9.0	0.095	9.9	0.085	12.0	0.065
DATA	7.0	0.015	7.5	0.10	8.4	0.095	10.9	0.09	11.6	0.075	14.0	0.06
			8.6	0.06	9.7	0.095	12.4	0.075	13.0	0.085	15.8	0.065
					11.1	0.035	13.7	0.05	14.4	0.08	17.6	0.06
							14.6	0.015	15.9	0.065	19.6	0.065
									17.0	0.05	20.7	0.065
									17.5	0.025	22.2	0.05
											23.3	0.02
Calculated Static head (cms)	1.54		1.6		1.75		1.88		1.97		2.28	
% Liquid in Dispersion	52%		64%		76.5%		88%		92.5%		95.6%	

Table 5 Insert 2 1/16" holes on 3/16" Triangular Pitch 3cm Weirs

Run No.	26	27	28	29	30	31
Vapour Rate based on active plate area (ft/sec)	1.98	2.61	3.16	3.78	4.4	5.25
F_A ($\rho_v^{\frac{1}{2}}$)	0.88	1.16	1.4	1.68	1.96	2.33
Liquid Rate (gpm)	0.17	0.22	0.26	0.31	0.37	0.44
Clear liquid height (cms)	2.2	1.9	1.7	1.4	0.8	0.5
Dynamic head (cms)	2.1	2.05	1.95	1.7	1.5	1.3

	Height (cms)	Dispersion Density	Height (cms)	Dispersion Density	Height (cms)	Dispersion Density	Height (cms)	Dispersion Density	Height (cms)	Dispersion Density	Height (cms)	Dispersion Density
DISPERSION DENSITY PROFILE DATA	0.4	0.475	0.4	0.435	0.4	0.405	0.4	0.36	0.4	0.295	0.4	0.22
	1.5	0.41	1.4	0.385	1.4	0.365	1.3	0.305	1.4	0.225	1.3	0.18
	2.4	0.275	2.2	0.28	2.2	0.28	2.2	0.245	2.2	0.18	2.2	0.165
	3.7	0.19	3.7	0.18	3.7	0.175	3.7	0.125	3.7	0.155	3.9	0.16
	4.6	0.185	4.9	0.155	4.7	0.155	5.3	0.15	5.5	0.13	5.8	0.145
	5.5	0.17	6.0	0.155	6.3	0.13	6.8	0.13	7.3	0.125	7.9	0.11
	6.4	0.115	7.1	0.15	7.6	0.14	8.2	0.13	9.1	0.105	9.7	0.11
	7.4	0.06	8.2	0.095	8.8	0.125	9.7	0.125	10.9	0.115	11.5	0.10
	8.3	0.15	9.4	0.04	10.1	0.095	11.1	0.10	12.7	0.10	13.4	0.10
					11.4	0.04	12.9	0.06	14.5	0.07	15.4	0.10
							13.8	0.03	16.0	0.035	17.1	0.085
											20.0	0.04
Calculated Static head (cms)	1.95		2.01		2.17		2.27		2.275		2.49	
% Liquid in Dispersion	51%		60.6%		72%		86.3%		88.5%		96%	

Table 6 Insert 2 1/16" holes on 3/16" Triangular Pitch 4 cm Weirs

Run No.	32		33		34		35		36		37	
Vapour Rate based on active plate area (ft/sec)	2.01		2.61		3.4		3.78		4.4		5.25	
F_A (ρv_s^2)	0.9		1.16		1.5		1.68		1.96		2.33	
Liquid rate (gpm)	0.16		0.22		0.28		0.31		0.39		0.44	
Clear liquid height (cms)	2.2		1.8		1.1		0.8		0.5		0.3	
Dynamic head (cms)	2.45		2.35		2.0		1.9		1.6		1.2	
	Height (cms)	Dispersion Density	Height (cms)	Dispersion Density	Height (cms)	Dispersion Density	Height (cms)	Dispersion Density	Height (cms)	Dispersion Density	Height (cms)	Dispersion Density
DISPERSION DENSITY PROFILE DATA	0.5	0.505	0.5	0.445	0.5	0.405	0.4	0.36	0.4	0.3	0.5	0.245
	1.2	0.475	1.2	0.43	1.2	0.405	1.2	0.315	1.4	0.24	1.5	0.185
	2.4	0.33	2.4	0.275	2.1	0.245	2.1	0.23	2.1	0.205	2.4	0.155
	3.4	0.245	3.4	0.22	3.3	0.21	3.2	0.185	3.3	0.16	3.3	0.15
	5.1	0.205	5.2	0.18	5.1	0.16	5.3	0.17	5.2	0.145	5.5	0.145
	6.3	0.185	6.4	0.175	6.3	0.155	6.6	0.14	6.6	0.145	7.3	0.125
	7.4	0.115	7.3	0.165	7.7	0.15	8.3	0.13	8.4	0.11	9.2	0.115
	8.4	0.065	8.4	0.125	9.0	0.14	9.9	0.13	9.9	0.11	11.0	0.10
	9.5	0.015	9.5	0.075	10.3	0.13	11.5	0.12	11.5	0.105	12.8	0.09
			10.2	0.035	11.5	0.09	12.8	0.08	13.2	0.10	14.6	0.08
					12.8	0.04	13.7	0.055	14.8	0.085	16.4	0.09
							14.6	0.025	16.4	0.05	18.2	0.08
									17	0.025	20.1	0.065
											21.9	0.03
Calculated Static head (cms)	2.36		2.3		2.47		2.44		2.42		2.67	
% Liquid in Dispersion	55.6%		64.8%		80%		87.4%		93.5%		96.4%	

Table 7 Insert 3 $\frac{1}{8}$" holes on $\frac{1}{4}$" Triangular Pitch 2cm Weirs

Run No.	38	39	40	41	42	43
Vapour Rate based on active plate area (ft/sec)	1.98	2.61	3.4	3.78	4.4	5.25
F_A ($\rho v^{\frac{1}{2}}$)	0.88	1.16	1.5	1.68	1.96	2.33
Liquid Rate (gom)	0.16	0.2	0.26	0.31	0.37	0.44
Clear Liquid height (cms)	1.5	1.4	1.2	1.0	0.9	0.7
Dynamic head (cms)	1.35	1.3	1.3	1.4	1.4	1.3

	Height (cms)	Dispersion Density	Height (cms)	Dispersion Density	Height (cms)	Dispersion Density	Height (cms)	Dispersion Density	Height (cms)	Dispersion Density	Height (cms)	Dispersion Density
DISPERSION DENSITY PROFILE DATA	0.6	0.38	0.6	0.315	0.6	0.295	0.6	0.27	0.6	0.245	0.6	0.225
	1.2	0.34	1.2	0.295	1.1	0.28	1.2	0.24	1.1	0.21	1.1	0.215
	2.7	0.15	2.8	0.12	2.8	0.12	2.8	0.145	2.8	0.15	2.8	0.1 5
	4.1	0.125	4.1	0.09	4.1	0.09	4.2	0.095	4.2	0.095	4.4	0.055
	5.4	0.115	5.4	0.085	5.3	0.085	5.7	0.085	5.7	0.085	5.8	0.07
	6.7	0.05	6.6	0.065	6.9	0.055	7.1	0.07	7.1	0.06	7.3	0.07
	7.1	0.02	7.9	0.05	8.2	0.055	8.6	0.07	8.6	0.065	9.1	0.05
			9.2	0.03	9.5	0.06	10.0	0.07	10.0	0.065	10.6	0.045
					10.8	0.035	11.7	0.055	11.5	0.055	12.0	0.05
					11.7	0.02	13.2	0.035	13.0	0.055	13.5	0.05
									14.4	0.05	15.1	0.055
									15.5	0.05	16.6	0.055
									16.5	0.035	18.0	0.055
									17.7	0.02	19.5	0.055
											22.5	0.02
Calculated Static head (cms)	1.34		1.27		1.31		1.53		1.6		1.80	
% Liquid in Dispersion	56.5%		63.8%		71.2%		81.2%		85.5%		1.3%	

Table 8 Insert 3 $\frac{1}{4}$" holes on $\frac{1}{4}$" Triangular Pitch 3 cm Weirs

Run No.	44	45	46	47	48	49
Vapour Rate based on active plate area (ft/sec)	1.98	2.61	3.4	3.78	4.4	5.25
F_A ($\rho^{\frac{1}{2}}$)	0.88	1.16	1.5	1.68	1.96	2.33
Liquid Rate (gpm)	0.16	0.2	0.26	0.31	0.36	0.44
Clear liquid height (cms)	2.5	2.1	1.6	1.2	1.0	0.7
Dynamic head (cms)	2.3	2.25	2.2	2.15	2.05	1.9

	Height (cms)	Dispersion Density	Height (cms)	Dispersion Density	Height (cms)	Dispersion Density	Height (cms)	Dispersion Density	Height (cms)	Dispersion Density	Height (cms)	Dispersion Density
	0.6	0.44	0.6	0.365	0.6	0.315	0.6	0.3	0.6	0.29	0.6	0.265
DISPERSION	1.5	0.435	1.5	0.375	1.5	0.32	1.6	0.28	1.5	0.25	1.5	0.2
	2.4	0.32	2.4	0.28	2.4	0.2 5	2.4	0.23	2.4	0.21	2.4	0.16
DENSITY	3.7	0.195	3.8	0.18	3.9	0.185	3.9	0.17	3.9	0.175	3.9	0.15
	4.6	0.15	5.3	0.14	5.3	0.14	5.7	0.125	5.9	0.115	6.0	0.12
PROFILE	5.5	0.145	6.8	0.13	6.7	0.11	7.5	0.11	8.0	0.115	8.3	0.095
	6.4	0.135	8.2	0.105	8.2	0.11	9.3	0.11	10.2	0.10	10.4	0.09
DATA	7.3	0.115	9.7	0.06	9.7	0.10	11.1	0.085	12.4	0.09	12.6	0.09
	8.2	0.085	11.1	0.035	11.1	0.07	12.9	0.06	14.6	0.07	14.7	0.09
	9.1	0.035			12.6	0.04	14.2	0.045	16.8	0.05	16.9	0.075
					13.2	0.02			18.2	0.03	19.2	0.06
											21.3	0.04

Calculated Static head (cms)	2.22	2.13	2.19	2.21	2.35	2.36
% Liquid in Dispersion	49%	61.6%	74.8%	82.4%	85.6%	91.6%

Table 9 Insert 3 $\frac{1}{8}$" holes on $\frac{1}{4}$" Triangular Pitch 4cm Weirs

Run No.	50	51	52	53	54
Vapour rate based on active plate area (ft/sec)	2.26	2.95	3.66	4.4	5.24
F_A ($\rho \cdot v_k^{\frac{1}{2}}$)	1.0	1.31	1.62	1.96	2.33
Liquid rate (gpm)	0.19	0.25	0.32	0.37	0.44
Clear liquid height (cms)	2.0	1.9	1.5	1.0	0.7
Dynamic head (cms)	2.9	2.75	2.7	2.5	2.2

	Height (cms)	Dispersion Density	Height (cms)	Dispersion Density	Height (cms)	Dispersion Density	Height (cms)	Dispersion Density	Height (cms)	Dispersion Density
DISPERSION DENSITY PROFILE DATA	0.6	0.42	0.6	0.39	0.6	0.36	0.6	0.33	0.6	0.295
	1.1	0.45	1.1	0.41	1.2	0.36	1.2	0.33	1.2	0.275
	2.4	0.37	2.4	0.32	2.1	0.305	2.2	0.26	2.3	0.215
	3.3	0.295	3.4	0.26	3.2	0.235	3.2	0.22	3.4	0.175
	5.1	0.19	5.1	0.21	5.0	0.20	5.2	0.165	5.0	0.14
	6.4	0.17	6.4	0.19	6.6	0.145	7.0	0.14	7.1	0.12
	7.7	0.14	7.9	0.145	8.2	0.14	8.8	0.13	9.3	0.115
	8.9	0.10	9.3	0.14	9.9	0.135	10.6	0.115	11.6	0.105
	10.2	0.05	10.8	0.055	11.5	0.09	12.6	0.125	13.7	0.095
			12.2	0.065	13.1	0.065	14.6	0.1	16.0	0.095
			13.3	0.04	14.7	0.035	16.4	0.07	18.2	0.095
							17.6	0.055	20.4	0.06
							19.0	0.025	22.2	0.035
Calculated Static head (cms)	2.63		2.7		2.6		2.8		2.8	
% Liquid in Dispersion	64.8%		71.5%		78.3%		87.6%		92%	

Table 10 Insert 4 $\frac{1}{8}$" holes on $\frac{3}{8}$" Triangular Pitch 2cm Weirs

Run No.	55	56	57	58	59
Vapour rate based on active plate area (ft/sec)	2.26	2.95	3.76	4,4	5.24
F_A ($\rho \cdot v^{\frac{1}{2}}$)	1.0	1.31	1.67	1.96	2.33
Liquid rate (gpm)	0.19	0.25	0.32	0.37	0.44
Clear liquid height (cms)	1.5	0.8	0.8	0.5	0.3
Dynamic head (cms)	1.7	1.55	1.5	1.3	1.1

	Height (cms)	Dispersion Density	Height (cms)	Dispersion Density	Height (cms)	Dispersion Density	Height (cms)	Dispersion Density	Height (cms)	Dispersion Density
	0.6	0.44	0.6	0.36	0.6	0.32	0.6	0.265	0.6	0.235
DISPERSION	1.2	0.40	1.2	0.33	[illegible]	0.255	1.2	0.20	1.2	0.20
	[illegible]	0.21	2.8	0.19	2.8	0.15	2.8	0.14	3.0	0.135
DENSITY	3.6	0.17	4.2	0.14	4.5	0.14	5.0	0.135	5.5	0.125
	4.6	0.17	5.7	0.14	6.1	0.145	7.2	0.135	8.1	0.125
DATA	5.4	0.175	7.2	0.145	7.7	0.14	9.3	0.135	10.6	0.1 5
	6.6	0.15	8.6	0.12	9.3	0.14	11.5	0.13	13.2	0.13
	7.4	0.045	10.1	0.03	11.2	0.115	13.7	0.075	15.3	0.13
					13.1	0.025	15.8	0.025	17.9	0.11
									19.7	0.085
									21.1	0.035

Calculated Static head (cms)	1.85	1.92	2.13	2.15	2.5
% Liquid in Dispersion	63.3%	84.2%	86.9%	93.5%	96.8%

Table 11 Insert 4 $\frac{1}{8}$" holes on $\frac{3}{8}$" Triangular Pitch 3 cm Weirs

Run No.	60	61	62	63	64
Vapour rate based on active plate area (ft/sec)	2.26	2.95	3.76	4.4	5.24
F_A ($\rho_v^{\frac{1}{2}}$)	1.0	1.31	1.67	1.96	2.33
Liquid rate (gpm)	0.19	0.25	0.32	0.37	0.44
Clear liquid height (cms)	2.0	1.2	0.8	0.6	0.4
Dynamic head (cms)		2.1	2.0	2.0	1.9

	Height (cms)	Dispersion Density	Height (cms)	Dispersion Density	Height (cms)	Dispersion Density	Height (cms)	Dispersion Density	Height (cms)	Dispersion Density
DISPERSION DENSITY PROFILE DATA	0.6	0.51	0.6	0.425	0.6	0.32	0.6	0.24	0.6	0.21
	1.6	0.45	1.6	0.35	1.6	0.21	1.6	0.155	1.6	0.15
	2.4	0.35	2.4	0.265	2.4	0.19	2.4	0.155	3.8	0.145
	3.7	0.225	3.8	0.19	3.8	0.195	3,9	0.18	5.5	0.155
	5.0	0.21	5.4	0.185	5.4	0.175	5.7	0.16	7.7	0.155
	6.3	0.215	7.0	0.185	7.0	0.16	8.1	0.16	11.0	0.125
	7.5	0.155	8.6	0.15	8.9	0.16	9.7	0.14	14.2	0.11
	8.8	0.05	10.3	0.075	10.5	0.155	11.7	0.135	17.3	0.10
			11.3	0.02	12.3	0.085	13.8	0.125	19.6	0.095
					14.1	0.025	16.4	0.045	22.0	0.02
Calculated Static head (cms)	2.62		2.49		2.53		2.6		2.93	
% Liquid in Dispersion	59.6%		78.1%		90.0%		94.0%		96.6%	

Table 12 Insert 4 $\frac{1}{8}$" holes on $\frac{3}{8}$" Triangular Pitch 4cm Weir

Run No.	65	66	67	68	69
Vapour rate based on plate active area (ft/sec)	2.26	2.95	3.76	4.4	5.24
F_A ($\rho_V^{\frac{1}{2}}$)	1.0	1.31	1.67	1.96	2.33
Liquid rate (gpm)	0.19	0.25	0.32	0.37	0.44
Clear liquid height (cms)	2.2	1.5	0.9	0.6	0.4
Dynamic head (cms)	2.6	2.6	2.3	2.3	2.2

DISPERSION DENSITY PROFILE DATA

Height (cms)	Dispersion Density	Height (cms)	Dispersion Density	Height (cms)	Dispersion Density	Height (cms)	Dispersion Density	Height (cms)	Dispersion Density
0.6	0.49	0.6	0.435	0.6	0.33	0.6	0.25	0.6	0.22
1.2	0.50	1.2	0.40	1.2	0 .275	1.2	0.235	1.2	0.215
2.3	0.365	2.4	0.275	2.3	0.225	2.3	0.215	2.3	0.195
3.4	0.26	3.4	0.255	3.4	0.225	3.4	0.205	3.4	0.185
5.2	0.245	5.4	0.21	5.2	0.23	5.2	0.205	5.0	0.185
6.5	0.225	7.4	0.20	6.8	0.195	7.0	0.175	7.2	0.16
7.9	0.145	9.7	0.155	8.5	0.16	9.2	0.145	9.4	0.14
9.4	0.045	11.5	0.065	10.1	0.15	11.4	0.145	11.6	0.115
		13.4	0.025	11.3	0.14	13.5	0.125	13.7	0.115
				12.5	0.125	15.5	0.095	15.9	0.11
				13.5	0.07	17.7	0.04	18.0	0.105
				14.2	0.045			∠0.2	0.06

Calculated Static head (cms)	2.8	2.86	2.86	2.96	3.15
% Liquid in Dispersion	59.5%	76%	89%	94.3%	97%

TABLE 13 Insert 3 2cm Weirs

Effect of Liquid and Vapour Rates on the Dispersion Density Profiles

Vapour Rate based on Plate Active Area (ft/sec)	1.98	3.78	3.78
$F_A(v_A \cdot \rho g^{\frac{1}{2}})$	0.88	1.68	1.68
Liquid Rate (gpm)	0.16	0.16	0.31

Height (cms)	Dispersion Density	Height (cms)	Dispersion Density	Height (cms)	Dispersion Density
0.6	0.38	0.6	0.265	0.6	0.27
1.2	0.34	1.2	0.235	1.2	0.24
2.7	0.15	2.8	0.105	2.8	0.145
4.1	0.125	4.2	0.06	4.2	0.095
5.4	0.115	5.7	0.055	5.7	0.085
6.7	0.05	7.1	0.055	7.1	0.07
7.1	0.02	8.8	0.055	8.6	0.07
		10.5	0.055	10.0	0.07
		12.2	0.05	11.7	0.055
		13.8	0.015	13.2	0.035

TABLE 14 Insert 4 3cm Weirs

Effect of Liquid and Vapour Rates on the Dispersion Density Profiles

Vapour Rate based on Plate Active Area (ft/sec)	2.26	3.76	3.76
$F_A(v_A \cdot \rho^{\frac{1}{2}})$	1.0	1.67	1.67
Liquid Rate (gpm)	0.19	0.19	0.32

Height (cms)	Dispersion Density	Height (cms)	Dispersion Density	Height (cms)	Dispersion Density
0.6	0.51	0.6	0.385	0.6	0.32
1.6	0.45	1.6	0.275	1.6	0.21
2.4	0.35	2.4	0.20	2.4	0.19
3.7	0.225	3.8	0.175	3.8	0.195
5.0	0.21	5.7	0.17	5.4	0.175
6.3	0.215	7.8	0.165	7.0	0.16
7.5	0.155	10.0	0.15	8.9	0.16
8.8	0.05	12.2	0.02	10.5	0.155
				12.3	0.085
				14.1	0.025

TABLE 15 Insert 2 2cm Weirs

Effect of Liquid and Vapour Rates on the Dispersion Density Profiles

Vapour Rate based on Plate Active Area (ft/sec)	1.98	3.78	3.78
$F_A(v_A \cdot \rho g^{\frac{1}{2}})$	0.88	1.68	1.68
Liquid Rate (gpm)	0.16	0.16	0.31

Height (cms)	Dispersion Density	Height (cms)	Dispersion Density	Height (cms)	Dispersion Density
0.4	0.45	0.6	0.325	0.6	0.305
1.3	0.38	1.2	0.285	1.2	0.28
2.8	0.165	3.0	0.15	2.9	0.165
3.7	0.145	3.9	0.13	3.9	0.135
4.3	0.155	5.2	0.105	5.2	0.105
5.6	0.12	6.3	0.085	6.3	0.095
6.5	0.04	7.6	0.085	7.6	0.09
7.0	0.015	9.0	0.085	9.0	0.095
		10.8	0.085	10.9	0.09
		12.3	0.06	12.4	0.075
		13.9	0.025	13.7	0.05
				14.6	0.015

PRESSURE DROP DATA

TABLE 16 INSERT 1 1/16" holes on $\frac{1}{8}$" Triangular Pitch

2 cm Weirs

Hole Velocity (ft/sec)	Hole F factor	ΔP_{TOTAL} cms pentane	Static head (ΔP_S) cms pentane	$\Delta P_T - \Delta P_S$ cms pentane	$\Delta P_{DRY\ PLATE}$ cms pentane	$\Delta P_{residual}$ cms pentane
12.8	5.7	3.8	1.4	2.4	0.7	1.7
16.8	7.5	4.3	1.3	3.0	1.2	1.8
21.8	9.7	5.4	1.3	4.1	2.0	2.1
24.3	10.8	5.9	1.4	4.5	2.4	2.1
28.4	12.6	6.8	1.5	5.3	3.1	2.2
33.7	14.9	7.7	1.7	6.0	4.2	1.8

4 cm Weirs

12.9	5.7	4.6	2.4	2.2	0.7	1.5
16.8	7.5	5.4	2.3	3.1	1.2	1.9
21.8	9.7	6.25	2.25	4.0	2.0	2.0
24.3	10.8	7.0	2.3	4.7	2.4	2.3
28.4	12.6	7.35	2.25	5.1	3.1	2.0
33.7	14.9	9.0	2.4	6.6	4.2	2.4

PRESSURE DROP DATA

TABLE 17 INSERT 2 1/16" holes on 3/16" Triangular Pitch

2 cm Weirs

Hole Velocity ft/sec	Hole F factor	h_T TOTAL cms pentane	Static head (h_S) cms pentane	$h_T - h_S$ cms pentane	h_{DP} DRY PLATE cms pentane	h_R RESIDUAL cms pentane
24.8	11	5.6	1.6	4.0	2.4	1.6
32.8	14.5	7.9	1.6	6.3	4.0	2.3
39.7	17.6	9.9	1.8	8.1	5.5	2.6
47.4	21.0	11.1	1.9	9.2	7.8	2.3
55.4	24.6	15.4	2.0	13.4	10.0	3.4
66	29.2	21.1	2.3	18.8	14.0	4.4

4 cm Weirs

25.4	11.4	6.6	2.4	4.2	2.6	1.6
32.8	14.5	8.2	2.3	5.9	4.0	1.9
44.0	19.5	10.6	2.5	8.1	6.1	2.0
47.4	21.0	12.0	2.5	9.5	7.8	1.7
55.4	24.6	17.9	2.5	15.4	10.0	5.4

PRESSURE DROP DATA

TABLE 18 INSERT 3 $\frac{1}{8}$" holes on $\frac{1}{4}$" Triangular Pitch

2 cm Weirs

Hole Velocity ft/sec	Hole F Factor	h TOTAL cms pentane	Static head (h_s) cms pentane	$h_T - h_S$ cms pentane	h DRY PLATE cms pentane	h RESIDUAL cms pentane
13.2	5.85	3.5	1.25	2.25	0.9	1.4
21	9.3	5.0	1.35	3.65	1.8	1.85
29	13.0	6.6	1.5	5.1	3.2	1.9

4 cm Weirs

13.1	5.8	5.0	2.7	2.3	0.9	1.4
18.2	8.1	5.8	2.5	3.3	1.4	1.9
23	10.2	6.7	2.5	4.2	2.1	2.3
28.4	12.6	7.6	2.6	5.0	3.2	1.8

PRESSURE DROP DATA

TABLE 19 INSERT 4 $\frac{1}{8}$" holes on $\frac{3}{8}$" Triangular Pitch

2 cm Weirs

Hole Velocity ft/sec	H ole F Factor	h_t TOTAL cms pentane	Static head (h_s) cms pentane	$h_T - h_S$ cms pentane	h_d DRY PLATE cms pentane	h_r RESIDUAL cms pentane
18	8.0	4.6	1.4	3.2	1.4	1.6
27.5	12.3	6.0	1.55	4.45	2.95	1.5
38.4	17.2	8.7	1.65	7.05	5.3	1.75
55	24.6	14.0	2.2	11.8	10	1.8
4 cm Weirs						
25.6	11.3	6.4	2.45	3.95	2.55	1.4
34	15.5	8.6	2.45	6.15	4.4	1.75
45	20.0	11.4	2.4	9.0	7.0	2.0
55	24.6	14.4	2.4	12.0	10.0	2.0

EVALUATION OF PRESSURE PROBE MEASUREMENTS IN THE DISPERSION

Run No. B-1

System: Air-Water

Column Air Rate: 1.5 ft/sec

Column F factor: 0.42

Hgt above Plate cms.	Dynamic Probe Rdg. cms. water	Time for 50000 counts secs.	Dispersion Density Vol.fraction liquid	Calc. Static Pressure cms. water
0	3.9			3.85
1	3.0	137	0.47	3.25
2	2.4	128	0.38	2.88
3	1.8	124.5	0.34	2.50
4	1.6	121	0.31	2.18
5	1.4	121	0.31	1.87
6	1.2	120.1	0.30	1.58
7	1.1	118.5	0.28	1.29
8	0.9	117.4	0.27	1.0
9	0.8	115.6	0.25	0.73
10	0.4	107.8	0.16	0.3
11		105.8	0.13	
12		101.5	0.075	
13		98	0.025	
14				

Liquid Hold Up by Integration of Density Profile 235 mls.

Liquid Hold Up by Draining Dispersion 244 mls.

Calibration Points:

Column empty	96.5 secs.
Column full of water	203 secs

Run No. B-2

System: Air-Water

Column Air Rate: 1.5 ft/sec.

Column F factor: 0.42

Hgt above Plate cms.	Dynamic Probe Rdg. cms. water	Time for 50000 counts secs.	Dispersion Density Vol. fract. liquid	Calc. Static Pressure cms. water
0	7.3			6.7
1	6.7	138	0.48	
2	5.8	133.5	0.44 (2.2cms)	5.7
3	5.3			
4	4.7	132	0.42 (4.3cms)	4.85
5	4.1			
6	3.7			4.0
7	3.3			
8	2.8	128	0.38 (8.3cms)	3.25
9	2.3			
10	1.9	124	0.34 (9.9cms)	2.5
11	1.5			
12	1.4	122	0.32	1.8
13	1.1			1.25
14	0.8	117.5	0.27	
15	0.6			
16	0.3	111.5	0.20	0.8
17	0.2			
18	0.2	106	0.13	0.45
19	0.1			
20	0.1	103.5	0.10	0.2
21.6		102	0.08	

Liquid Hold Up by Integration of Density Profile 413 mls.

Liquid Hold Up by Draining Dispersion 460 mls.

Run No. B-3

System: Air-Water

Column Air Rate: 2.7 ft/sec.

Column F factor: 0.66

Hgt above Plate cms.	Dynamic Probe Rdg. cms. water	Time for 50000 counts secs.	Dispersion Density Vol. fract. liquid	Calc. Static Pressure cms. water
0	3.8			3.5
1	2.9	126.5	0.37	3.0
2	2.1	125.5	0.36	2.6
3	1.7	123.5	0.335	2.3
4	1.3	120	0.30	2.0
5	1.1	119.5	0.29	1.7
6	0.8	117.5	0.27	1.4
7	0.7	116.5	00.26	1.13
8	0.6	115.5	0.25	0.93
9	0.5	114	0.23	0.64
10	0.4	110	0.18	0.48
11	0.4	107.5	0.15	0.32
12		104.5	0.11	0.2
13		100.5	0.06	0.12
14		98.5	0.04	0.06
15		98	0.03	0.03

Liquid Hold Up by Integration of Density Profile 215 mls.

Liquid Hold Up by Draining the Dispersion 234 mls.

DERIVATION OF EQUATION 5.2.2.

The Navier Stokes equation for a fluid in the x direction may be written in the form

$$-\frac{\partial p}{\partial x} = \rho\left\{g + U_x\frac{\partial U_x}{\partial x} + U_y\frac{\partial U_x}{\partial y} + U_z\frac{\partial U_x}{\partial z} - \mu\nabla^2 U_x\right\}$$

where p = instantaneous hydrostatic pressure in the medium

ρ = fluid density

g = acceration due to gravity

U_x = fluid velocity in the x direction

U_y = " " " " y "

U_z = " " " " z "

μ = fluid viscosity

∇ = Laplacian operator

$$\frac{\partial^2}{\partial x^2} + \frac{\partial^2}{\partial y^2} + \frac{\partial^2}{\partial z^2}$$

Assuming the applicability of the Navier Stokes equation to turbulent flow, U can be written

$$U_x = \bar{u}_x + u^1_x$$

where $\bar{u}_x$ = mean velocity in the x direction

u^1_x = turbulent fluctuation in the x direction about this mean velocity

- and similarly for U_y and U_z

hence $$-\frac{\partial p}{\partial x} = \rho\left\{g + \bar{u}_x\frac{\partial \bar{u}_x}{\partial x} + \bar{u}_y\frac{\partial \bar{u}_x}{\partial y} + \bar{u}_z\frac{\partial \bar{u}_x}{\partial z} + \frac{\partial}{\partial x}\overline{u^{1\,2}_x} + \frac{\partial}{\partial y}\overline{u^1_x u_y} + \frac{\partial}{\partial z}\overline{u^1_x u^1_z} - \mu\nabla^2 v_x\right\}$$

In the present case we have a two phase liquid-vapour system, for which the liquid phase is stationary and the vapour phase has a uniform mean velocity in the x-direction. Thus:

$$\bar{u}_x = \bar{u}_y = \bar{u}_z = 0$$

$$\bar{v}_y = \bar{v}_z = 0 \quad \text{and} \quad \bar{v}_x = \text{constant}$$

- where u refers to velocities in the liquid phase, and v velocities in the vapour phase. If further we write

ε = vol fraction liquid in the dispersion

ρ_L = liquid density

ρ_V = vapour density

Then

$$-\frac{\partial \bar{p}}{\partial x} = \rho_L \varepsilon \left\{ g + \frac{\partial \overline{u'^2_x}}{\partial x} + \frac{\partial}{\partial y}\overline{u'_x u'_y} + \frac{\partial}{\partial z}\overline{u'_x u'_z} \right.$$

$$\left. + \rho_g (1-\varepsilon) \left\{ g + \frac{\partial \overline{v'^2_x}}{\partial x} + \frac{\partial}{\partial y}\overline{v'_x v'_y} + \frac{\partial}{\partial z}\overline{v'_x v'_z} \right.\right.$$

From homogeneity, all derivatives of mean values with respect to y and z vanish, hence

$$-\frac{\partial \bar{p}}{\partial x} = g\left\{\rho_L \varepsilon + \rho_V (1-\varepsilon)\right\} + \left\{ \varepsilon \rho_L \frac{\partial \overline{u'^2_x}}{\partial x} + (1-\varepsilon)\rho_V \frac{\partial \overline{v'^2_x}}{\partial x} \right.$$

Now the foam density ρ_F at any point is given by:

$$\rho_F = \rho_L \varepsilon + \rho_V (1-\varepsilon)$$

Hence by integration we get:-

$$-\bar{p} = g \int \rho_F dx + \varepsilon \rho_L \overline{u'^2_x} + (1-\varepsilon) \rho_V \overline{v'^2_x} - \int (\rho_L \overline{u'^2_x} - \rho_V \overline{v'^2_x}) \, d\varepsilon + \text{const}$$

The normal Reynold's stresses $(\rho_L \overline{u'^2_x})$ and $(\rho_V \overline{v'^2_x})$ probably have similar magnitudes in the two phases, so that to a first order approximation the second integral may be neglected.

Using the boundary conditions at the surface of the dispersion $(x = h_f)$ we have:

$$-\bar{p} = g \int_x^{h_f} \rho_F dx - \varepsilon \rho_L \left\{ \overline{u'^2_x} - (u'^2_x) \right\}_{h_f} - (1-\varepsilon) \rho_V \left\{ \overline{v'^2_x} - (v'^2_x) \right\}_{h_f}$$

The term $\int_x^{h_f} \rho_F \, dx$ is simply the static head at the point x due to the weight of dispersion above it.

Table 20. EXPERIMENTAL DATA.

Run No.	% ISO PENTANE PLATE INLET	% ISO PENTANE PLATE OUTLET	% EO_G
INSERT 3.	2 CM. WEIR.		
1	24.5	22.4	41
2	24.2	22.2	39.5
3	23.1	20.5	52
4	22.1	19.3	59
INSERT 4.	2 CM. WEIR.		
5	21.4	18.9	54
6	21.1	18.4	59
7	20.8	18.0	63
8	20.1	17.1	67
INSERT 3.	4 CM. WEIR.		
9	19.6	17.1	57
10	19.5	16.5	62
11	19.3	16.0	74
12	18.5	15.2	80.5
INSERT 4.	4 CM. WEIR.		
13	19.5	16.9	72
14	19.3	15.9	83
15	18.7	14.9	89.5

Table 21. TABULATION OF PLATE EFFICIENCY RESULTS.

Run No.	Hole Velocity ft/sec.	Static Head cms.	% Liquid Holdup in Dispersion.	Gas Holdup ϕ ft^3/ft^2 bubbling area.	VA ft/sec.	$t_G = \frac{\phi}{VA}$ secs.	EO_G %	N_G
	INSERT 3.		23% FREE AREA.			2 CM. WEIRS.		
1	13.8	1.3	56	0.2	2.08	0.096	41	0.527
2	17.7	1.46	68	0.26	2.67	0.097	39.5	0.503
3	23.0	1.48	75	0.346	3.46	0.100	52	0.733
4	27.6	1.63	82	0.425	4.15	0.102	59	0.891
	INSERT 4.		10% FREE AREA.			2 CM. WEIRS.		
5	27.0	1.6	60	0.14	2.0	0.07	54	0.775
6	34.5	1.73	71	0.192	2.67	0.072	59	0.89
7	44.8	1.93	79	0.252	3.46	0.073	63	0.99
8	53.6	2.08	85	0.321	4.15	0.077	67	1.11

Table 22. . TABULATION OF PLATE EFFICIENCY RESULTS.

Run No.	Hole Velocity ft/sec.	Static Head cms.	% Liquid Holdup in Dispersion.	Gas Holdup $\emptyset$ ft^3/ft^2 bubbling area.	VA ft/sec.	$\frac{\emptyset}{VA} = \pm_G$	EO_G %	N_G
	INSERT 3.		23% FREE AREA.			4 CM. WEIRS.		
9	13.4	2.35	53	0.248	2.06	0.123	57	0.844
10	18.2	2.41	67	0.33	2.75	0.120	62	0.966
11	23.2	2.43	74	0.438	3.5	0.125	74	1.34
12	27.0	2.62	78	0.502	4.1	0.123	80.5	1.63
	INSERT 4.		10% FREE AREA.			4 CM. WEIRS.		
13	26.2	2.6	65	0.197	2.05	0.096	72	1.27
14	39.0	2.63	76	0.299	3.0	0.100	83	1.77
15	52.5	2.75	89	0.43	4.1	0.105	89.5	2.25

Refrigerant Cycle Design Calculations

Boiling Point Pentane	$98^{\circ}F$
Allowing Overall Temp.Drop across Reboiler	$25^{\circ}F$
Freon Condensing Temp.	$123^{\circ}F$ (164 psig)
Condensing Temp. Pentane Mixture	$91^{\circ}F$
For an Overall Temp. Drop over Condenser	$25^{\circ}F$
Freon Evaporating Temp.	$66^{\circ}F$ (65 psig)
Actual gas shift of compressor between 65 psig suction and 164 psig deliver	137 cfm
Enthalpy change between these limits from Molier Diagram	47.21 BTU/lb.
Refrigerant Specific Volume at Suction Conditions	0.508 ft^3/lb.
Available heat duty from the cycle	7.65×10^5 BTU/hr.
Latent heat pentane mixture	153 BTU/lb.
Total boil up	5000 lb/hr.
Cross Sectional Area 15.5" I.D. column	1.31 ft^2
Max.superficial vapour rate	5.4 ft/sec.
Total reflux rate	14 gpm.

By-Pass Condenser Design

From Freon-12 Molier Diagram, 32.5 lb/min of Freon @ 164 psig and superheated to $140^{\circ}F$ has to be condensed to balance heat loadings at reboiler and condenser.

Heat duty on by-pass condenser 1.085×10^5 BTU/hr.

For a cooling water temperature rise from 65 to 110°F and a Freon condensing temperature of 123°F, the LMTD is 30°F.

For an assumed overall coefficient of 150 BTU/hr.ft^2 °F

surface area required 24 ft^2

cooling water requirement 4 gpm.

Nearest standard Hall's condenser is a 12 pass tubular exchanger with 46 x 0.58" bore x 3'9" long tubes having a surface area of 40 ft^2.

Check overall coefficient for this condenser on the basis of a readily available 4 gpm water supply to the condenser

From page 267 Kern "Process Heat Transfer"

h condensing = 350 BTU/hr.ft^2.°F

Using $h_w = 0.023 \left(\frac{k}{D}\right) h_e^{0.8} P_r^{0.4}$

h_w = 164 BTU/hr.ft^2.°F

giving U overall = 114 BTU/hr.ft.^{2} °F

Thus condensing capacity of this condenser is in excess of that required.

Calculation of Surface Area Requirements of Reboiler and Condenser

According to the manufacturer, there had been no previous application of these secondary surface exchangers in heat exchange between a condensing vapour and a boiling liquid and no established design procedure was available. Much of the experimental data available in the literature for boiling and condensing coefficients

had been obtained in test rigs with 0.3" I.D. tubes and greater and no data was available for passages of the small hydraulic radius used in the Marston exchangers. It appeared reasonable to design on the basis that such relationships were valid for the Marston exchangers providing a suitable design margin to allow for departure from these conditions.

Condensing coefficients for both pentane and Freon 12 were estimated using Equation 12.42, page 266 and relationship 12.45, page 269 quoted in Kern, "Process Heat Transfer"[48].

$$h_e = 1.51\ k\ (\frac{\rho^2 g}{4uG})^{\frac{1}{3}}$$

where h_e = condensing film coefficient BTU/hr.ft^2.$^\circ$F

k = thermal conductivity of the condensate, BTU/hr.ft^2.$^\circ$F/ft.

ρ = condensate density lb/ft^3.

g = acceleration due to gravity ft/hr^2.

u = viscosity of the condensate centipoise

G = condensate loading lb/hr.ft.

$= W/L$

W = mass of condensate lb/hr.

L = sum of all the corrugation passage lengths ft.

For estimating boiling coefficients both on the pentane and Freon sides, the relationship proposed by Holladay[38] was used:

$$h_b = 5.0\ q^{0.5}$$

where h_b = boiling film coefficient BTU/hr.ft^2.$^\circ$F.

q = heat flux, BTU/hr.ft^2

Basis of Calculations

15" Square matrix

Pentane side	25 passages
Freon side	26 passages (6 passes)
Heat load (Q)	1.07×10^6 BTU/hr.ft^2.°F
Boil Up Rate (W)	7360 lb/hr.

Estimate of Condenser Surface Area

Pentane Side (Condensing Vertical Passages)

Total surface area	296 ft^2
Total length of passages	5640 ft^2
Condensate load (G)	1310 lb/hr.ft.

$$h_c = 1.51\ k\ \left(\frac{g^2}{4Gu}\right)^{\frac{1}{3}}$$

$$= 495 \text{ BTU/hr.ft}^2\text{.°F}$$

and $$T_c = \frac{Q}{h_c \cdot A_c} = 7.3^\circ F$$

Freon Side (Boiling - horizontal passages)

Total surface area 308 ft^2

Heat flux $q = \frac{Q}{A_b} = 3480$ BTU/ft^{2}hr

and $T_B = 0.2\ q^{\frac{1}{2}} = 11.8^\circ F$

i.e. $h_B = \frac{q}{\Theta B} = 295$ BTU/hr.ft^2.°F

Total $T_c = 19.1^\circ F$

Estimate of Reboiler Surface Area

Freon Side (Condensing - horizontal passages)

Total surface area 308 ft^2

Total passage length 5860 ft.

Condensate load (G) 3.48 lb/hr.ft.

$$he = 1.51\ k\ (\frac{g^2}{4Gu})^{\frac{1}{3}}$$

$$= 385\ BTU/hr.ft^2.{}^oF.$$

and $$Tc = \frac{Q}{A.hc} = 9^oF$$

Pentane Side (Boiling - vertical passages)

Total surface area 296 ft^2

Heat flux q 3610 $BTU/hr.ft^2$

$$TB = 0.2\ q^{\frac{1}{2}} = 12^oF$$

and $$hB = \frac{q}{TB} = 301\ BTU/hr.ft^2.{}^oF$$

Total $TR = 21^oF$

Validity of Estimated Coefficients

The major source of uncertainty in the method is the applicability of relationships based on experimental data obtained in 0.3" diameter tubes and larger to the passages of small hydraulic radius used in this matrix. Work done within this Department indicates condensing coefficients of the order of 450 $BTU/hr.ft^2.{}^oF$ inside overflow type corrugated packings[61]. On the other hand, Potter and Patel[62] found Freon 12 condensing coefficients of the same value in ½" I.D. horizontal tubes with a 12^oF temperature difference at a heat flux of 6200 $BTU/hr.ft^2$. It appears from

this that the calculated coefficients are reasonable estimates of the true condensing coefficients in this matrix.

Holladay's relationship for boiling film coefficients was based on experimental data obtained in 5/8" I.D. tubes and gives concervative results when applied to the data of Ashley[4] and Baker[5]. It should be noted that Watzig[27] obtained a value of 270 BTU/hr.ft^2.$^\circ$F for the boiling coefficient of Freon 12 inside horizontal, 0.3" I.D. tubes, a value less than the design coefficient of 295 BTU/hr.ft^2.$^\circ$F. The boiling coefficient for pentane calculated from Holloday's relationship appears satisfactory in the light of generally accepted values. Even if no recirculation were to occur in this reboiler, a pool boiling coefficient of 250 BTU/hr.ft^2.$^\circ$F. for a 12°F temperature difference (Kern, Fig.15-11, page 474) would apply.

To allow for the uncertainty of these relationships when applied to the Marston matrix, the design was based on a heat duty approximately 30% greater than the desired duty. Even using this increased heat duty, the overall exchanger temperature drops were lower than those allowed for in the refrigerant cycle conditions. On these grounds, it was believed that the matrix so designed incorporated sufficient design margin to compensate for any inaccuracy in the method.

Distillation Column Design Calculations

Column Diameter

A compromise had to achieve between the desire to have both

a large column and a high column vapour velocity since the total boil up was fixed by the refrigerant cycle heat duty. A column fabricated from sections of 16" O.D. x 15.5" I.D. seamless steel pipe with a cross sectional area of 1.31 ft^2 giving a maximum vapour velocity of 5 ft/sec was considered to be the most satisfactory.

Plate Spacing

The plate spacing was fixed at 18". This was considered to be typical of many industrial columns.

Plate Layout

Weir length

Length of chord weirs was fixed at 10.5" giving a weir length/diameter ratio of 0.68, that is within the normal design range of 0.6-0.8.

Downcomer Area

Segmental type downcomers with cross sectional area of 0.098 ft^2 were provided. Liquid residence time is of the order of 4 seconds with a liquid velocity in the downcomer of 0.25 ft/sec, both requirements meeting the criterion proposed by Hughmark and O'Connell[40].

Perforated Insert

First plate fitted had 1/8" holes on 3/8" triangular pitch with 10% free area. This was chosen as having the same drilling

pattern as an insert tested in the 4" column as well as approaching the type of perforations used in small industrial columns.

Plate Stability

Calculations were made to check the stability of this plate at the deepest weir as regarding weeping and flooding as well as providing an estimate of total plate pressure drops needed to specify the range of the Foxboro Differential Pressure Cell used for plate pressure drop measurements.

The method given by Hughmark and O'Connell[40] was used in these calculations:

Dry Plate Drop at Max.Vapour Velocity

Diameter hole/plate thickness = 1

hence $C = 0.81$

$$h_{DP} = \frac{0.003\ Fh^2\ (1 - B^2)}{C^2}$$

Fh = $52.8/\sqrt{0.2}$ at max.column vapour rate

B = 0.1

$$= \frac{0.003 \times 23.5^2 \times 0.99}{0.81^2}$$

$$= 4.0 \text{ ins pentane}$$

Head over 4" Weir

The normal Francis Weir formula has been modified for use in column calculations, allowance being made for velocity of approach. For liquid flow of 0.04 ft^3/sec over the weir, weir crest is 0.20 ins.

Effective Liquid Head

At Fh of 23.5, heff is given as 2.25 ins from Figure 4.

Wet Plate Pressure Drop

$$h_T = h_{DP} + heff$$

$$= 6.25 \text{ ins pentane}$$

On this basis, the column should not flood at the maximum column velocity since the downcomer level is running about 70% full, which is satisfactory in the case of a non foaming liquid such as pentane.

Bearing in mind the use of smaller % free area plates, a Foxboro Differential Pressure Cell calibrated over the range 0-10" W.G. should cover the entire range of pressure drops to be enccuntered.

Weep Point

Using Hughmark and O'Connell's weep point correlation, weeping should occur below 22 ft/sec in the holes, i.e. at column superficial velocities less than 2.25 ft/sec.

Column Piping

Column Vapour Piping and Liquid Reflux lines were sized in the normal way.

10'-11" APPROX.

6" 2'-2" 3'-2" 1'-9" 2'-10" 6"

1'-4" 9" 1'-6" 1'-11" 6" 1'-6" 1'-1" 9" 3" 6"

6" DEEP 'KNITMESH' DE-ENTRAINER.

6" N/B M.S. CONNECTION TO REBOILER SEE DWG 3101/C

1½" C/RAD

1'-4" RAD

⅛" THK

½" B.S.P. BOSS P.C.

4" NOM BORE M.S. BRANCH FLANGE B.S.T.D. DRILLED OFF CENTRES.

1½" DIA REFLUX CONNECTION

RECTANGULAR SIGHT CLASS 2" WIDE 23" LONG SEE DRG. Nº 3090/1

¼" B.S.P. BOSS (P.G.)

4" DIA BORE TAKE OFF CONNECTION

3½"

— VIEW ON ARROW 'A' —

SEE PLAN FOR TRUE POSITIONS OF FITTINGS

6" DEEP M.S. "KNITMESH" DE-ENTRAINER SEE DRG. Nº 3090/7

1'-10½"

1½" NOM BORE REFLUX CONNECTION

2½"

1'-4" RAD

⅛" THK

3" NOM BORE M.S. BRANCH FLANGE B.S.T.D. ⅜" THK DRILL 4 HOLES - 11/16" DIA OFF CENTRES.

4¾"

℄ LIGHT CLASS

6" NOM BORE CONNN TO REBOILER

¾" × ¾" × ⅛" THK M.S. ANGLE RING AND 1" × ⅛" THK M.S. FLAT "ON EDGE" USED TO SUPPORT 'KNITMESH' DE-ENTRAINERS SEE DRG. Nº 3090/6

'A'

'B'

'B'

'A'

℄ 4" DIA TAKE OFF CONNN AND BOTH 1½" REFLUX CONNNS

℄ LEVEL GAUGE

— PLAN — SHOWING TRUE POSITION OF ALL FITTINGS

5¼" 5¼"

9½"

2"

10½"

7½" 9" CRS 10½"

M.S. DOWNCOMER 17 SWG

— FRONT —

— PLAN VIEW OF TRAY 1 — ARROW SHOWS FLOW DIRECTION

5¼" 5¼"

9½"

¼" R.C. BOSS

30°

¼" AG BOSS

— FRONT —

— PLAN VIEW OF TRAY 2 — ARROW SHOWS FLOW DIRECTION

⅝" ⅛ LEVEL GAUGE TYPE E25S

M.S. DOWNCOMERS

A BACKING RINGS.

2'-4½"

1'-0"

5¼" 5¼"

ADJUSTABLE WEIR AND SUPPORT BOTH 16 SWG THK

1" HIGH × 16 SWG THK WEIR

— PLAN VIEW OF TRAY 3 — ARROW SHOWS FLOW DIRECTION

5¼" Ø DIA DRILL 4 HOLES 9/16 DIA OFF CRS 3⅜ PCD 1½" NOM BORE ¼ ½"

10" 6½" 10½" 4¾" 4½" 5¼" 10" 1'7" 1'-11" 2'-2"

ADJUSTABLE WEIR ×16 SWG THK ADJUSTABLE HEIGHT - "2" TO 4"

16 SWG THK M.S. 'D' SHAPED DOWNCOMERS × 17½" LONG TRAYS 1 AND 2 ONLY.

16 SWG THK M.S. WEIRS 1" HIGH ON TRAYS 1 2. AND 3.

⅜ 7½" INSIDE 9" CRS 10½" 16 OFF ½" BSW STUDS ⅛" TOW

M.S. ADJUSTABLE BAFFLE SEE SK Nº 1509

8½" Ø DIA 7" P.C.D. 4" NOM. BORE DRILL 4 HOLES - 11/16" DIA OFF CENTRES.

6" DEEP M.S. 'KNITMESH' DE-ENTRAINER

6" NOM BORE 9¼" PCD 11" Ø DIA

DRILL 8 HOLES - ¾" DIA OFF CENTRES

DRILL 20 HOLES - 11/16" DIA OFF CENTRES.

45°

1'-3½" DIA 1'-4" DIA 1'-6" PCD 1'-8" DIA

— SECTION 'B-B' WITH ENDS REMOVED —

SEE 'PLAN' FOR TRUE POSITION OF ALL FITTINGS

JOHN DORE & Co LTD.
BROMLEY HIGH STREET
BOW.
LONDON E3

DETAILS OF 1'-3½" DIA MILD STEEL DISTILLATION COLUMN.

SCALE - 3" = 1 FOOT | DATE - 14.3.61

DRAWN - F.M | OB -

CLIENT THE IMPERIAL COLLEGE OF SCIENCE AND TECHNOLOGY

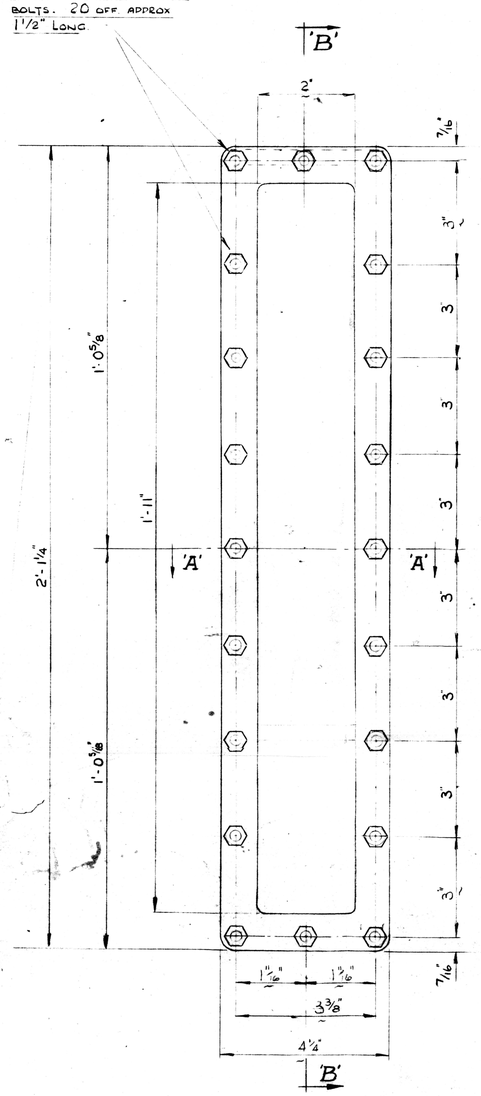
DRAWING NUMBER 3089/B

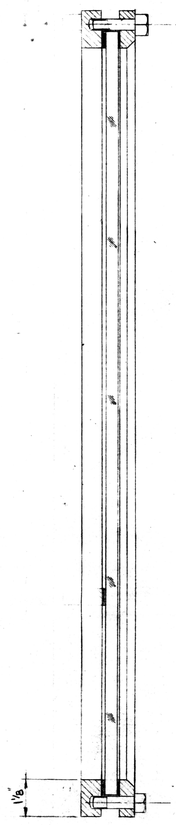
LETTER	REVISION	SIGN & DATE
A	REVISED TO SUIT CLIENT	1.5.61

IF IN DOUBT ASK

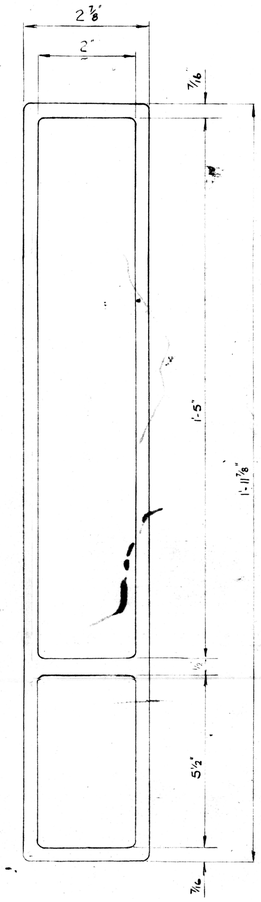
DO NOT SCALE

3/8" B.S.F. MILD STEEL SET BOLTS. 20 OFF. APPROX 1 1/2" LONG.



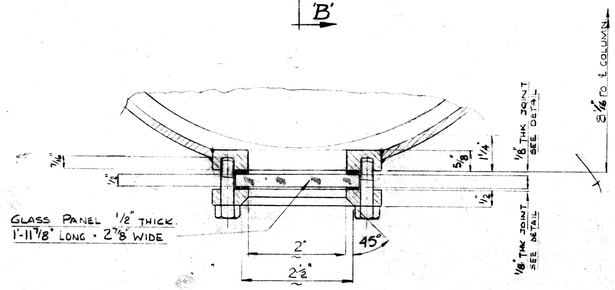


— Section 'B-B' —



1 off As Above - 1/8 Thk.
1 off As Above But Without Centre Bar - 1/8 Thk.

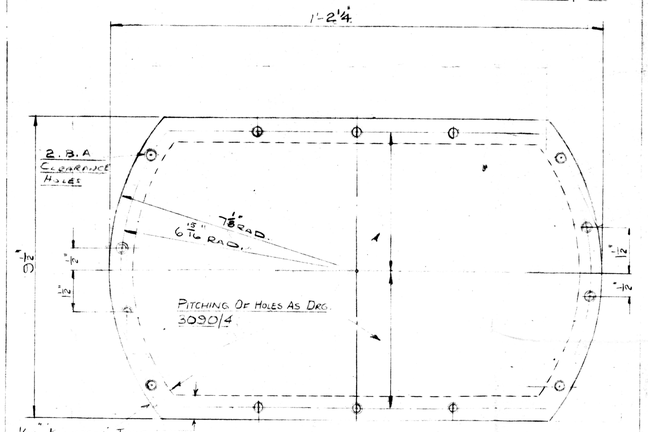
— Joint On Drg 3090/1 —
C A F



— Section 'A-A' —

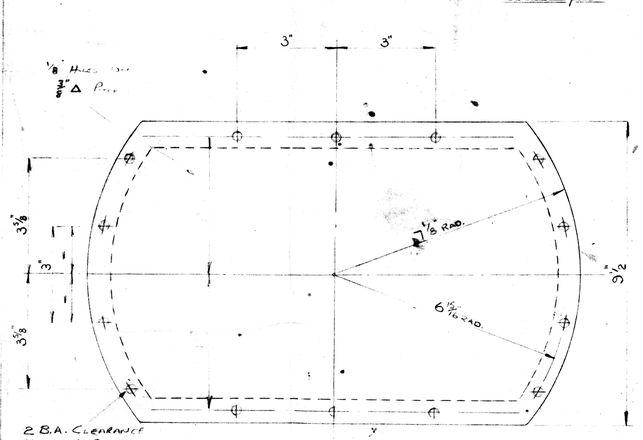
3090/1

3090/2



— Details of Removable Trays 1 and 2 — 1/8 Thk M.S.

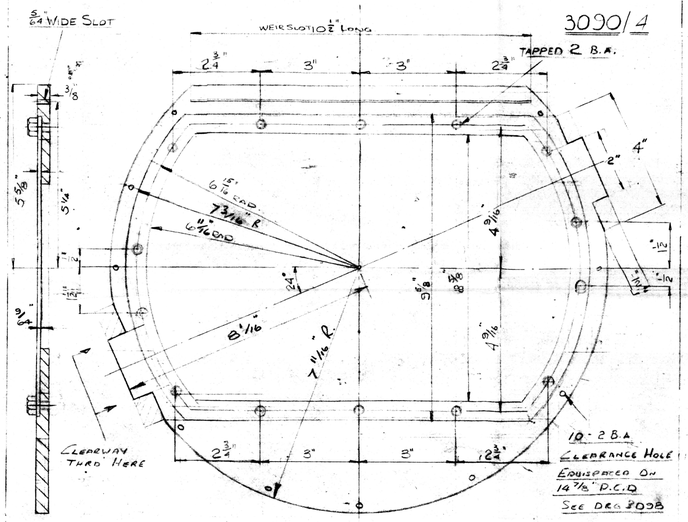
3090/3



2 B.A. Clearance Holes As Drg 3090/5

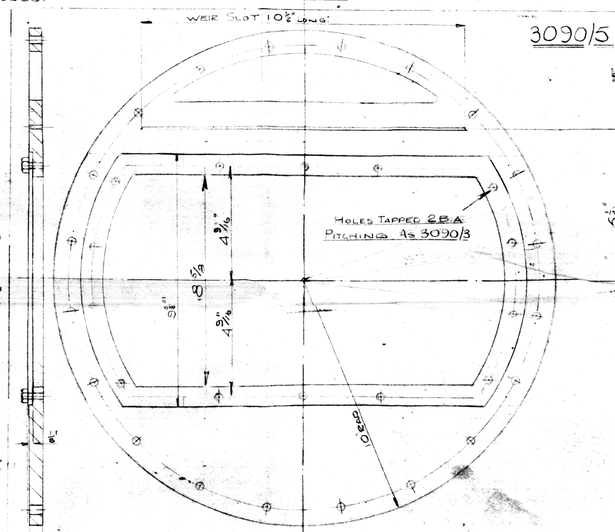
— Details of Removable Tray 3 —

3090/4



— Supporting For Removable Trays 1 & 2 —

3090/5

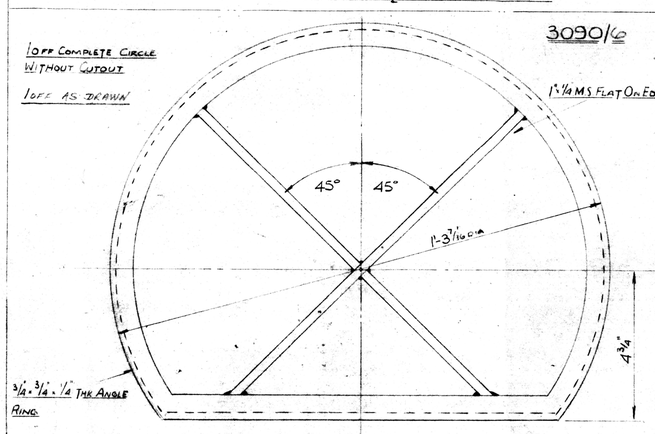


— Supports For Removable Tray 3 —

3090/6

1 off Complete Circle Without Cutout

1 off As Drawn

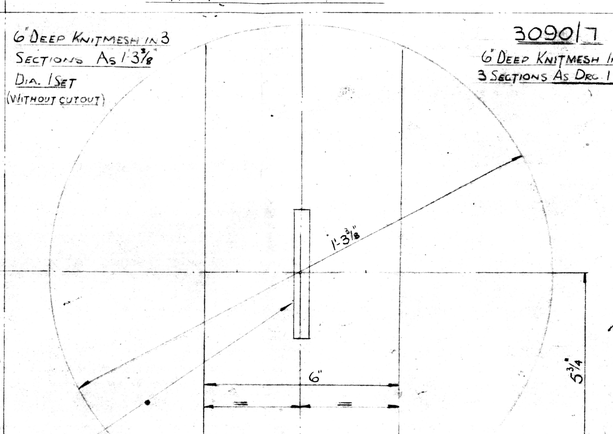


— Knitmesh Support —

3090/7

6" Deep Knitmesh In 3 Sections As 1'-3 7/16" Dia. 1 Set (Without Cutout)

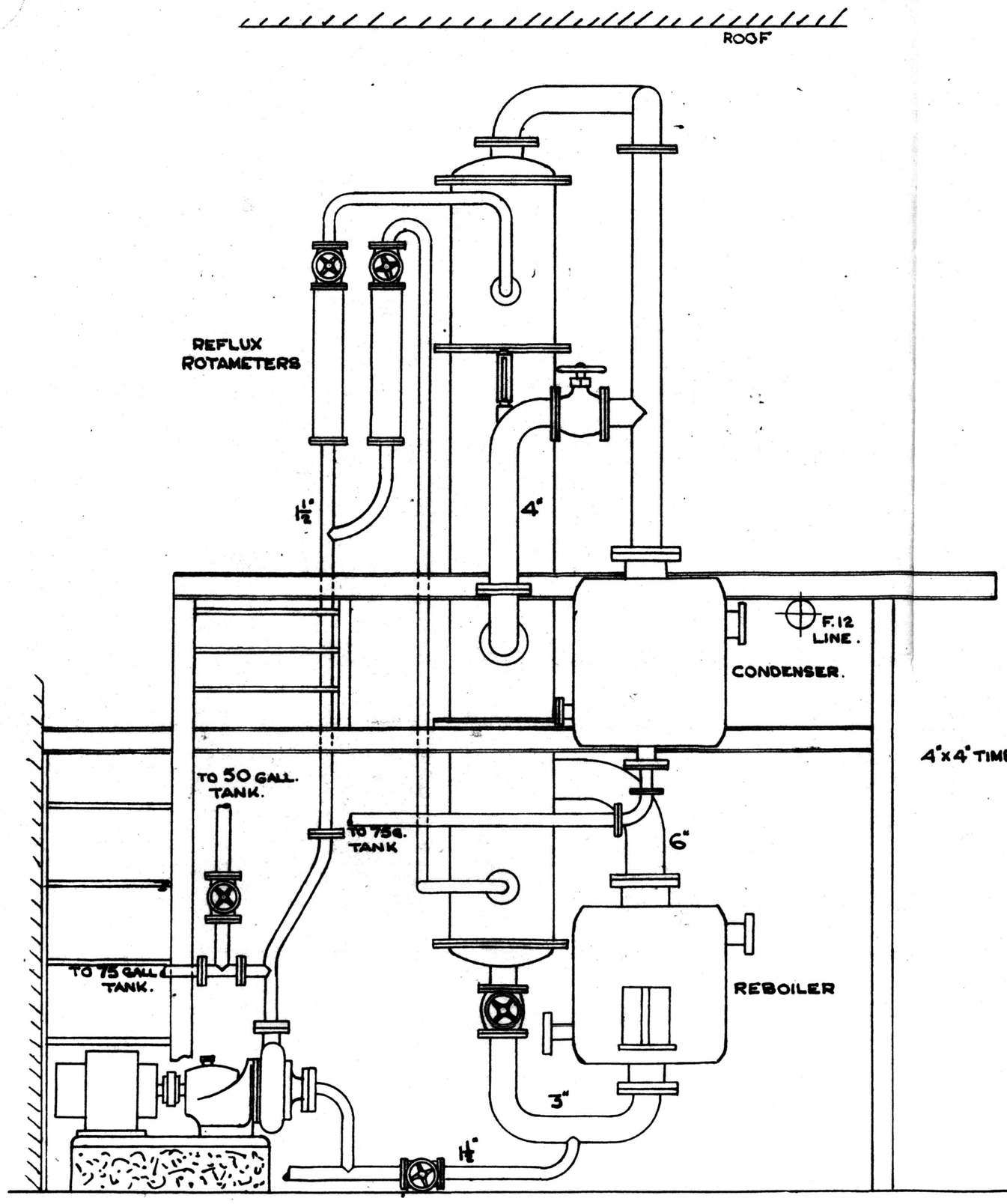
6" Deep Knitmesh In 3 Sections As Drg. 1 Set

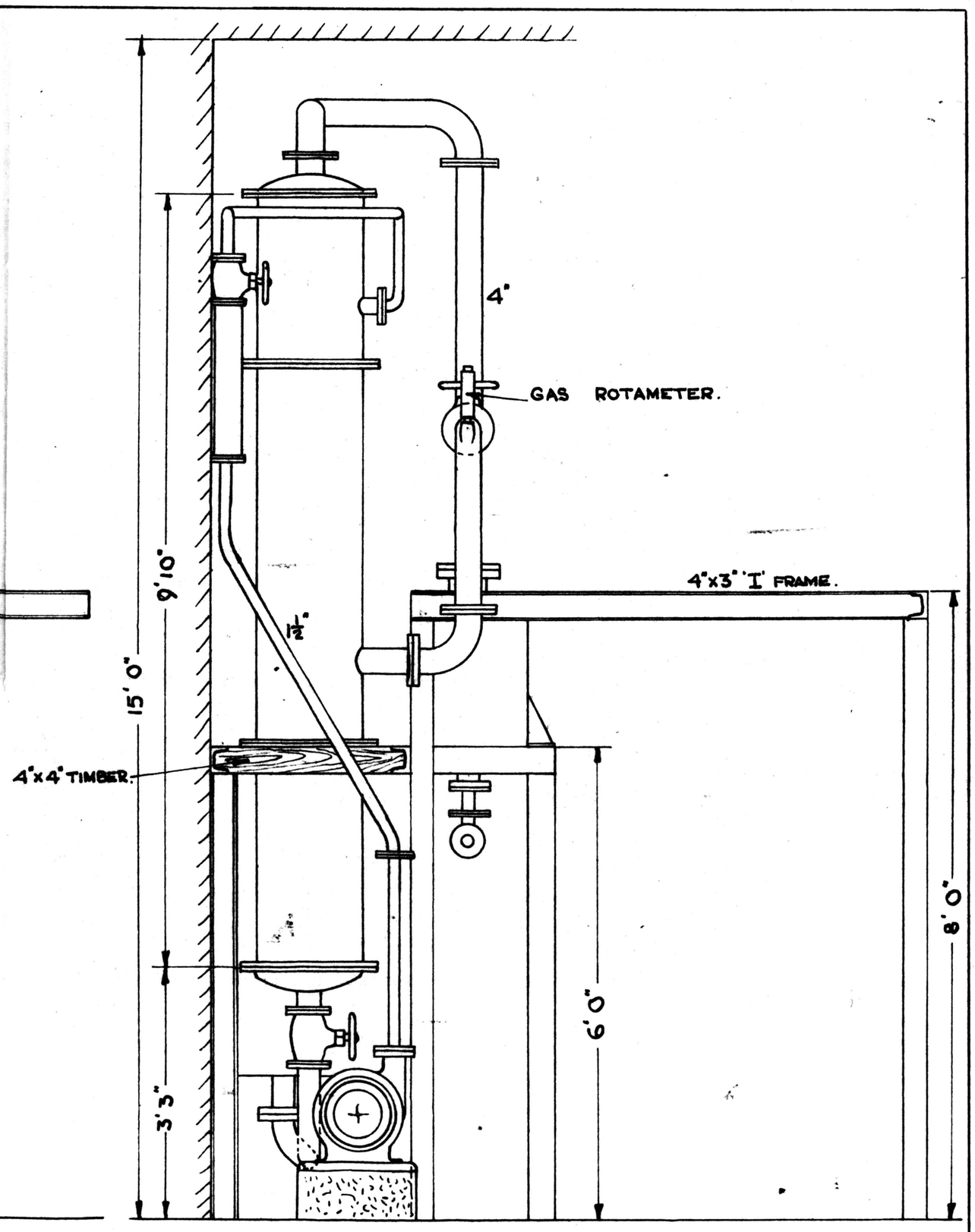


Lifting Handle

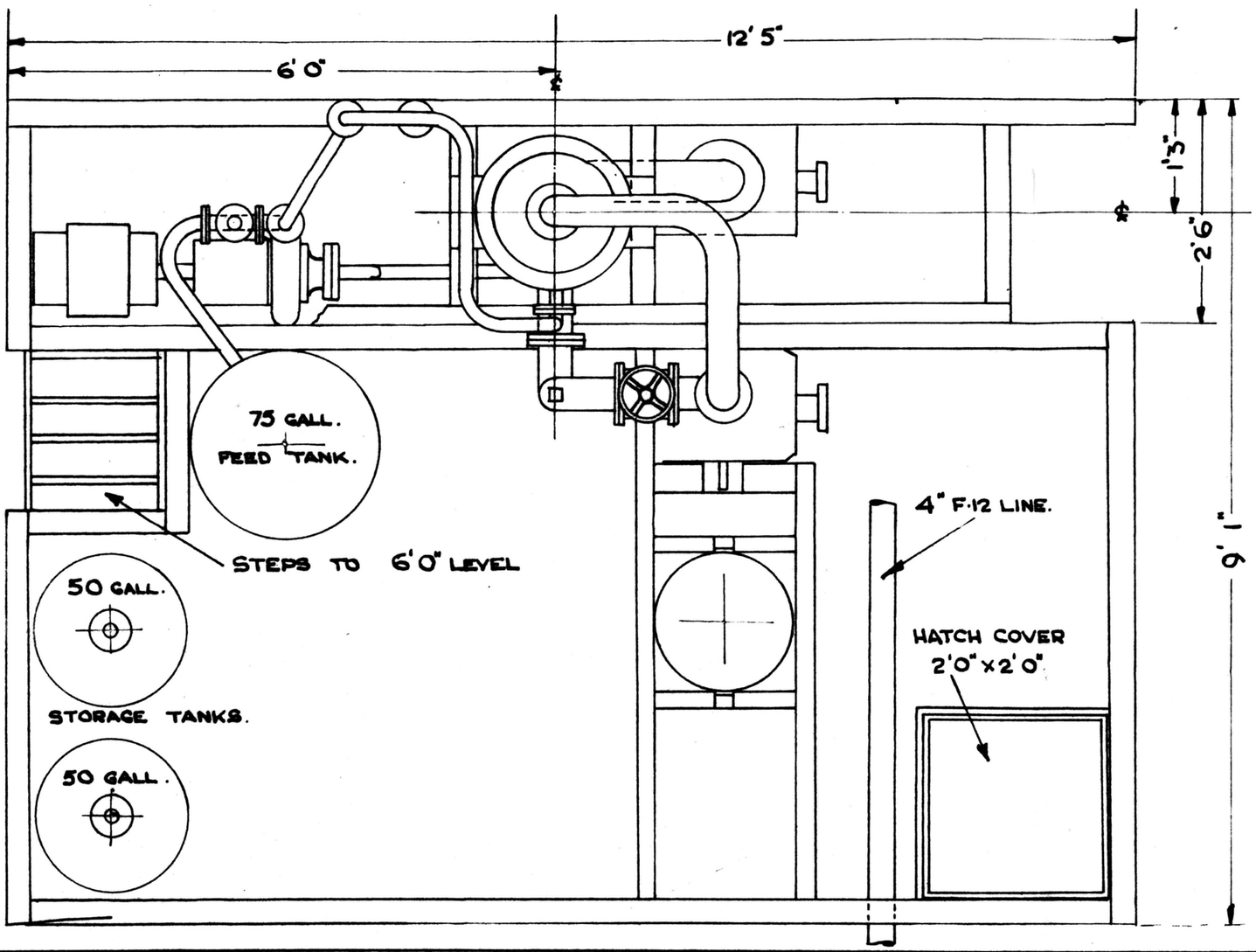
PATT. LETTER	REVISION	SIG. & DATE
A	Slot Added Bolster	7-7-61
B	Sight Glass Position Revised 4.5"	25.5.61

CLIENT		SCALE	1/8 Full Size	Q'NTY.	DRG. No.	PATT. No.	DESCRIPTION	MATERIAL	ITEM
Imperial College Of Science And Technology	Details Of Sightglass & Tray Supports	DRAWN		CHECKED			FOOD & CHEMICAL PLANT SPECIALISTS JOHN DORE & CO. LTD., COPPERSMITHS BROMLEY HIGH ST. BOW. LONDON. E.3.	DRG. No. 3090/8	
		DATE	17-3-61	APPROVED					
		DRAWING REFERENCES		3098/SA/1509.					
		JOB No.							





SIGMUND PUMP,
TYPE N-NE4.
ON CONCRETE PLINTH



GENERAL ARRANGEMENT of 16" DISTILLATION COLUMN.

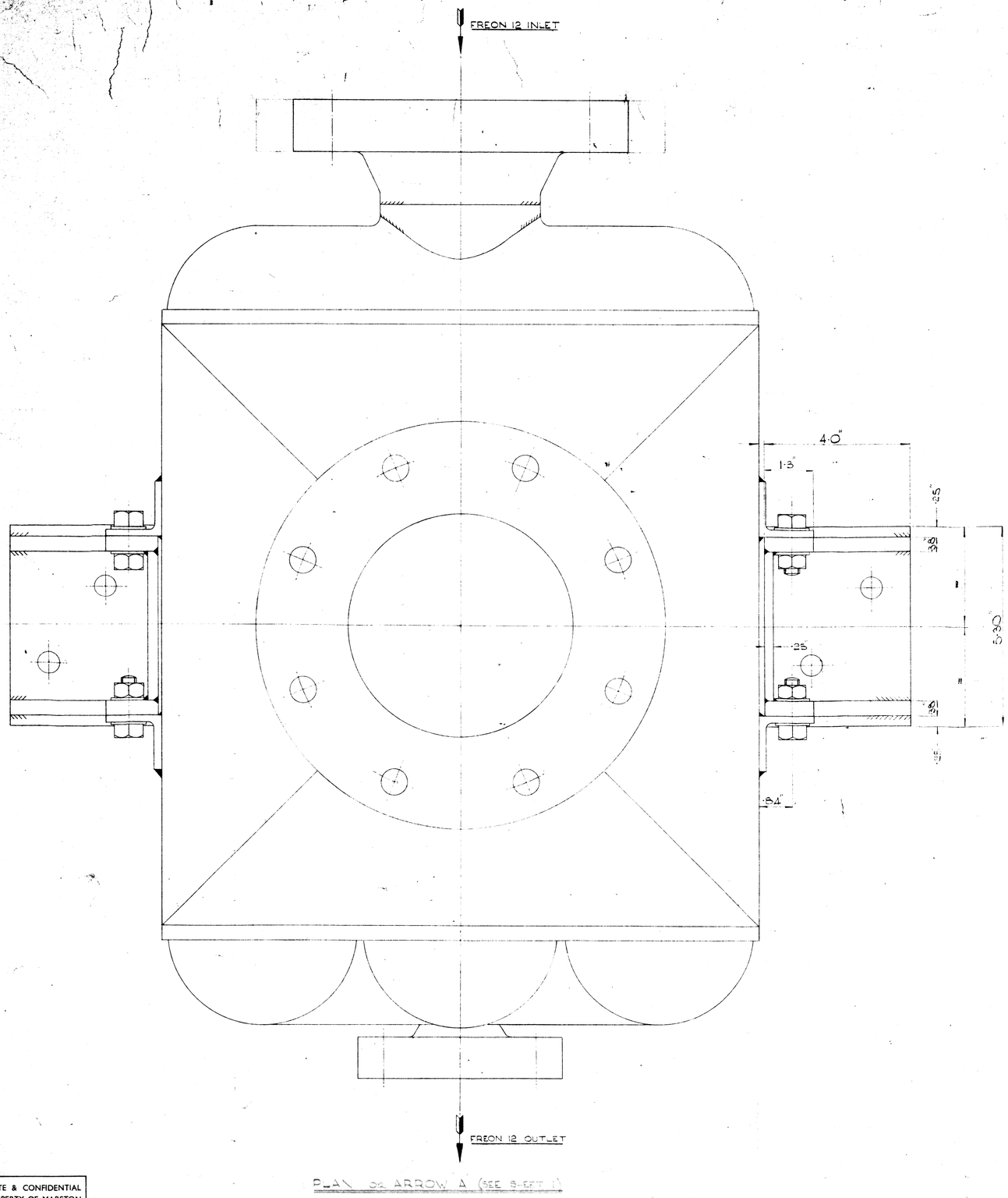
SCALE ~ ¾" = 1'0" (1/16TH.)

DRG. Nº 3101/CES.

ASSEMBLED ON	
	G/A

DRG. No. D1431-1A Sheet 2

ALTERATIONS PRIOR TO H.O.S. INTRODUCTION		
ISSUE	DATE	ALTERATION
A	6-4-60	DRAWN



PLAN on ARROW A (SEE SHEET 1)

NOTES :-

1. ALL BOLT HOLES TO BE POSITIONED OFF CENTRE
2. ARGON ARC WELD PENTANE INLET TANK (ITEM 14), OUTLET TANK (ITEM 21), FLANGES & MOUNTING ANGLES IN POSITION
3. ARGON ARC WELD IN A/W BS.277/D USING FILLER ROD BS.1475 : NG3
4. WELD SHOWN THUS ⌊ ////////
5. TORCH BRAZE ALL FREON TANKS (ITEMS 7,8,9,12,15,16,17,20) & LABEL PLATFORM IN POSITION
6. TORCH BRAZE IN A/W BS.877/B USING FILLER ROD BAIG
7. TEST FITTINGS TO BE IN ACCORDANCE WITH BS.71 SHEETS 7,8 & 9
8. HYDRAULIC TEST UNIT FIRST FOLLOWED BY LEAK DETECTION TEST
9. TREATMENT : INTERNAL — BS 53 X
   EXTERNAL — BS 53 Q

TESTS :-

	FREON SIDE	PENTANE SIDE
HYDRAULIC	440 PS.I.G @ AMBIENT T.	10 PS.I.G @ AMBIENT TEMP
A.L.D.W.	250 PS.I.G @ AMBIENT T.	5 PS.I.G @ AMBIENT TEMP

ITEM No.	DRG OR PART No.	DESCRIPTION	No. REQ'D PER UNIT	No. REQ'D PER ASSY.	MATERIAL SPEC.	MATERIAL SIZE	REMARKS
24	D891-30C	LABEL CLIP	2	-	-	-	
23	CP2480	LABEL	1	-	-	-	
22	SS2604/D60	WELD NECK FLANGE 6 NB	1	-	"	-	
21	D1431-1A/Q	TANK	1	-	BS1470 N.S.3	10 SWG (128)	
20	D1431-1A/P	TANK	1	-	BS1470 N.S.3	6 SWG (192)	
19	D1431-1A/N	FREON INLET/OUTLET	1	-	BS1471 N.S.3	4 NB x 6 SWG TUBE	
18	SS2604/4D	WELD NECK FLANGE 4 NB	1	-	-	-	
17	D1431-1A/M	TANK	1	-	BS1470 N.S.3	6 SWG (192)	
16	D1431-1A/L	TANK	2	-	BS1470 N.S.3	6 SWG (192)	
15	D1431-1A/K	TANK	1	-	BS1470 N.S.3	8 SWG (160)	
14	D1431-1A/J	INLET/OUTLET TANK	1	-	BS1470 N.S.3	10 SWG (128)	
13	SS2604/6D	WELD NECK FLANGE 6 NB	1	-	-	-	
12	D1431-1A/H	INLET/OUTLET TANK	1	-	BS1470 N.S.3	16 SWG (064)	
11	D1431-1A/G	FREON INLET/OUTLET	1	-	BS1471 N.S.3	12 NB x 6 SWG TUBE	
10	SS2604/12D	WELD NECK FLANGE 12 NB	1	-	-	-	
9	D1431-1A/F	TANK	1	-	BS1470 N.S.3	6 SWG (192)	
8	D1431-1A/E	TANK	2	-	BS1470 N.S.3	6 SWG (192)	
7	D1431-1A/D	TANK	1	-	BS1470 N.S.3	6 SWG (192)	
6	D1431-1A/C	MOUNTING FOOT	2	-	BS1449 N.S.3	-	
5	D1431-1A/B	MOUNTING ANGLE	4	-	BS1449 N.S.3	12 x 12	BSA23/4A
4	D1431-1A/A	WASHER 3/8 N.DIA	32	-	BS1083	-	F.D.P. ST STEEL
3	WN3069/-	NUT 3/8 B.S.W.	16	-	BS1083	-	F.D.P. ST STEEL
2	WB1096/10	BOLT 3/8 B.S.W.	16	-	BS1083	-	F.D.P. ST STEEL
1	D1431-10A	MATRIX.	1	-	-	-	

ALL ERRORS AND DISCREPANCIES NO MATTER HOW SMALL, ARE TO BE REPORTED TO THE DRAWING OFFICE USING THE W.Q. FORM PROCEDURE.

NOTE : DIRECTION OF FLOWS INDICATED ARE FOR THE REBOILER. FLOWS ARE REVERSED FOR THE CONDENSER.

TITLE :- DISTILLATION COLUMN REBOILER & CONDENSER - IMPERIAL COLLEGE OF SCIENCE

LIMITS ± .060 UNLESS OTHERWISE STATED
TREATMENT :- SEE NOTE 9
SCALE :- 1/4 F.S. 1/1

	DRAWN	R.H.	18-4-60
	CHECKED		
	STRESSED		
	TRACED		
	APPROVED		

ISSUE No.
MOD. OR AMEND No.
APP. FOR CS(A)

MARSTON EXCELSIOR LTD. WOLVERHAMPTON
PROPRIETOR, IMPERIAL CHEMICAL INDUSTRIES LIMITED.

ORG. No. D1431-1A SHEET 2

THIS DRAWING IS A PRIVATE & CONFIDENTIAL COMMUNICATION & THE PROPERTY OF MARSTON EXCELSIOR LTD. (SUBSIDIARY OF I.C.I. METALS), AND MUST NOT BE COPIED LOANED OR USED FOR THE MANUFACTURE OF ANY PART OR PARTS WITHOUT THE WRITTEN CONSENT OF MARSTON EXCELSIOR LTD., WOLVERHAMPTON.

1ST. 3RD. ANGLE PROJECTION